

AD-A069 796

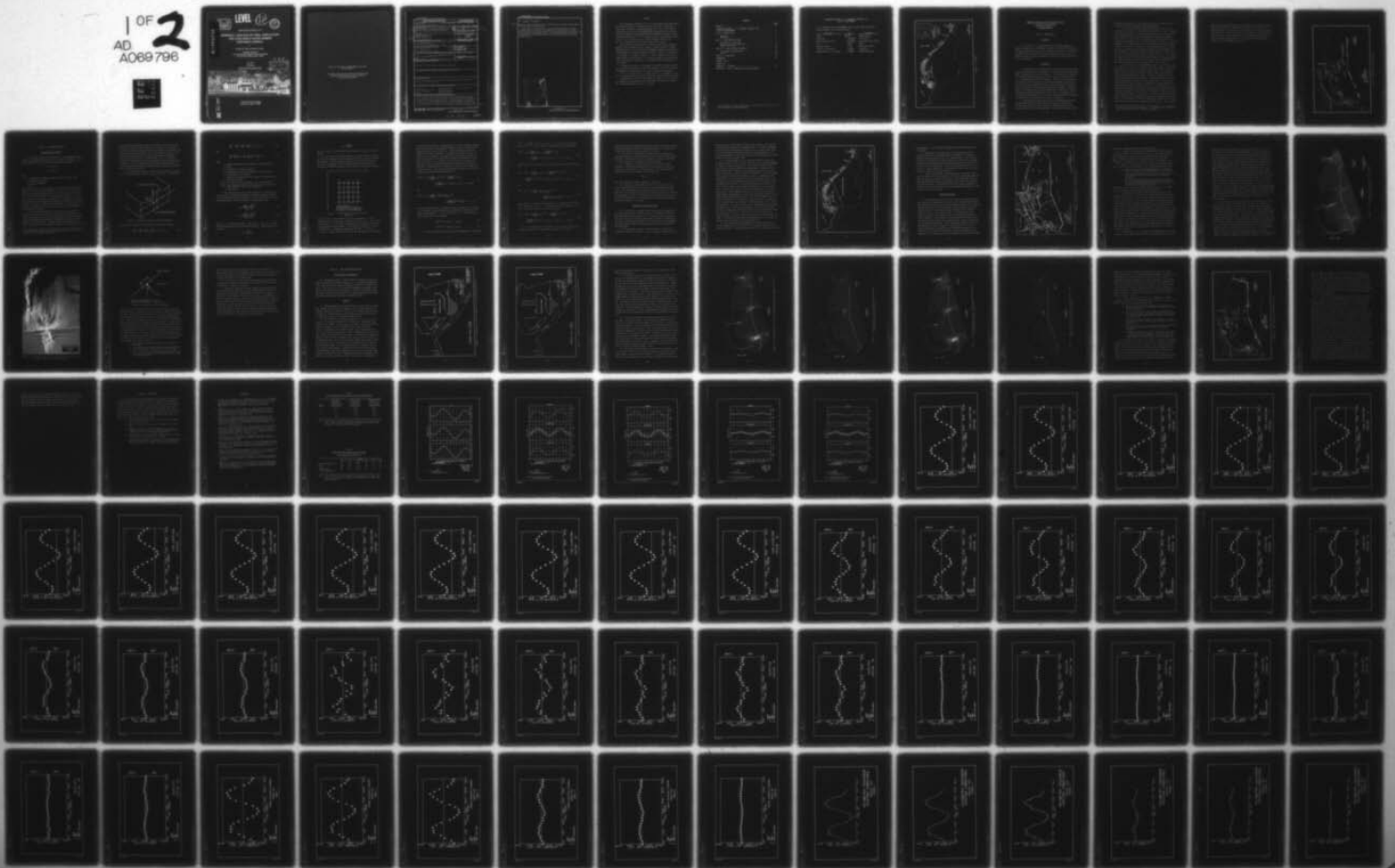
ARMY ENGINEER WATERWAYS EXPERIMENT STATION VICKSBURG MISS F/6 13/13
NUMERICAL ANALYSIS OF TIDAL CIRCULATION FOR LONG BEACH OUTER HA--ETC(U)
MAY 79 D 6 OUTLAW, D C RANEY

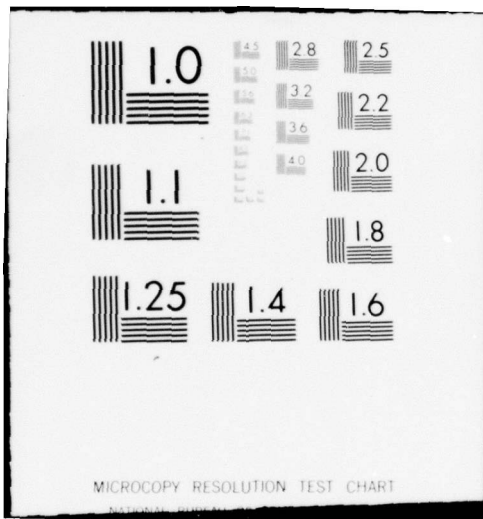
UNCLASSIFIED

WES-MP-HL-79-5

NL

1 OF 2
AD
A069 796





AD A 069796



LEVEL

12



MISCELLANEOUS PAPER HL-79-5

NUMERICAL ANALYSIS OF TIDAL CIRCULATION FOR LONG BEACH OUTER HARBOR PROPOSED LANDFILL

by

Douglas G. Outlaw and Donald C. Raney

Hydraulics Laboratory

U. S. Army Engineer Waterways Experiment Station
P. O. Box 631, Vicksburg, Miss. 39180

May 1979

Final Report

Approved For Public Release; Distribution Unlimited

DDC
RECEIVED
JUN 13 1979
RECEIVED
C



DDC FILE COPY

Prepared for Port of Long Beach
Long Beach, California 90801

79 06 14 168

Destroy this report when no longer needed. Do not return
it to the originator.

The findings in this report are not to be construed as an official
Department of the Army position unless so designated
by other authorized documents.

Unclassified

SECURITY CLASSIFICATION OF THIS PAGE (When Data Entered)

REPORT DOCUMENTATION PAGE		READ INSTRUCTIONS BEFORE COMPLETING FORM
1. REPORT NUMBER Miscellaneous Paper HL-79-5	2. GOVT ACCESSION NO.	3. RECIPIENT'S CATALOG NUMBER
4. TITLE (and Subtitle) NUMERICAL ANALYSIS OF TIDAL CIRCULATION FOR LONG BEACH OUTER HARBOR PROPOSED LANDFILL	5. TYPE OF REPORT & PERIOD COVERED Final report. May-Aug 78	6. PERFORMING ORG. REPORT NUMBER
7. AUTHOR(s) Douglas G./Outlaw Donald C./Raney	8. CONTRACT OR GRANT NUMBER(s) 12 98 p.	10. PROGRAM ELEMENT, PROJECT, TASK AREA & WORK UNIT NUMBERS
9. PERFORMING ORGANIZATION NAME AND ADDRESS U. S. Army Engineer Waterways Experiment Station Hydraulics Laboratory P. O. Box 631, Vicksburg, Miss. 39180	11. CONTROLLING OFFICE NAME AND ADDRESS Port of Long Beach P. O. Box 570 Long Beach, California 90801	12. REPORT DATE May 1979
13. MONITORING AGENCY NAME & ADDRESS (if different from Controlling Office)	14. NUMBER OF PAGES 93	15. SECURITY CLASS. (of this report) Unclassified
14 WES-MP-HL-79-5	15a. DECLASSIFICATION/DOWNGRADING SCHEDULE	
16. DISTRIBUTION STATEMENT (of this Report) Approved for public release; distribution unlimited.		
17. DISTRIBUTION STATEMENT (of the abstract entered in Block 20, if different from Report)		
18. SUPPLEMENTARY NOTES Vector plots showing tidal circulation velocity patterns are presented in a separate volume as Appendix B.		
19. KEY WORDS (Continue on reverse side if necessary and identify by block number) Earthfills Long Beach Harbor Tidal circulation Finite difference method Mathematical models Harbor oscillations Numerical analysis Harbors Tanker terminals		
20. ABSTRACT (Continue on reverse side if necessary and identify by block number) A study was conducted for Long Beach Harbor to numerically investigate tidal circulation in existing basins and to define and evaluate the impact of a proposed oil terminal adjacent to pier J on existing harbor circulation. A two-dimensional depth-averaged formulation of the hydrodynamic equations was used in the model and an implicit-explicit finite difference scheme was used to numerically solve the equations. The numerical model had been verified in a (Continued) →		

DD FORM 1473 JAN 73 EDITION OF 1 NOV 65 IS OBSOLETE

Unclassified

SECURITY CLASSIFICATION OF THIS PAGE (When Data Entered)

038 100 Luu

Unclassified

SECURITY CLASSIFICATION OF THIS PAGE(When Data Entered)

20. ABSTRACT (Continued).

CONT'

previous study using tide and velocity data from the prototype and from physical model tests conducted at WES.

Two landfill configurations for the oil terminal along with a channel dredging project in the Port of Los Angeles were considered in the study. Tidal currents were relatively unaffected by the proposed plans except near the oil terminal and the dredging project. Net discharges through the harbor entrances and through Cerritos Channel in the inner harbor were not changed significantly.

Accession For	
NTIS GRA&I	<input checked="" type="checkbox"/>
DDC TAB	<input type="checkbox"/>
Unannounced	
Justification	
By _____	
Distribution / _____	
Availability Codes	
Dist .	Avail. 4/or special
A	

Unclassified

SECURITY CLASSIFICATION OF THIS PAGE(When Data Entered)

PREFACE

This study was conducted at the U. S. Army Engineer Waterways Experiment Station (WES) with funding provided by the Port of Long Beach, Long Beach, California, under WES Agreement No. 78-05. The study was conducted during the period from May 1978 to August 1978 in the Harbor Wave Action Branch, Wave Dynamics Division, Hydraulics Laboratory, WES, under the direction of Mr. H. B. Simmons, Chief of the Hydraulics Laboratory, Dr. R. W. Whalin, Chief of the Wave Dynamics Division, and Mr. C. E. Chatham, Chief of the Harbor Wave Action Branch.

The study was conducted and this report prepared by Mr. Douglas G. Outlaw, Project Engineer, and Dr. Donald C. Raney, Professor of Engineering Mechanics at the University of Alabama, assigned to WES under an Intergovernmental Personnel Exchange Agreement. Messrs. H. Lee Butler, L. A. Barnes, S. A. Adamec, and Ms. J. I. Jones assisted with various tasks during the investigation. Vector plots showing tidal circulation velocity patterns are presented in a separate volume as Appendix B to this report.

A significant portion of the numerical computation associated with this study was performed on a CYBER 176 computer at the Air Force Weapons Laboratory at Kirtland Air Force Base, Albuquerque, New Mexico.

Mr. C. T. Johnson, Dr. D. B. Bright, and Mr. B. R. McDaniel of the Port of Long Beach visited WES for conferences associated with the study.

Commander and Director of WES during the course of this study and the preparation and publication of this report was COL John L. Cannon, CE. Technical Director was Mr. F. R. Brown.

CONTENTS

	<u>Page</u>
PREFACE	1
CONVERSION FACTORS, U. S. CUSTOMARY TO METRIC (SI)	
UNITS OF MEASUREMENT	3
PART I: INTRODUCTION	5
Objective	5
Background	5
PART II: THE NUMERICAL MODEL	9
Formulation of the Model	9
Application to San Pedro Bay	15
Model Verification	18
PART III: TIDAL CIRCULATION RESULTS	26
Oil Terminal Configurations	26
Results	26
PART IV: CONCLUSIONS	38
REFERENCES	39
TABLES 1 and 2	
PLATES 1-52	
APPENDIX A: NOTATION	A1
APPENDIX B: TIDAL CIRCULATION VELOCITY PATTERNS*	

* This appendix is bound separately.

CONVERSION FACTORS, U. S. CUSTOMARY TO METRIC (SI)
UNITS OF MEASUREMENT

U. S. customary units of measurement used in this report can be converted to metric (SI) units as follows:

<u>Multiply</u>	<u>By</u>	<u>To Obtain</u>
acres	4046.856	square metres
cubic feet	0.02831685	cubic metres
cubic feet per second	0.02831685	cubic metres per second
feet	0.3048	metres
feet per second	0.3048	metres per second
miles (U. S. statute)	1.609344	kilometres
square miles (U. S. statute)	2.589988	square kilometres

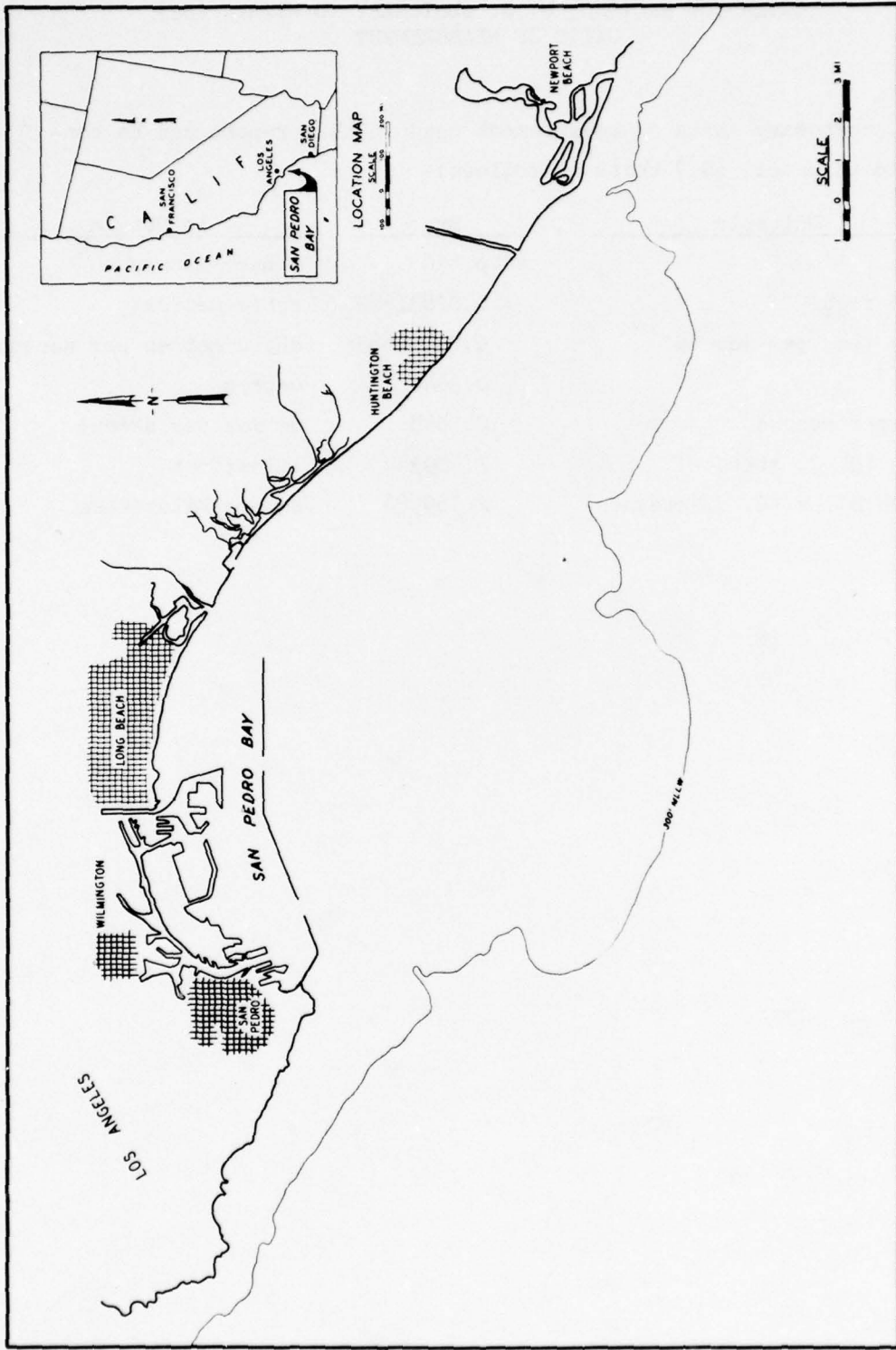


Figure 1. Site map

NUMERICAL ANALYSIS OF TIDAL CIRCULATION FOR
LONG BEACH OUTER HARBOR
PROPOSED LANDFILL

PART I: INTRODUCTION

Objective

1. The purpose of the Long Beach Harbor numerical analysis of tidal circulation was to investigate the effect on harbor circulation by a proposed landfill adjacent to the southerly side of pier J. The numerical model used had been verified for existing conditions in previous numerical studies of tidal circulation in the Port of Long Beach and the Port of Los Angeles.

Background

2. Los Angeles and Long Beach Harbors are located on San Pedro Bay along the southern coast of California. A location map and the existing harbor configuration are shown in Figure 1. Various plans for expansion of the harbors have been proposed over the years by each Port and the U. S. Army Engineer District, Los Angeles. Proposed port modifications and additions have been extensive, requiring comprehensive analyses to assure that tidal circulation, energy oscillatory patterns, and water quality remain within established and desirable standards. A physical model of Los Angeles and Long Beach Harbors was constructed at the U. S. Army Engineer Waterways Experiment Station (WES) to investigate tidal circulation characteristics of the present and proposed harbor plans and to investigate wave-induced oscillations in the harbors.

3. An extensive prototype data collection program was conducted by WES during 1971-1972 and is described in detail in Reference 1. The prototype data were used to describe existing conditions in the harbors and to verify the physical model. Base tidal circulation tests

(described in Reference 2), and tests on several other proposed expansion plans have been conducted in the physical model.

4. In 1976, during a period when the hydraulic model was in use for wave tests, the Port of Long Beach requested WES to conduct a numerical study of the effect on tidal-generated circulation of various alternative configurations for the outer harbor oil terminal and landfill south of pier J. The proposed configurations consisted primarily of a landfill of approximately 120 acres* and variations thereof, a protective breakwater on the seaward side of the oil terminal, and channel depths of -65 or -82 ft mllw. A plan with a reduced landfill and oil storage facilities provided by two 250,000-dwt permanently moored tankers also was considered. The results of these previous numerical studies for the various oil terminal plans are given in References 3 and 4. Conclusions from the study were that the proposed plans resulted in only minor overall changes in tidal circulation in Los Angeles and Long Beach Harbors and that the primary circulation changes were local in nature.

5. After completion of the numerical study for the preceding plans, the proposed outer harbor development concept was revised. The revised plan included a landfill of approximately 60 acres. The southwestern edge of the new landfill was shifted slightly toward the Long Beach Harbor entrance channel and possibly could tend to obstruct flow into the inner harbor and Cerritos Channel. In May 1978, the Port of Long Beach requested WES to conduct a study of the effect of the revised landfill plan on tidal circulation considering both the proposed plan and a modified plan with a 40-acre landfill. In the modified plan, the southwesterly portion of the landfill was decreased, thereby increasing the distance between the landfill and the navigation channel, thus presenting less obstruction to tidal flow. Included in this study with the pier J landfill were the proposed oil terminals and breakwater south of pier J, the deepening of Los Angeles Harbor main channel to -45 ft mllw, and the associated landfill of approximately 200 acres. These proposed

* A table of factors for converting U. S. customary units of measurement to metric (SI) units is presented on page 3.

projects are shown in Figure 2 and are referred to as the phase I plan. The alternate landfill configuration is referred to as phase I with modified landfill. Due to time constraints and the fact that the physical model was in use for wave studies, the numerical tidal circulation model was used to predict the effects of the proposed modifications on tidal circulation. The model is a two-dimensional, depth-averaged solution of the hydrodynamic equations.

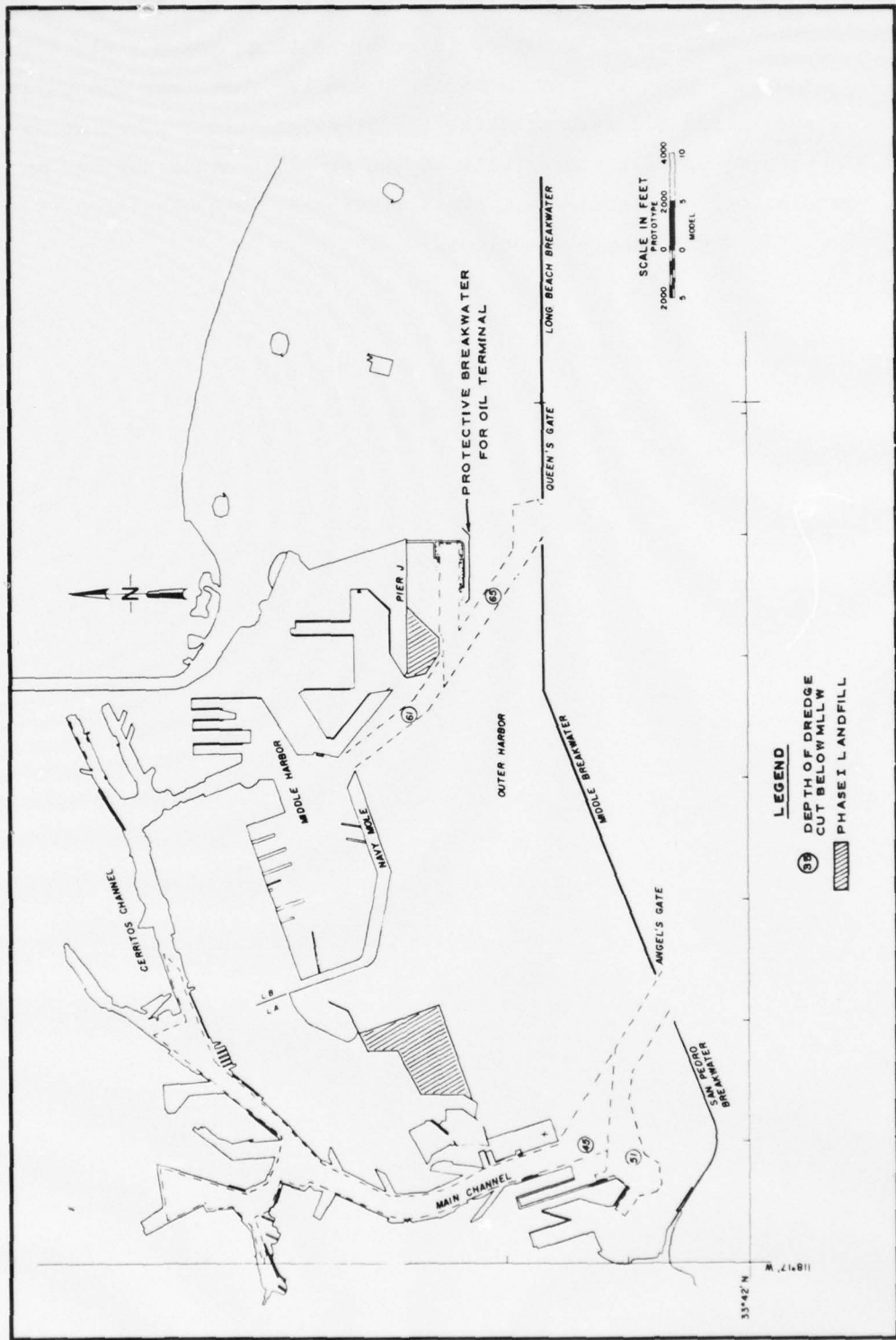


Figure 2. Elements of the phase I plan

PART II: THE NUMERICAL MODEL

Formulation of the Model

6. A complete mathematical description of the hydrodynamic flow in a harbor or estuary would require that the velocity and density be completely specified for every point in the system at all times:

$$u = u(x,y,z,t)$$

$$\rho = \rho(x,y,z,t)$$

where

x = longitudinal coordinate measured along the estuary axis*

y = transverse coordinate

z = vertical coordinate

t = time

Unfortunately, with existing computers, a generalized three-dimensional model with the needed time and spatial resolution is not feasible for practical engineering applications (due to time and cost of computer time and the state of the art of three-dimensional modeling). Because of the practical difficulties in formulation and execution of a three-dimensional model for engineering applications, researchers have devised a variety of numerical models of various degrees of simplification. In general, the simpler the model the less reliable and less adaptable it is to changing conditions.

7. A two-dimensional approach⁵ that produces a pseudothree-dimensional effect was utilized in this numerical investigation. The vertical components of velocity and acceleration are neglected and the general three-dimensional governing hydrodynamic equations are integrated over the water depth. A depth-averaged two-dimensional flow field is obtained but three-dimensional geometry can be considered. The

* For convenience, symbols and unusual abbreviations are listed and defined in the Notation (Appendix A).

most important approximations used in the model are those of constant density and relatively small variations of velocity over the depth, conditions which are reasonably valid in most harbors. Where these conditions are approximately valid, this type of numerical model can provide accurate representations of tidal elevations and velocities. Although the model output is two-dimensional, it has a pseudothree-dimensional character since the actual bathymetric data are used in the calculations. The two-dimensional depth-averaged model appears to be the most sophisticated numerical model presently available for study of tidal circulation in harbors.

8. The rectangular coordinate system used is located in the plane of the undisturbed water surface as shown in Figure 3. The equations

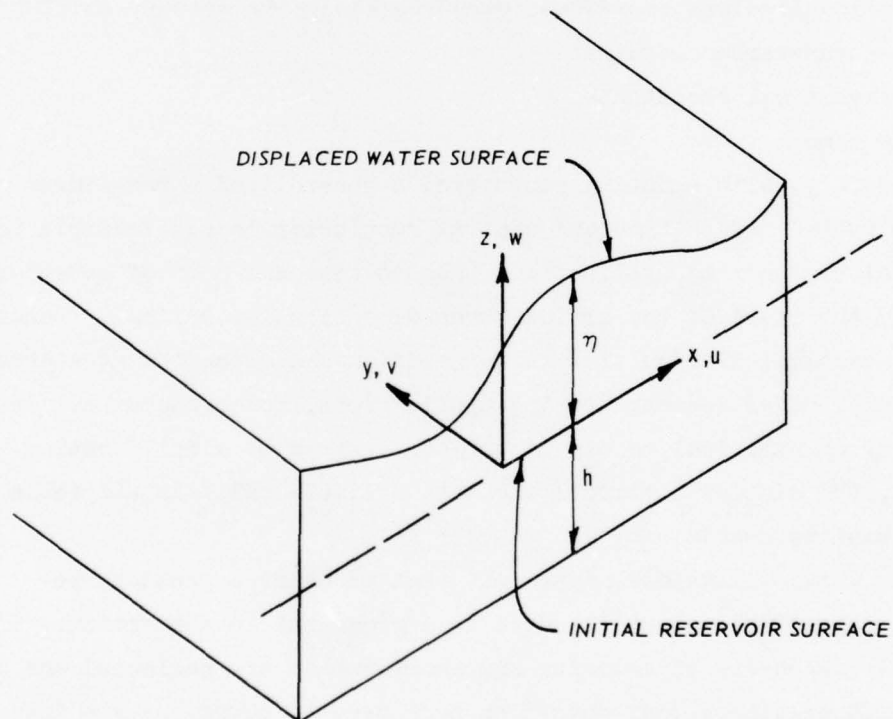


Figure 3. Coordinate system for problem formulation of motion and the equation of continuity are written as follows:

$$\frac{\partial u}{\partial t} + u \frac{\partial u}{\partial x} + v \frac{\partial u}{\partial y} + g \frac{\partial \eta}{\partial x} - fv = R_x + L_x \quad (1)$$

$$\frac{\partial v}{\partial t} + u \frac{\partial v}{\partial x} + v \frac{\partial v}{\partial y} + g \frac{\partial \eta}{\partial y} + fu = R_y + L_y \quad (2)$$

and

$$\frac{\partial \eta}{\partial t} + \frac{\partial}{\partial x} [(h + \eta)u] + \frac{\partial}{\partial y} [(h + \eta)v] = 0 \quad (3)$$

where

u = depth-averaged velocity component in the x-direction

t = time

x, y = rectangular coordinate variables

v = depth-averaged velocity component in the y-direction

g = acceleration due to gravity

η = water-level displacement with respect to datum elevation

f = Coriolis parameter

R_x, R_y = the effect of bottom roughness in x- and y-directions

L_x, L_y = the acceleration effect of the wind stress acting on the water surface in the x- and y-directions

h = water depth

9. The continuity equation has been obtained by integrating over the water depth and applying kinematic and dynamic boundary conditions at the surface and bottom of the harbor. The bottom friction terms are represented using a Chezy coefficient in the following form:

$$R_x = \frac{-gu(u^2 + v^2)^{1/2}}{C^2(h + \eta)} \quad (4)$$

$$R_y = \frac{-gv(u^2 + v^2)^{1/2}}{C^2(h + \eta)} \quad (5)$$

where C is the Chezy coefficient. The terms L_x and L_y represent the wind shear stress effect on the water surface. These terms are of the form:

$$L_x = \frac{T_x}{(h + \eta)} \quad (6)$$

$$L_y = \frac{T_y}{(h + \eta)} \quad (7)$$

where T_x and T_y are the wind stress components acting on the water surface.

10. To solve the governing equations, a finite difference approximation of the equations and an alternating direction solution technique are employed. A space-staggered scheme is used in which velocities, water-level displacement, bottom displacement, and water depth are described at different locations within a grid cell as shown in Figure 4.

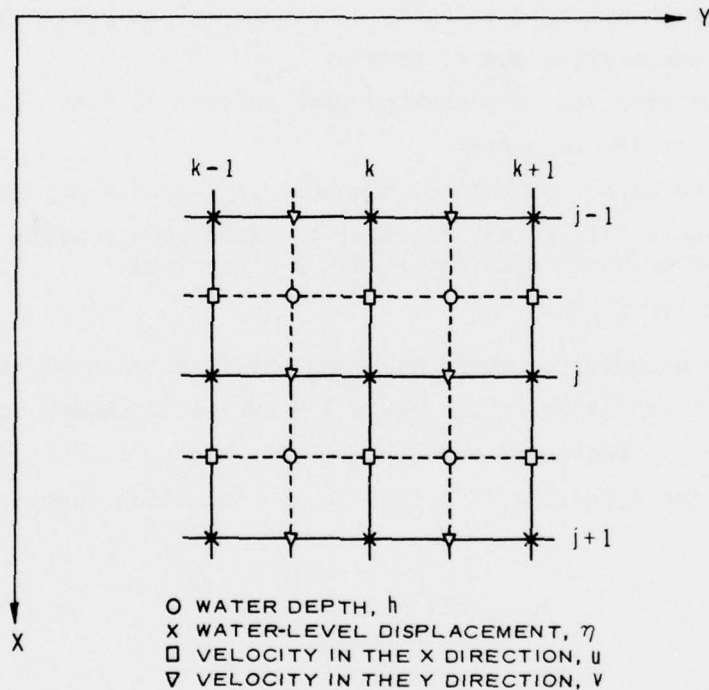


Figure 4. Grid system and variable definition locations

The first step in the calculation consists of computing u and η implicitly and v explicitly, advancing from time $n\Delta t$ to $(n + 1/2)\Delta t$. The parameter n is an integer representing the time-step at which the calculations are being conducted. The second step computes η and v implicitly and u explicitly, advancing from time $(n + 1/2)\Delta t$ to $(n + 1)\Delta t$. Central differences are used for evaluating all derivatives

in the governing equations. The application of these difference approximations gives rise to corresponding difference equations centered about different points within a grid cell. These expressions require the evaluation of certain quantities at locations different from those defined in the grid system. Such quantities are replaced by values computed from a one- and two-dimensional averaging of neighboring values. The time interval Δt is taken as the time required to complete the full cycle in the computational procedure; however, each half cycle is treated by a different set of equations so a system of six operational equations is used. The difference approximations used in the first step of the alternating direction technique are:

$$\begin{aligned}
 u^{n+1/2} = u^n - \frac{g}{2} \left(\frac{\Delta t}{\Delta x} \right) \langle \langle \eta_x \rangle \rangle^{n+1/2} - \frac{1}{4} \left(\frac{\Delta t}{\Delta x} \right) u^{n+1/2} \langle u_x \rangle^n \\
 - \frac{1}{4} \left(\frac{\Delta t}{\Delta y} \right) v^n \langle u_y \rangle^n + \frac{1}{2} \Delta t (R_x + L_x)^n \quad \text{at } j+1/2, k
 \end{aligned} \tag{8}$$

and

$$\begin{aligned}
 \eta^{n+1/2} = \eta^n - \frac{1}{2} \left(\frac{\Delta t}{\Delta x} \right) \langle \langle (\overline{h + \eta}) u \rangle \rangle_x^{n+1/2} \\
 - \frac{1}{2} \left(\frac{\Delta t}{\Delta y} \right) \langle \langle (\overline{h + \eta}) v \rangle \rangle_y^n \quad \text{at } j, k
 \end{aligned} \tag{9}$$

where superscripts refer to multiples of time increments. For simplicity of notation, some terms have been maintained in differential form within angle brackets $\langle \rangle$ or double brackets $\langle \langle \rangle \rangle$. The differential forms are defined by the examples:

$$\langle \eta_x(j, k) \rangle = \eta_{j+1/2, k} - \eta_{j-1/2, k} \tag{10}$$

$$\langle \langle u_x(j, k) \rangle \rangle = u_{j+1, k} - u_{j-1, k} \tag{11}$$

11. These two equations can be solved simultaneously for quantities

$u^{n+1/2}$ and $\eta^{n+1/2}$ along a grid line k . The additional velocity component $v^{n+1/2}$ can be determined explicitly from the expression

$$v^{n+1/2} = v^n - \frac{g}{2} \left(\frac{\Delta t}{\Delta y} \right) \langle \langle \eta_y \rangle \rangle^n - \frac{1}{4} \left(\frac{\Delta t}{\Delta x} \right) u^{n+1/2} \langle v_x \rangle^n - \frac{1}{4} \left(\frac{\Delta t}{\Delta y} \right) v^{n+1/2} \langle v_y \rangle^n + \frac{1}{2} \Delta t (R_y + L_y)^n \text{ at } j, k+1/2 \quad (12)$$

The equations for the second step of the alternating direction technique are:

$$v^{n+1} = v^{n+1/2} - \frac{g}{2} \left(\frac{\Delta t}{\Delta y} \right) \langle \langle \eta_y \rangle \rangle^{n+1} - \frac{1}{4} \left(\frac{\Delta t}{\Delta x} \right) u^{n+1/2} \langle v_x \rangle^{n+1/2} - \frac{1}{4} \left(\frac{\Delta t}{\Delta y} \right) v^{n+1} \langle v_y \rangle^{n+1/2} + \frac{1}{2} \Delta t (R_y + L_y)^{n+1/2} \text{ at } j, k+1/2 \quad (13)$$

and

$$\eta^{n+1} = \eta^{n+1/2} - \frac{1}{2} \left(\frac{\Delta t}{\Delta x} \right) \langle \langle [(\overline{h + \eta})_u] \rangle \rangle^{n+1/2} - \frac{1}{2} \left(\frac{\Delta t}{\Delta y} \right) \langle \langle [(\overline{h + \eta})_v] \rangle \rangle^{n+1} \text{ at } j, k \quad (14)$$

These equations are solved simultaneously for the quantities v^{n+1} and η^{n+1} along a grid line j . The additional velocity component u^{n+1} can be determined explicitly from the expression

$$u^{n+1} = u^{n+1/2} - \frac{g}{2} \left(\frac{\Delta t}{\Delta x} \right) \langle \langle \eta_x \rangle \rangle^{n+1/2} - \frac{1}{4} \left(\frac{\Delta t}{\Delta x} \right) u^{n+1} \langle u_x \rangle^{n+1/2} - \frac{1}{4} \left(\frac{\Delta t}{\Delta y} \right) v^{n+1} \langle u_y \rangle^{n+1/2} + \frac{1}{2} \Delta t (R_x + L_x)^{n+1/2} \text{ at } j+1/2, k \quad (15)$$

12. The formulation of the problem in this way (ADI method) considerably simplifies the computational procedure. The implicit

equations are solved simultaneously during each half time-step. However, with this formulation scheme the coefficient matrix is tridiagonal and a relatively simple solution procedure is available.

13. Two types of boundaries are involved in the calculations: the solid boundaries at fixed coastlines and the artificial tidal input boundaries arising from the need to truncate the region of computation (in order to minimize computational time requirements).

14. A condition of complete reflection is adopted at solid boundaries. While some dissipation does occur at the shoreline, this should not be significant in this application. The actual boundary condition for the solid boundary can be written as

$$\vec{V}_n = 0 \quad (16)$$

where \vec{V}_n denotes the normal component of velocity.

15. Artificial tidal boundaries were used in the model to describe the tidal action that occurs at the ocean computational boundaries. These boundaries must be accurately defined since the tides applied at these boundaries represent the major forcing function driving the hydrodynamic system. The water-surface elevation time-history for the desired tidal cycle is specified at each such boundary and applied during the operation of the model.

Application to San Pedro Bay

16. San Pedro Bay is formed by the curvature and indentation of the southern California coastline (Figure 1). Sheltered to the west by Point Fermin, the bay is open to the south and southeast except for the slight protection offered by Santa Catalina Island. Originally an open bay, the protection afforded by its orientation has been augmented by an 8-mile-long breakwater extending from Point Fermin eastward to near Seal Beach.

17. The breakwater consists of three sections. The San Pedro breakwater (oldest of the three) is 11,000 ft long and extends from the

shoreline east of Point Fermin to Angel's Gate, which is the 2,100-ft-wide navigation opening for Los Angeles Harbor. The Middle breakwater is 18,500 ft long and extends from Angel's Gate to Queen's Gate, which is the 1,800-ft-wide navigation opening for Long Beach Harbor. The Long Beach breakwater is the third section of the breakwater and extends 13,350 ft due east of Queen's Gate.

18. A detailed study of the circulation patterns in San Pedro Bay was necessary in order to predict the effect on circulation patterns of changes in harbor configuration. Some recent advances at WES^{6,7,8} have resulted in several significant improvements to numerical tidal circulations models; however, this investigation used the identical model to that used in previous numerical studies^{3,4} of tidal circulation in Los Angeles and Long Beach Harbors in order to completely assure compatibility of these results with those in References 3 and 4 (also to minimize costs by eliminating the necessity to verify another model and prepare another grid). To obtain the required resolution of the harbor basins, channels, and proposed modifications it was necessary to use a 300-ft step size in the finite difference grid. For proper application of tidal boundary conditions the region of study was extended seaward approximately 1.4 miles from the Middle breakwater. The tidal boundary was taken as parallel to the Middle breakwater and the region of application of the model is shown in Figure 5. A region of about 60 square miles was included in the model coverage with a finite grid dimension of 101 cells by 199 cells or approximately 20,000 finite difference cells. There were approximately 12,000 water cells where the velocity components and tidal elevations were calculated each time-step during a tidal cycle. A time-step of 45 sec was used in the numerical model so a 25-hr tidal cycle required 2,000 calculation time-steps. The numerical model required approximately 0.8 hr of CYBER 176 computer time to simulate 25 hr of prototype time.

19. The model required approximately 5 hr of prototype time (10 min of computer time) to "warm up" due to transients associated with starting the model. Actual calculations for a 25-hr tidal cycle required

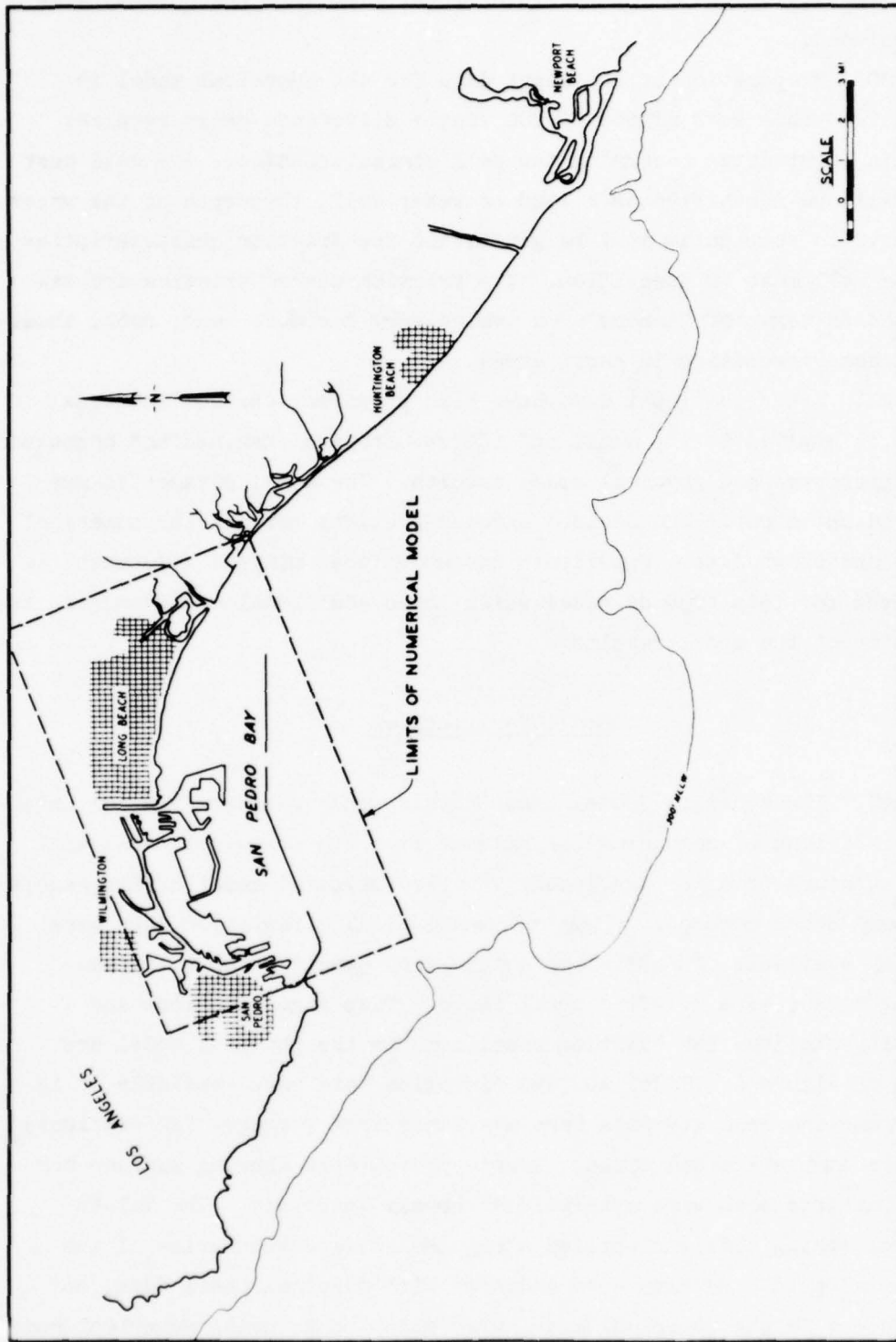


Figure 5. Site map and limits of numerical model

approximately 1.0 hr of CYBER 176 computer time when the warm-up time is included.

20. Preparation of the input data for the numerical model is extensive since each of the 20,000 finite difference cells requires certain input data concerning the cell characteristics. The cell must initially be identified as a land or water cell, the depth of the water relative to some datum must be given, and the friction characteristics of the cell must be identified. The friction characteristics are expressed in terms of Manning's n which vary for mud, sand, rock, shoaling areas, vegetation in marsh areas, etc.

21. After the input data have been prepared, the desired tidal cycle is applied to the model and the results are examined and compared with prototype and physical model results. The model parameters are then adjusted until the desired agreement exists between the numerical model and known data. Experience has shown that minimal adjustment is required for this type of model which lends additional confidence in the veracity of the model results.

Model Verification

22. The numerical model used in this study was verified for existing conditions by comparing the results from the numerical model with data obtained from the previously verified physical model of Los Angeles and Long Beach Harbors.⁴ Physical model tidal circulation data were readily available of sufficient quality and quantity for a typical spring tide with a 7.1-ft diurnal range. Tide gage locations and velocity stations for existing conditions in the physical model are shown in Figure 6. Tidal surface elevation data were available at 13 locations and velocity data were available from 7 ranges (22 stations) for the complete tidal cycle. Mosaic photographs showing surface current patterns also were available at hourly intervals. The 7.1-ft diurnal spring tide was applied along the seaward boundaries of the numerical grid. Results were compared with physical model data, and parameters in the numerical model were adjusted to bring numerical model

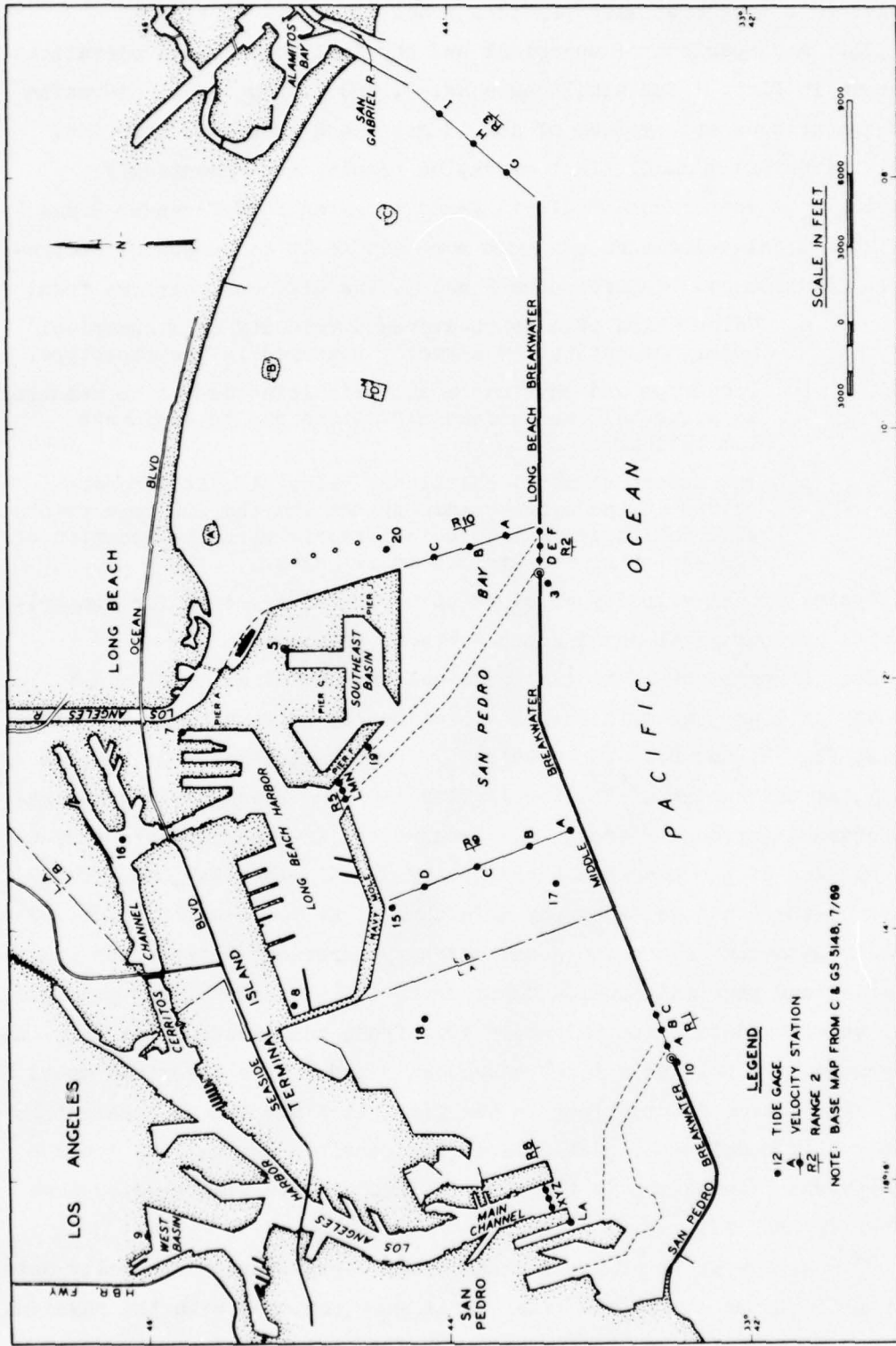


Figure 6. Gage locations for circulation study

results into agreement with physical model results.

23. A comparison of numerical and physical model tidal elevations is shown in Plate 1 for tidal gages LA, 3, and 5. The tidal elevation data comparisons are typical of all 13 gages and show that numerical model and physical model tidal elevation results are essentially identical. A comparison of all 13 gages is given in References 3 and 4.

24. Tidal velocities are much more difficult to adequately reproduce. As discussed in References 2 and 3, the difficulty arises from:

- a. Calculation of a depth-averaged velocity in a numerical model, an entity not directly measured in the prototype.
- b. Prototype and physical model velocities cannot be measured as accurately as surface elevations due to equipment limitations.
- c. The numerical model calculates velocities at discrete points in the hydrodynamic system and the discrete points will not in general coincide exactly with the location of the prototype or physical model gages.

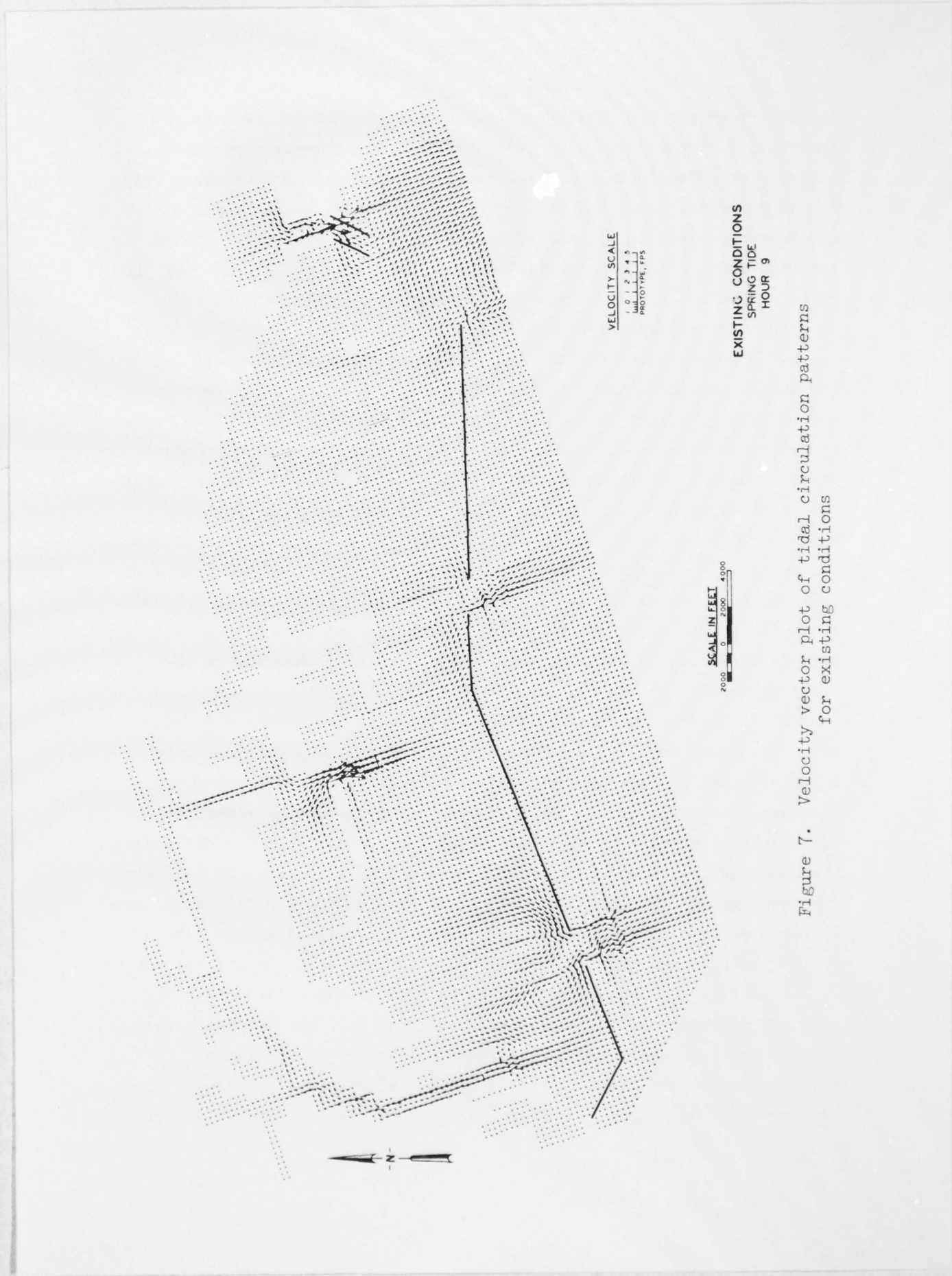
The physical model velocity at midpoint depth was selected for comparison with the numerical model depth-averaged velocities.

25. Comparisons of typical physical and numerical model tidal velocity data are shown in Plates 2-5 at hourly intervals for velocity sta 1B, 2E, 3H, and 8Y. These velocity stations are located, respectively, at the center of the Los Angeles and Long Beach Harbors navigation channel entrances through the breakwater, at the midpoint between the east end of the Long Beach breakwater and Alamitos Bay, and in the center of the Los Angeles Harbor main channel at Reservation Point. The velocity data comparison shows satisfactory agreement between the numerical model and physical model. Considering the accuracy of the physical model velocity data² (approximately ± 0.2 fps), the agreement is particularly good. As pointed out in References 3 and 4, the numerical model data exhibit some fluctuations in the flow which are not as apparent in the physical model data, particularly for Cerritos Channel stations. The apparent fluctuation in the numerical model data will be discussed further in PART III.

26. Vector plots of the instantaneous depth-averaged velocity data at specific times during the tidal cycle were compared with the physical

model surface current patterns. As discussed in References 3 and 4, the results of the comparison indicated that the overall circulation patterns observed in the physical model were reproduced reasonably well in the numerical model and the major gyres observed in the physical model were present in the numerical model velocity data and extended over essentially the same spatial region. However, the strength of the gyres generally appeared lower in the numerical model results. The apparent differences between the numerical and physical model results may be associated with variation in the strength of the gyre between the surface strength and the average strength over the water depth or, more likely, the fact that these gyres probably take 3 or 4 tidal cycles (based on physical model observations) to develop fully to a steady-state condition. A typical velocity vector plot of hour 9 in the tidal cycle for existing conditions is shown in Figure 7. At hour 9, the large gyre in the outer harbor east of Angel's Gate was near the maximum strength. At the scale shown in Figure 7, the large gyre was apparently confined to a relatively small area, however plotted at the larger scale shown in Figure 8, the actual extent of the spatial area covered by the gyre is more clearly shown as being similar to that observed in the physical model.

27. In the model verification process, the volumetric flow rates were calculated across the various velocity ranges and compared with physical model apparent discharge data. The physical model apparent discharge was calculated using the total current velocity regardless of its orientation relative to the velocity range. In the numerical model, the adjusted discharge across a range was calculated using the velocity component normal to the range. The apparent and adjusted discharges are illustrated in Figure 9. It was necessary to use the apparent discharge for the model flow rate since model velocity data were identified only as ebb or flood. The adjusted discharge will always be less than the apparent discharge by the cosine of the angle θ . The two discharges will be equal if the current velocities are normal to the range. Range 8 is across a rectangular channel and should have relatively close agreement between the apparent and adjusted discharge. The volumetric



VELOCITY SCALE
 0 1 2 3
 PROTOTYPE, FPS

SCALE IN FEET
 0 2000 4000

EXISTING CONDITIONS
 SPRING TIDE
 HOUR 9

Figure 7. Velocity vector plot of tidal circulation patterns for existing conditions

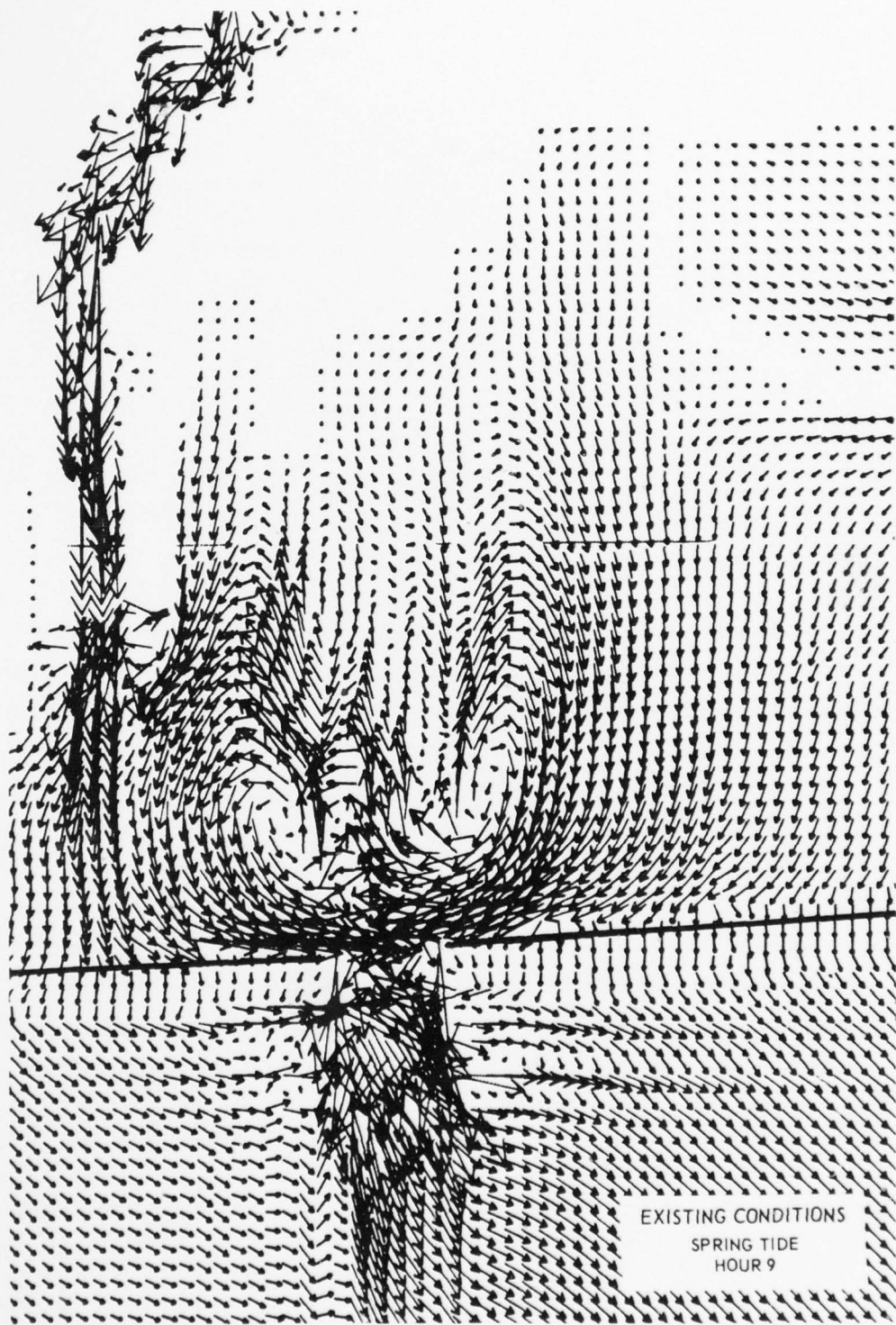
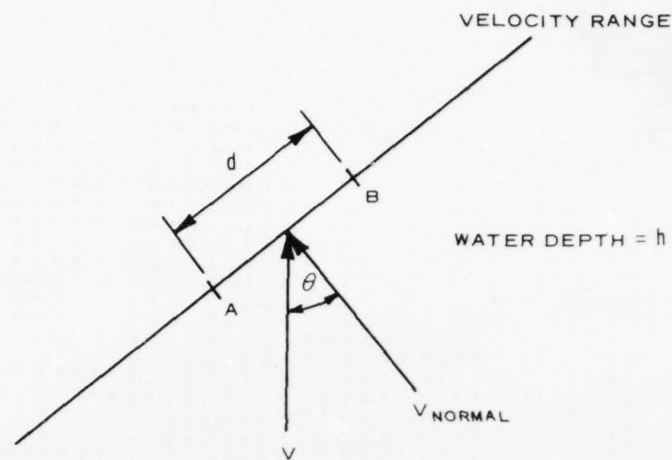


Figure 8. Large-scale vector plot of tidal circulation patterns east of Angel's Gate for existing conditions



$$\text{APPARENT FLOW ACROSS AB} = (V) (d) (h)$$

$$\text{ADJUSTED FLOW ACROSS AB} = (V_{\text{NORMAL}}) (d) (h)$$

Figure 9. Apparent and adjusted discharge

flow rates may be integrated over a tidal cycle to obtain a net flow through a range. In the tidal verification process during the previous numerical studies reported in References 3 and 4, the hourly volumetric flow data were used to compute net flows from the adjusted discharge data. Because of the apparent presence of oscillations in the numerical model velocity data, the adjusted net discharge rates for ranges 1-3 and 8 were recomputed using discharge data from each time-step (45 sec) in lieu of the hourly values and are compared with physical model apparent net discharge rates in Table 1. At range 8 agreement between the physical model apparent net discharge and the numerical model adjusted net discharge is excellent as should be expected. At the other three ranges, the numerical model adjusted net discharge is less than the physical model apparent net discharge due to:

- a. Differences in calculating apparent and adjusted net discharges.
- b. Use of physical model velocity data at hourly intervals and numerical model velocity data at each time-step.
- c. Use of velocity data from all numerical model grid cells in a range versus use of selected stations over a range in the physical model.

The prototype adjusted net discharge² at range 1 was $310(10^6)$ cu ft which compares well with the numerical model results [$351(10^6)$] and indicates the magnitude of the differences which can be expected between apparent and adjusted net discharge data.

28. The net flows shown in Table 1 represent small differences, particularly for range 8, between large flood and ebb flows and should be used only to indicate flow trends.

29. Numerical model data also were compared with physical model data in the previous study for a proposed harbor expansion plan which included a large landfill (approximately 750 acres) in Los Angeles Harbor and an oil terminal and associated landfill of approximately 300 acres in Long Beach Harbor. Results from the comparison were similar to the data comparison for existing conditions and are discussed in References 3 and 4. Results of the comparison of numerical and physical model data indicate that the numerical model is capable of being used to predict changes in tidal circulation patterns and will apparently yield essentially the same results as those which would be obtained from the physical model for large-scale circulation features.

PART III: TIDAL CIRCULATION RESULTS

Oil Terminal Configurations

30. The proposed phase I 60-acre landfill configuration and outer harbor oil terminal are shown in Figure 10. An alternate configuration with a modified landfill (decreased westward extension) is shown in Figure 11. The location of the oil terminal breakwater and dredged channels was the same for each configuration. The Corps of Engineers dredging project and associated landfill in Los Angeles Harbor were included with each configuration tested and are shown in Figure 2.

Results

31. Numerical model tidal elevation data for phase I and the alternate landfill configuration are compared with the tidal elevations for existing conditions in Plates 6-18 for the 13 tide gage locations shown in Figure 6. The tidal elevation data show that tidal elevations were not affected by either of the harbor expansion plans.

32. The velocities calculated at ranges 1, 2, 3, 5, 8, 9, and 10 (Figure 6) are shown in Plates 19-40 for each hour. Generally, tidal velocities are similar for both phase I and phase I with modified landfill at all ranges. At sta 1B (Angel's Gate), tidal velocities (Plate 20) with phase I were slightly smaller at the maximum ebb near hour 0, at maximum flood near hour 4, and at maximum ebb near hour 12 but were similar on the second flood near hour 19. Ebb and flood velocities shown in Plate 23 at sta 2E (Queen's Gate) follow a similar trend, but the maximum velocity for the second flood for phase I was slightly lower. At sta 3H (east end of the harbor) tidal velocities shown in Plate 26, with and without phase I, were similar and with no consistent trend in the slight variation present. Differences in the tidal velocity were more apparent at range 8 near Reservation Point in the Los Angeles main channel, as shown in Plate 32. Maximum ebb velocities with phase I were lower by 0.15 fps and 0.16 fps near hour 0 and hour 12, respectively.

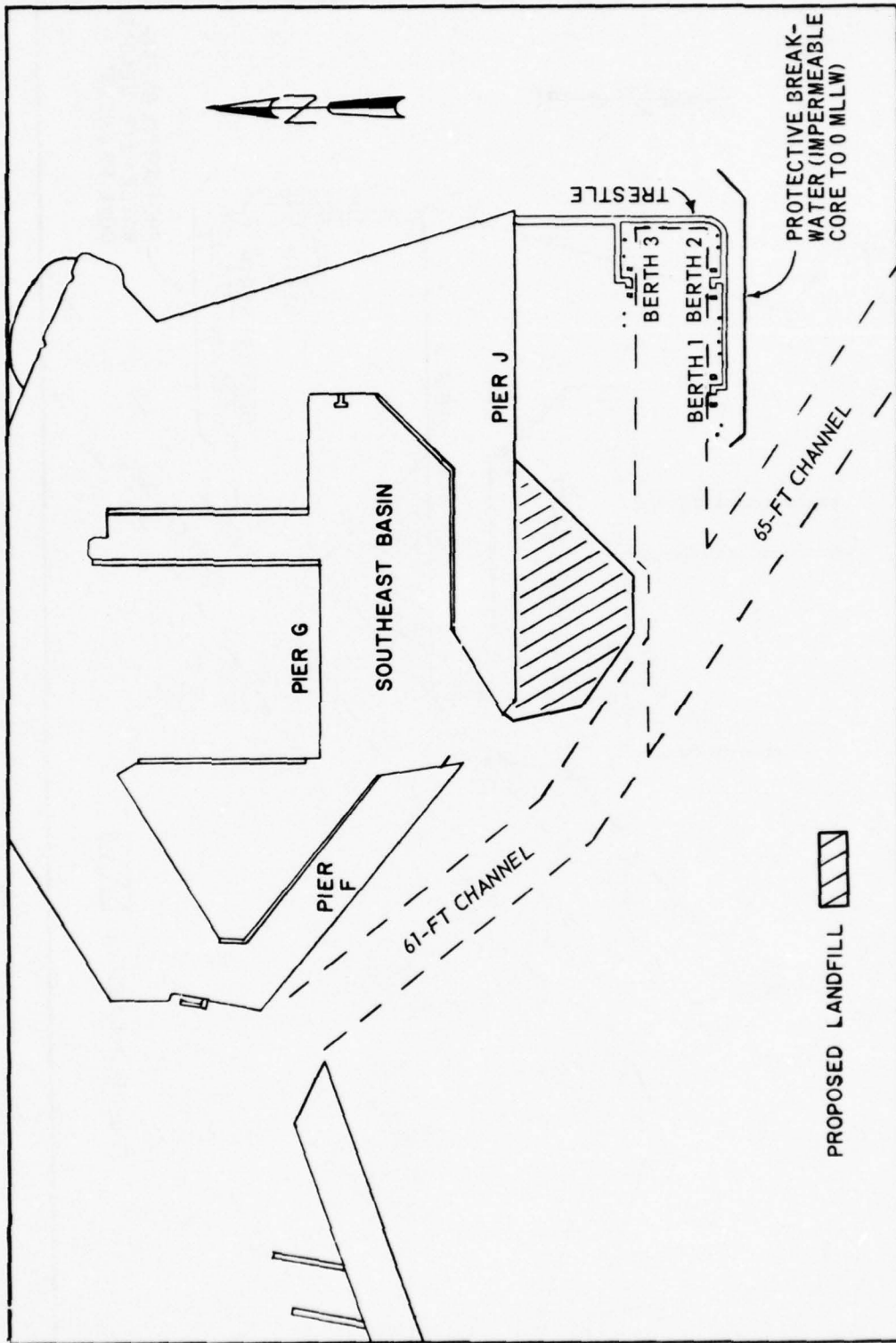


Figure 10. Proposed phase I 60-acre landfill and oil terminal configuration

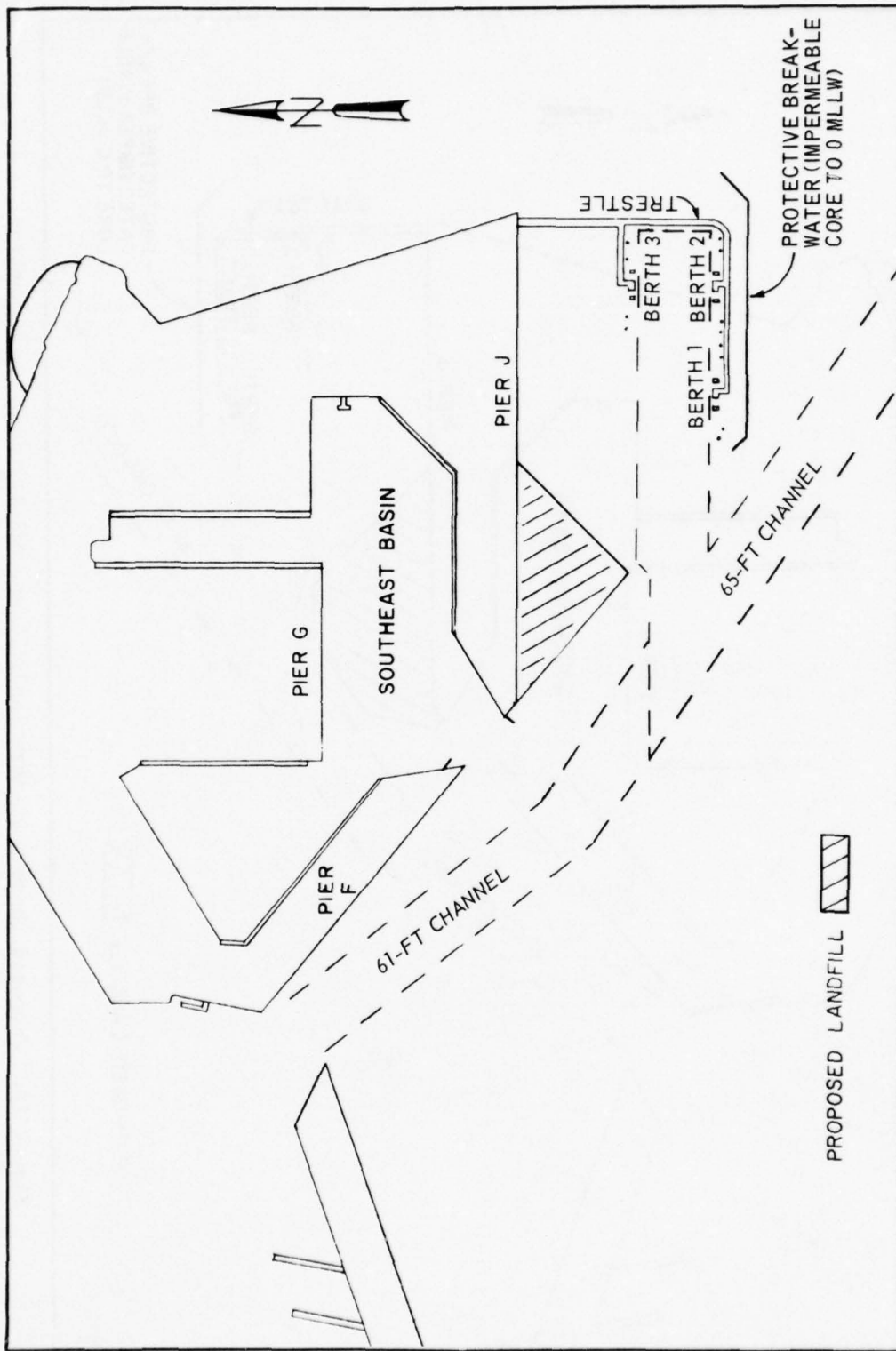


Figure 11. Proposed phase I modified landfill and oil terminal configuration

Flood velocities were lower by 0.11 fps and 0.07 fps near hour 5 and hour 19, respectively.

33. To properly interpret the velocity results, the effect on velocity of the changed depths in the dredged areas should be recognized. The relation between depth-averaged velocity and volumetric flow rate is not the same for existing conditions and for the modifications. Depth-averaged velocity for the modifications may be less than that for existing conditions even though the volumetric flow rate through the finite difference cell is greater. This results from the greater depths in the dredged areas of the modifications. This qualification is limited to the dredged regions and affects only velocity ranges 1, 2, 8, and 10, and vector plots of overall tidal circulation in the dredged portion of the bay. For example, while velocities at ranges 1 and 2 are observed to be lower than those for existing conditions, there is an increase in the volumetric flow rate through this range for the modifications considered. At range 8, the increase in depth is approximately 28 percent while the average velocity near maximum ebb and flood was approximately 23 percent less.

34. Vector plots showing the calculated circulation patterns for the phase I plan and the phase I plan with modified landfill are presented in a separate volume as Appendix B to this report. Vector plots indicating changes in circulation patterns from existing conditions and between the phase I plan and phase I with a modified landfill also are presented in Appendix B. The vector plots show the changes that occurred primarily near the proposed Outer Harbor oil terminal, in Cerritos Channel and near the Los Angeles landfill. Differences between the phase I plan and the phase I plan with the modified landfill were not appreciable except near the local pier J areas. Examples of the velocity plots and the difference plots are shown in Figures 12-15 for hour 18 for the phase I plan and the modified phase I plan.

35. The hourly average volumetric flow rates across ranges 1-3 and 8 are shown in Plates 41-44 for existing conditions, the phase I plan, and the phase I plan with modified landfill. The average volumetric flow rate is the average of the calculated flow rates at each time-step



Figure 12. Velocity vector plot of tidal circulation patterns for phase I at hour 18



Figure 13. Tidal circulation velocity difference between phase I and existing conditions at hour 18



Figure 14. Velocity vector plot of tidal circulation patterns for phase I with a modified landfill at hour 18



Figure 15. Tidal circulation velocity difference between phase I with a modified landfill and existing conditions

summed over one-hour intervals centered about the hour. The hourly average was used due to oscillations which were present in the numerical discharge data and the data from the time-step at the hour may not accurately represent discharge over an hourly interval. Two additional ranges, 8A and 8B in Cerritos Channel, were used in the numerical study to accurately define the new flow in the channel. The positive direction of flow and location of range 8A (near the ARCO oil terminal in Long Beach Harbor) and range 8B (near the center of Cerritos Channel) are shown in Figure 16. Volumetric discharge data for the two ranges are shown in Plates 45 and 46.

36. Specific observations made from the comparison of average volumetric flow data for existing conditions, the phase I plan, and the phase I plan with the modified landfill were:

- a. Volumetric flow rates for the phase I plan and for the phase I plan with modified landfill are essentially identical for all ranges.
- b. The flow rate at range 1 was similar at maximum ebb and flood flow for phase I and existing conditions except for a slight decrease (approximately 1 percent) at the second ebb near hour 19.
- c. A decrease occurred at range 2 for the phase I plan for maximum ebb and flood flows (maximum decrease of 10 percent near hour 0).
- d. Maximum flows at range 3 are similar for phase I and existing conditions with little difference in maximum discharges.
- e. Volumetric flow data for ranges 8, 8A, and 8B are similar for existing conditions, phase I, and phase I with modified landfill with the maximum ebb and flood flows for range 8 generally slightly higher for the proposed plan.

37. Net flows over a tidal cycle across the volumetric flow ranges are given in Table 2. Net flow into the harbor is increased by approximately 5 percent and 11 percent at ranges 1 and 2, respectively, with phase I. Net ebb flow at range 3 is increased by approximately 3 percent. The net westward flow through Cerritos Channel was essentially identical for existing conditions and for the expansion plans. At ranges 8, 8A, and 8B, the net flows represent small differences between large total ebb and flood flows, and variations between the flow into

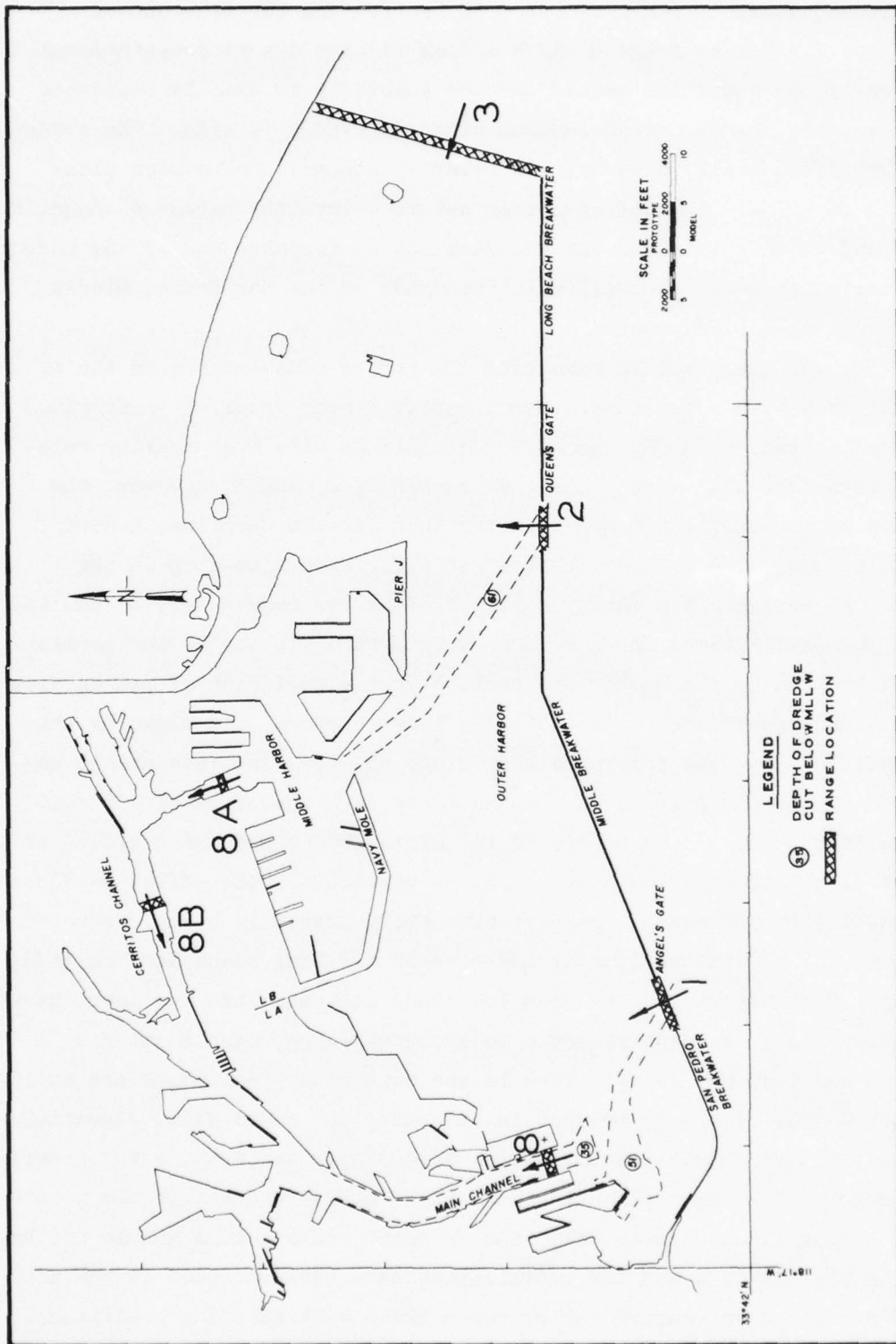


Figure 16. Range locations and directions of flow

Cerritos Channel at range 8A (31×10^6 cu ft) and the flow out of Cerritos Channel at range 8 (43×10^6 cu ft) are due to computational errors of the numerical method and the inability to exactly reproduce the variable channel cross section with a 300-ft grid size. The error is considered small, however, and relative comparisons between plans should be valid. The difference in net flow into the harbor at Angel's Gate and Queen's Gate and the net flow out at the east end of the harbor is attributed to a net outflow in the voids of the San Pedro, Middle, and Long Beach breakwaters.⁵

36. As discussed in paragraph 33, strong oscillations in the volumetric flow with a period of approximately 1 hour occurred in Cerritos Channel at ranges 8, 8A, and 8B. Oscillations of a much smaller relative magnitude also were present at ranges 1, 2, and 3; however, the period of the oscillation was shorter than for the Cerritos Channel oscillations. The volumetric flow rates for each time-step in the numerical analysis are shown in Plates 47-52 for ranges 1-3, 8, 8A, and 8B. The oscillations in flow rates were apparently due to the geometric configuration of the harbor and could have a significant effect on flow conditions and residence times in the inner harbors. As shown by the volumetric flow data for range 8 in Plate 50, the flow rate at the entrance to the Los Angeles main channel may vary approximately 20×10^3 cfs within 33 min. The source of the oscillations and their effect on tidal circulation in the harbor and, in particular, the effect on flushing of Cerritos Channel, are part of a study presently being conducted in connection with the general Los Angeles and Long Beach Harbors model study. Preliminary results from the study indicate that the inner harbor area has a resonant response to incident energy near a one-hour period and that the oscillations in the numerical tidal model are excited by low levels of energy present in the numerical model tidal elevation input boundary data. The low energy levels near one hour in the numerical model tidal input elevation data would not be present in the prototype spring tide; consequently, the resonant oscillations should not be excited by the tide and the oscillations have been smoothed in the net flow data used to compare the proposed plans with existing conditions.

However, oscillations near a one-hour period are known to occur in the inner harbor area and are probably excited by lower level incident prototype wave energy present at periods near one hour. Results of the Cerritos Channel oscillation study are being conducted separately and will be published during the latter half of this calendar year.⁹

PART IV: CONCLUSIONS

39. The proposed landfill configuration and channel dredging plans for Long Beach Harbor and Los Angeles Harbor considered in this study resulted in minor overall changes to the net tidal circulation relative to that for existing conditions. Although tidal currents were significantly affected near the oil terminal and in the dredged areas, the net discharges through the harbor entrances and through Cerritos Channel were not significantly changed. Specific changes in tidal circulation produced by the proposed expansion plans were:

- a. Small increase in net flow into the harbor through Angel's Gate and Queen's Gate.
- b. Small increase in net flow out of the harbor at the east end.
- c. Negligible effect on the net westward flow in Cerritos Channel, but with a decrease in maximum velocities in the dredged area due to the increased channel depth.
- d. Little effect on tidal circulation patterns east of Queen's Gate except near the proposed oil terminal.
- e. Little effect on tidal circulation in the Los Angeles and Long Beach outer harbor area except near the proposed Long Beach outer harbor oil terminal and Los Angeles landfill.

REFERENCES

1. Pickett, E. B., Durham, D. L., and McAnally, W. H., Jr., "Los Angeles and Long Beach Harbors Model Study; Prototype Data Acquisition and Observations," Technical Report H-75-4, Report 1, Jun 1975, U. S. Army Engineer Waterways Experiment Station, CE, Vicksburg, Miss.
2. McAnally, W. H., Jr., "Los Angeles and Long Beach Harbors Model Study; Tidal Verification and Base Circulation Tests," Technical Report H-75-4, Report 5, Sep 1975, U. S. Army Engineer Waterways Experiment Station, CE, Vicksburg, Miss.
3. Raney, D. C., "Numerical Analysis of Tidal Circulation for Long Beach Harbor; Existing Conditions and Alternate Plans for Pier J Completion and Tanker Terminal Study," Miscellaneous Paper H-76-4, Report 1, Sep 1976, U. S. Army Engineer Waterways Experiment Station, CE, Vicksburg, Miss.
4. _____, "Numerical Analysis of Tidal Circulation for Long Beach Harbor; Existing Conditions and Alternate Plans for Pier J Completion and Tanker Terminal Study with -82 Ft Channel," Miscellaneous Paper H-76-4, Report 3, Sep 1976, U. S. Army Engineer Waterways Experiment Station, CE, Vicksburg, Miss.
5. Leendertse, J. J., "Aspects of a Computational Model for Long Period Water Wave Propagation," RM-5294-pr, May 1967, Rand Corporation, Santa Monica, Calif.
6. Butler, H. Lee, "Numerical Simulation of Tidal Hydrodynamics; Great Egg Harbor and Corson Inlets, New Jersey," Technical Report H-78-11, Jun 1978, U. S. Army Engineer Waterways Experiment Station, CE, Vicksburg, Miss.
7. Butler, H. Lee, "Numerical Simulation of the Coos Bay - South Slough Complex," Technical Report H-78-22, Dec 1978, U. S. Army Engineer Waterways Experiment Station, CE, Vicksburg, Miss.
8. Butler, H. Lee, "Coastal Flood Simulation in Stretched Coordinates," Proceedings, 16th International Conference on Coastal Engineering, Aug 1978.
9. Raney, D. C. and Whalin, R. W., "Los Angeles and Long Beach Harbors Model Study; Analysis of Cerritos Channel Oscillation," Technical Report (in preparation), U. S. Army Engineer Waterways Experiment Station, CE, Vicksburg, Miss.

Table 1
Net Discharge per Tidal Cycle for Existing Conditions

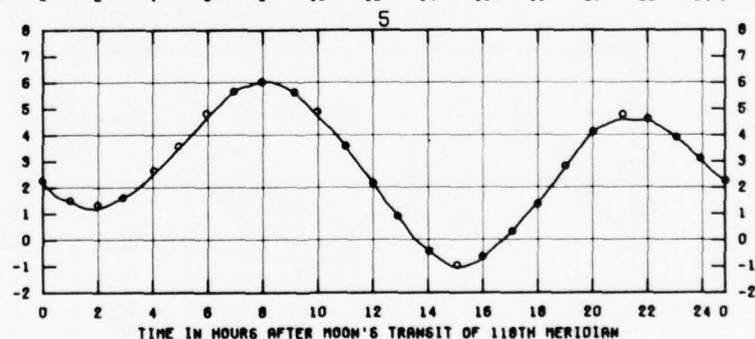
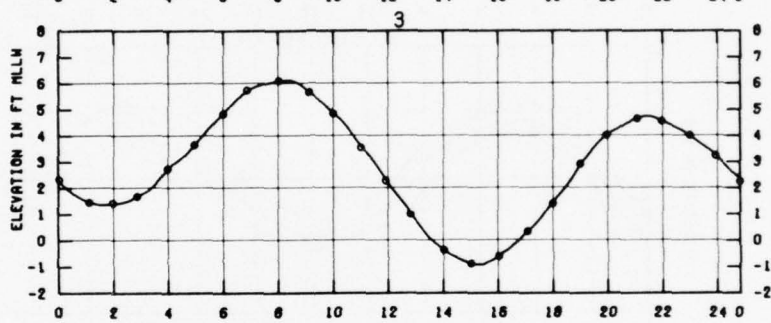
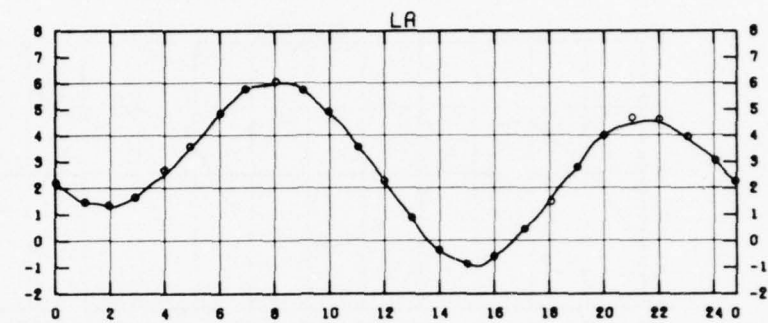
<u>Range</u>	<u>Prototype Apparent Net Discharge 10⁶ cu ft</u>	<u>Physical Model Apparent Net Discharge 10⁶ cu ft</u>	<u>Numerical Model Adjusted Net Discharge 10⁶ cu ft</u>
1	+310	+1230	+351
2	--	+ 520	+324
3	--	-1700	-478
8	-160	- 50	- 43

Note: A plus sign = net flood condition; a minus sign = net ebb condition. Numerical model adjusted net discharge calculated using volumetric flow data from each time-step.

Table 2
Numerical Model Adjusted Net Discharge
per Tidal Cycle, 10⁶ cu ft

	<u>Range</u>					
	<u>1</u>	<u>2</u>	<u>3</u>	<u>8</u>	<u>8A</u>	<u>8B</u>
Existing Conditions	351	324	-478	-43	31	33
Phase I	368	359	-495	-32	27	32
Phase I with modified landfill	368	364	-499	-32	27	32

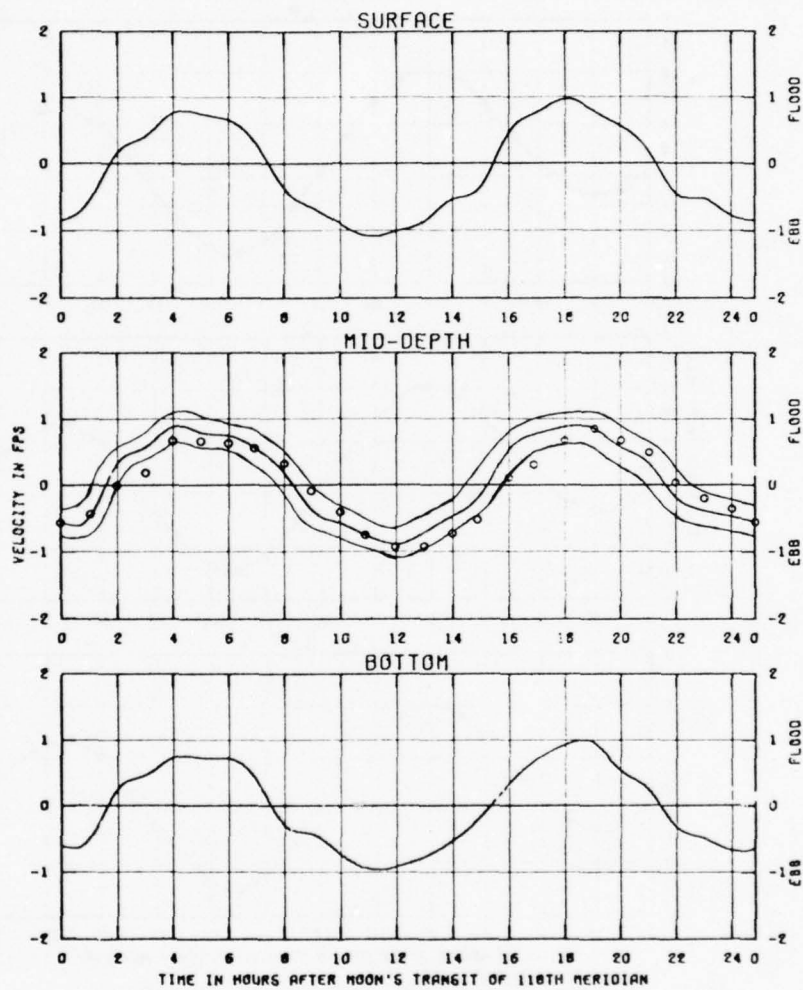
Note: A plus sign = net flood condition; a minus sign = net ebb condition. Net discharge calculated using volumetric flow data from each time-step.



TEST CONDITIONS
 TIDAL RANGE AT QUEENS DATE = 7.1 FT

LEGEND
 — PHYSICAL MODEL RESULTS
 ○ DEPTH-AVERAGED NUMERICAL MODEL RESULTS

TIDAL ELEVATIONS
 BASE TEST
 SPRING TIDE
 STATIONS
 LA, 3, AND 5

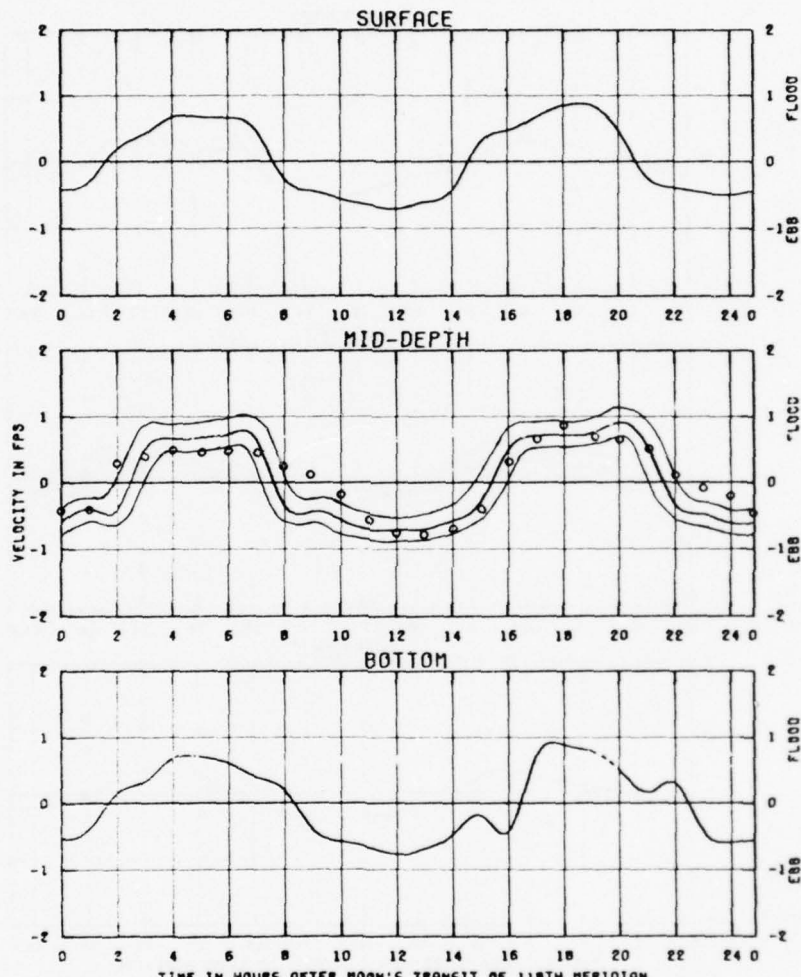


VELOCITIES
BASE TEST
SPRING TIDE
STATION
18

LEGEND

- PHYSICAL MODEL RESULTS
- DEPTH-AVERAGED NUMERICAL MODEL RESULTS

NOTE: ± 0.2 FPS PHYSICAL MODEL ACCURACY
LIMITS ARE SHOWN AT MIDDEPTH



TEST CONDITIONS
 TIDAL RANGE AT QUEENS DATE = 7.1 FT

LEGEND
 — PHYSICAL MODEL RESULTS
 ○ DEPTH-AVERAGED NUMERICAL MODEL RESULTS

VELOCITIES
 BASE TEST
 SPRING TIDE
 STATION
 2C

NOTE: ±0.2 FPS PHYSICAL MODEL ACCURACY
 LIMITS ARE SHOWN AT MIDDEPTH

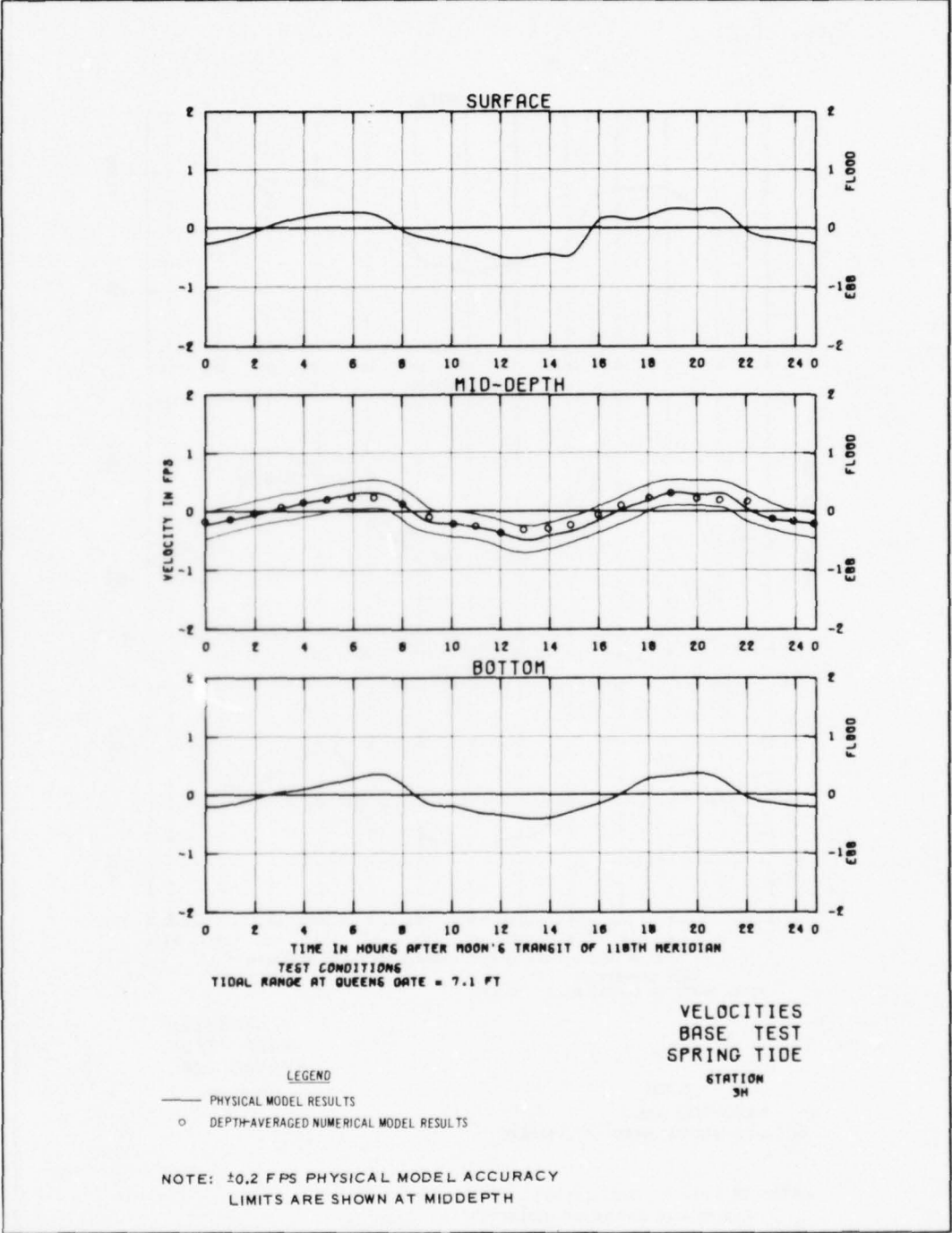
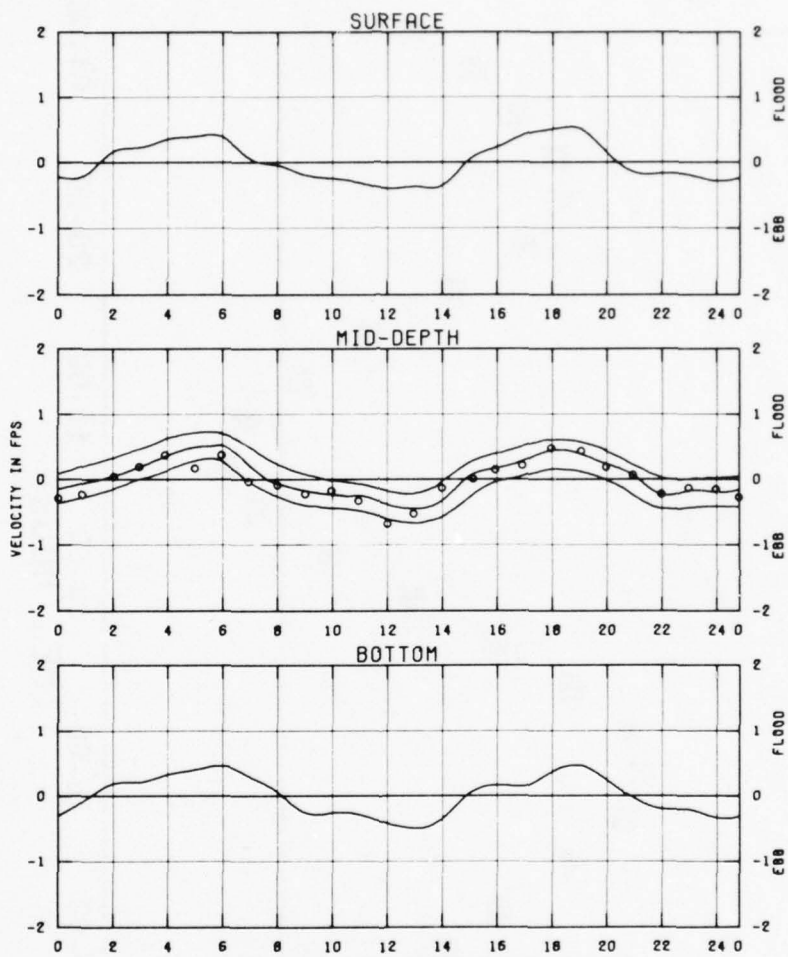


PLATE 4



TEST CONDITIONS
TIDAL RANGE AT QUEENS BAY = 7.1 FT

LEGEND
— PHYSICAL MODEL RESULTS
○ DEPTH-AVERAGED NUMERICAL MODEL RESULTS

NOTE: ± 0.2 FPS PHYSICAL MODEL ACCURACY
LIMITS ARE SHOWN AT MIDDEPTH

VELOCITIES
BASE TEST
SPRING TIDE
STATION
BY

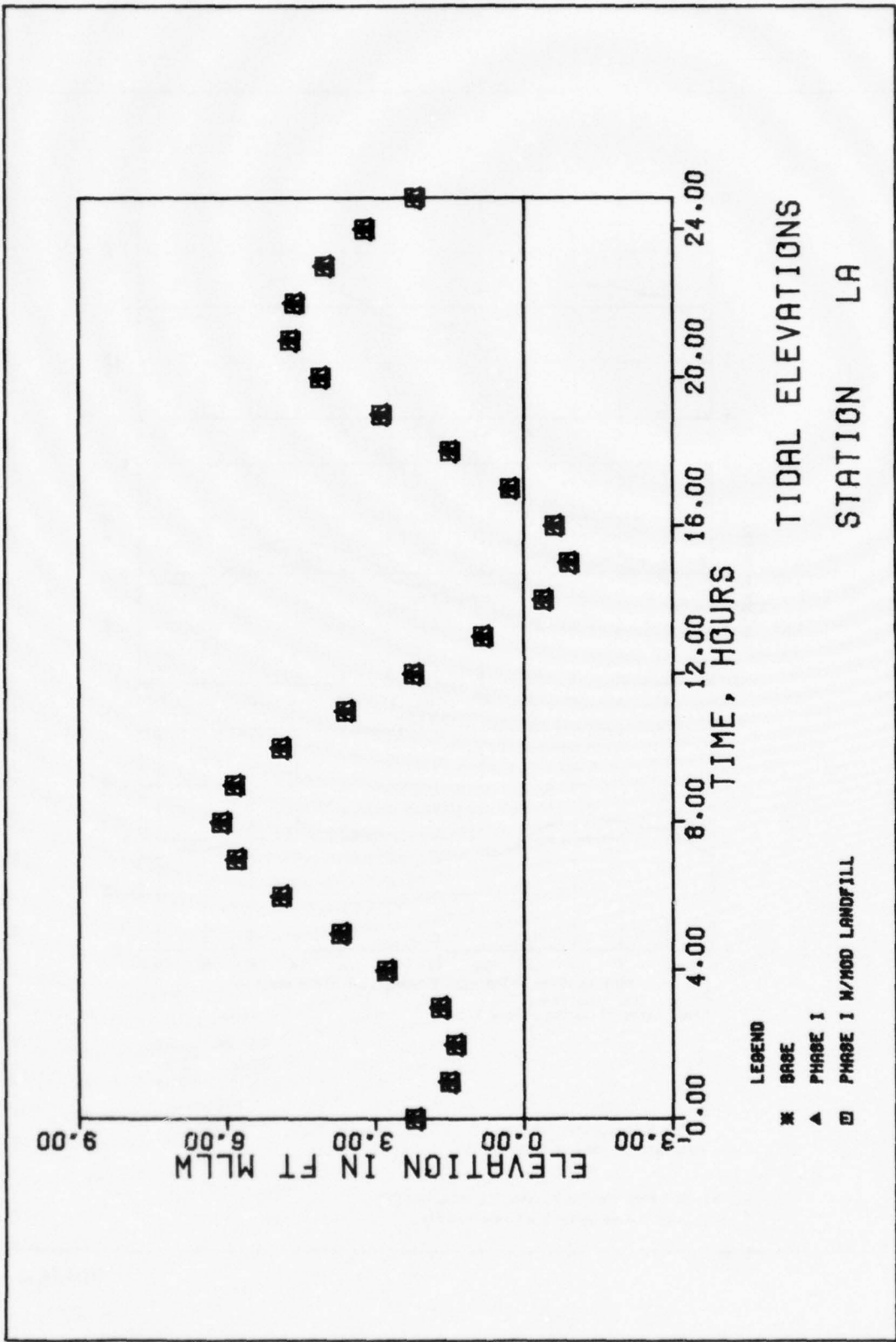


PLATE 6

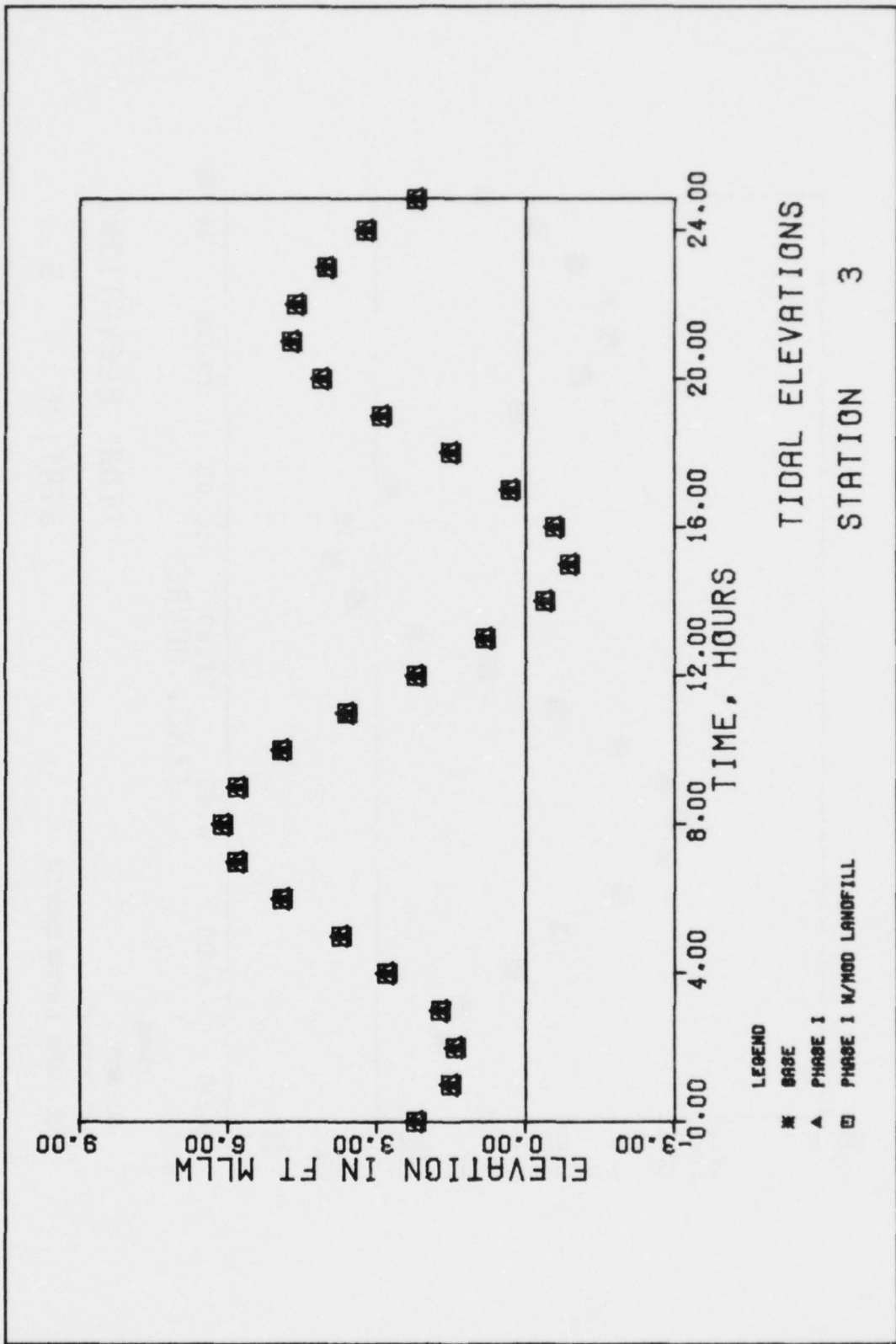


PLATE 7

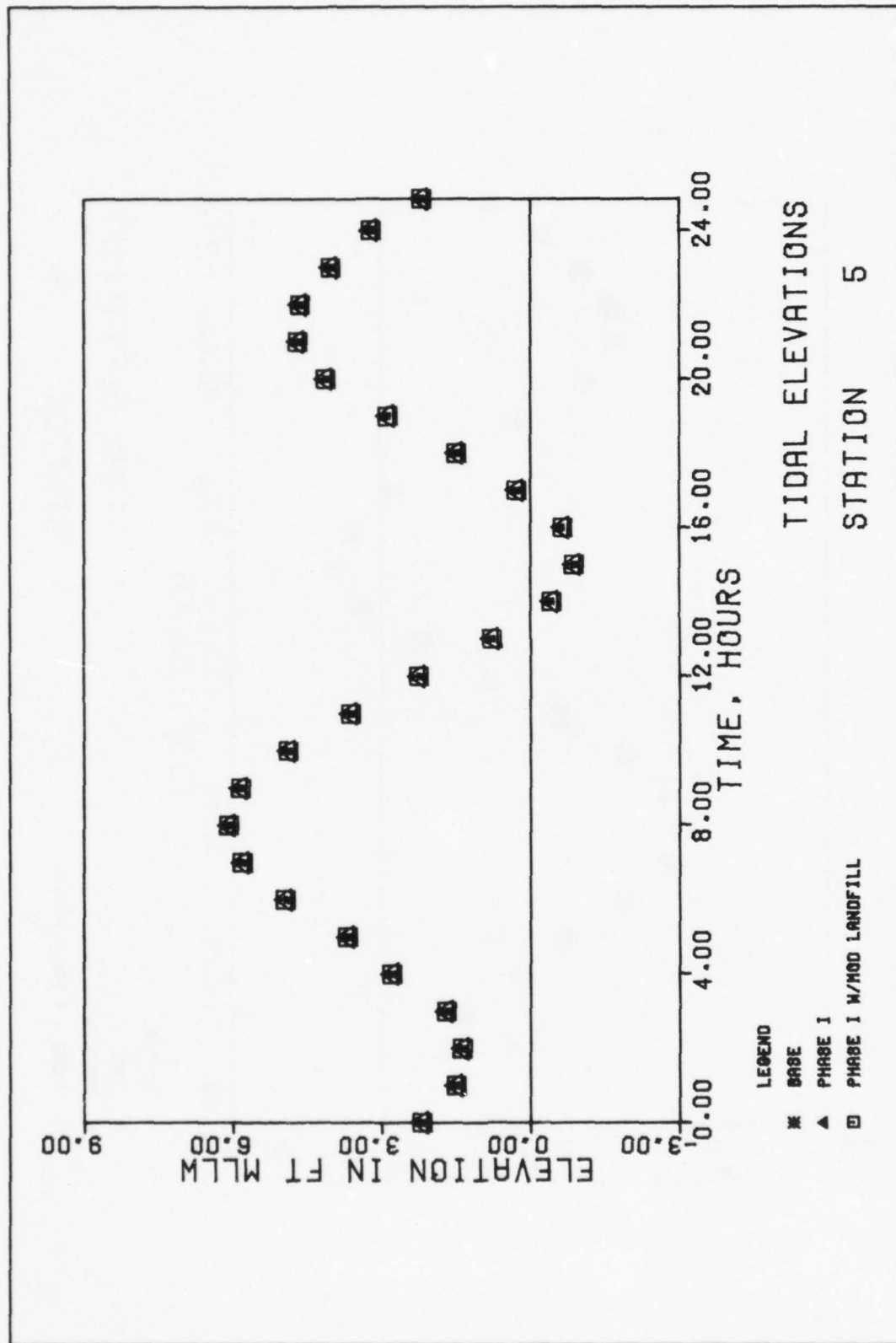
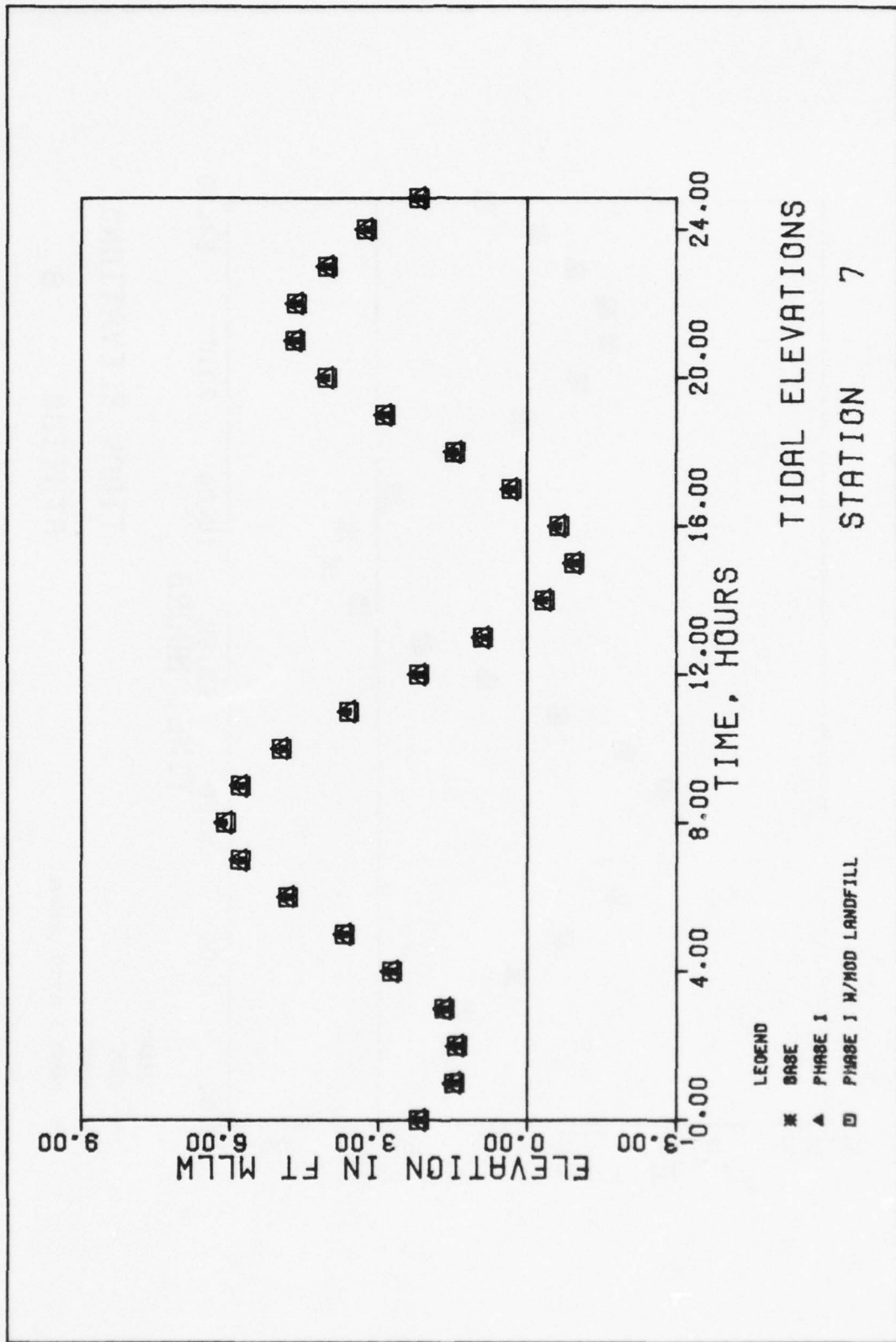


PLATE 8



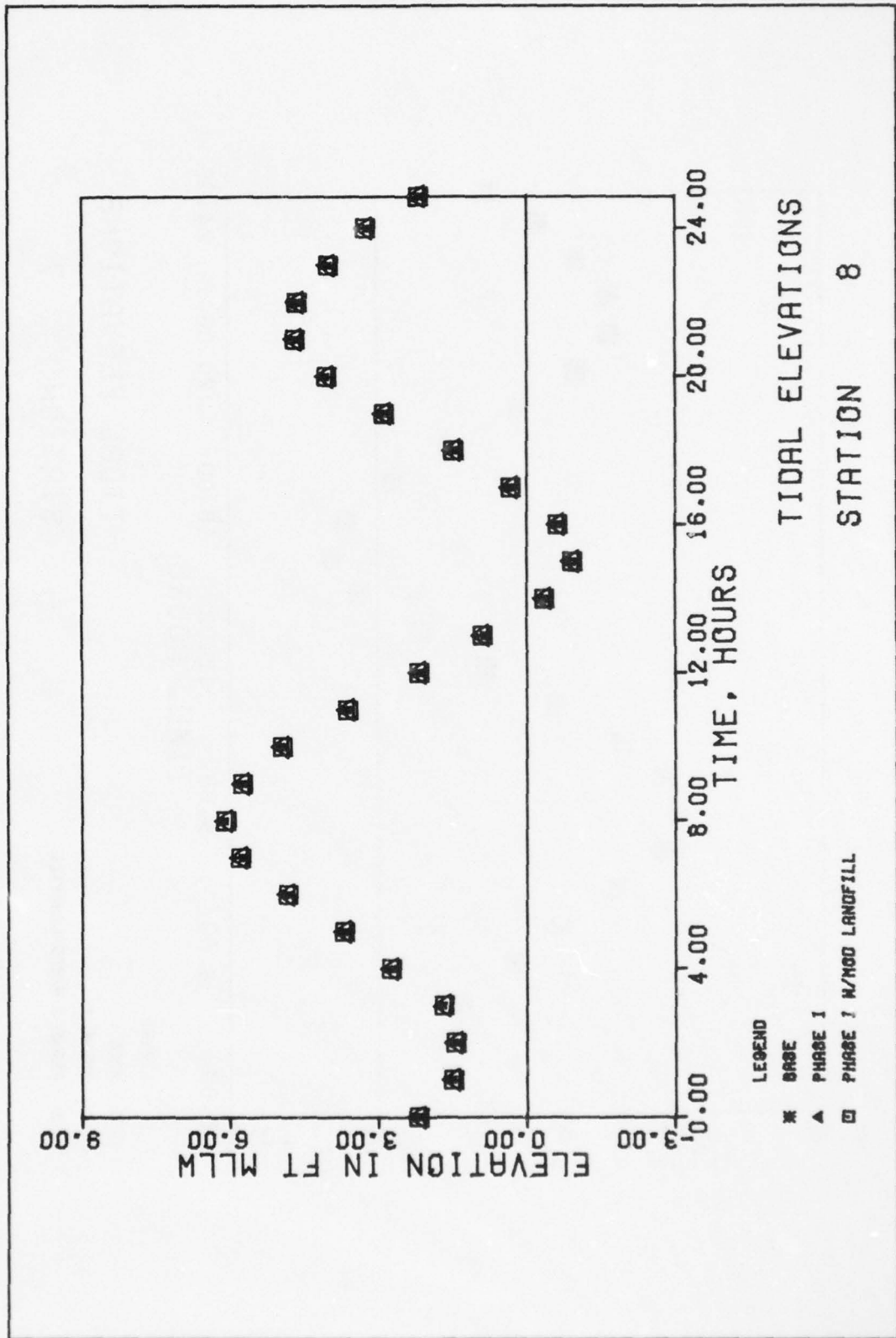
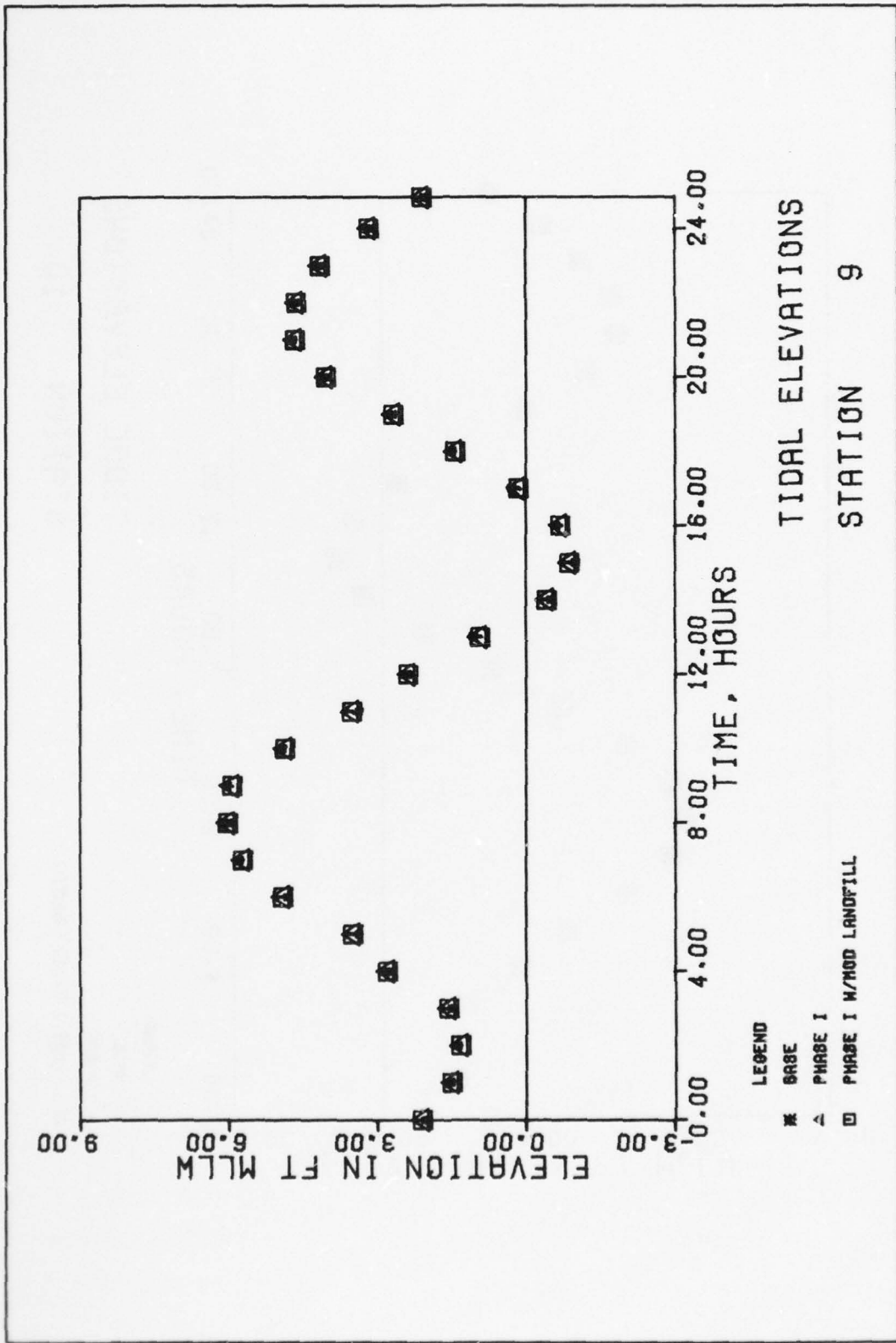


PLATE 10



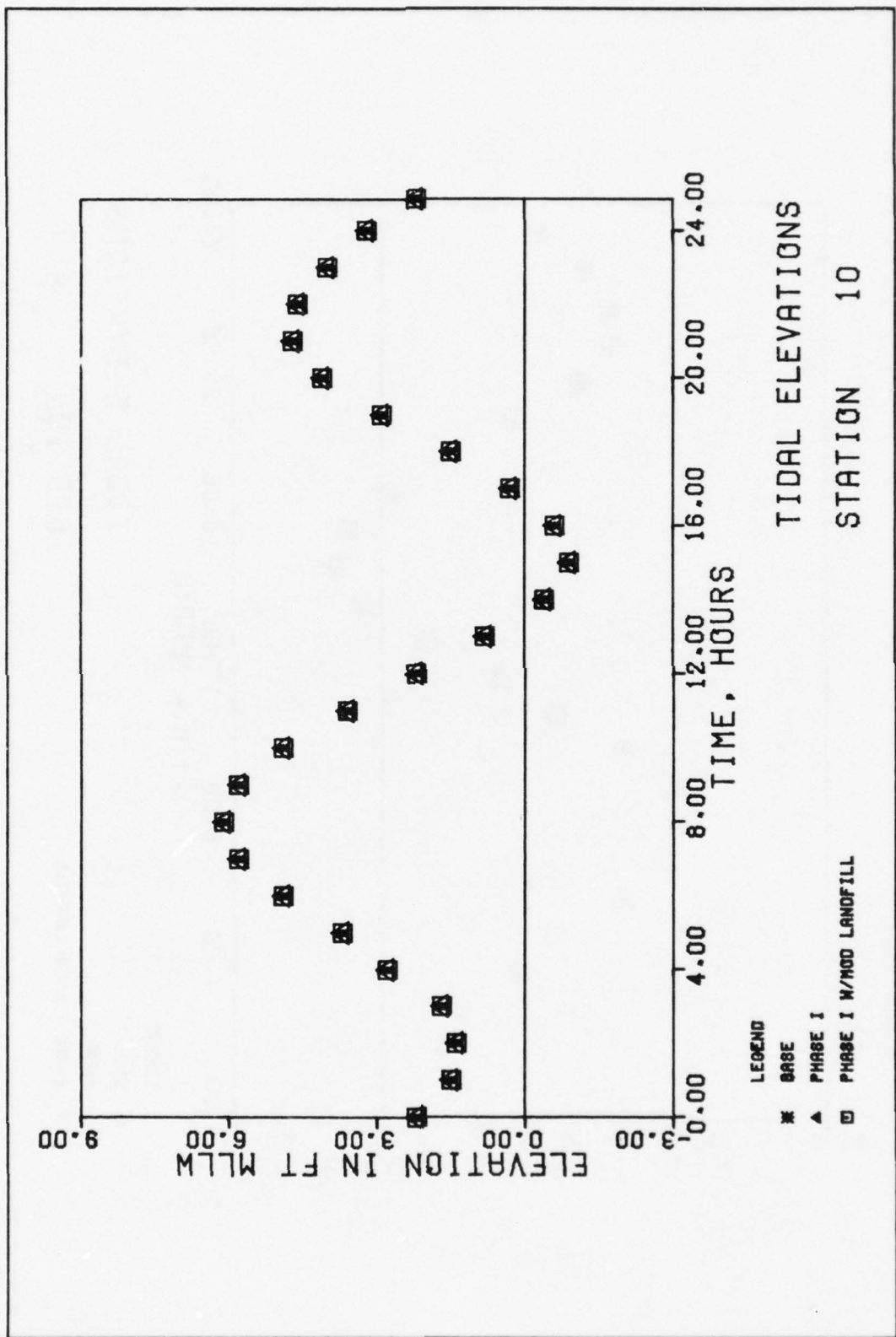


PLATE 12

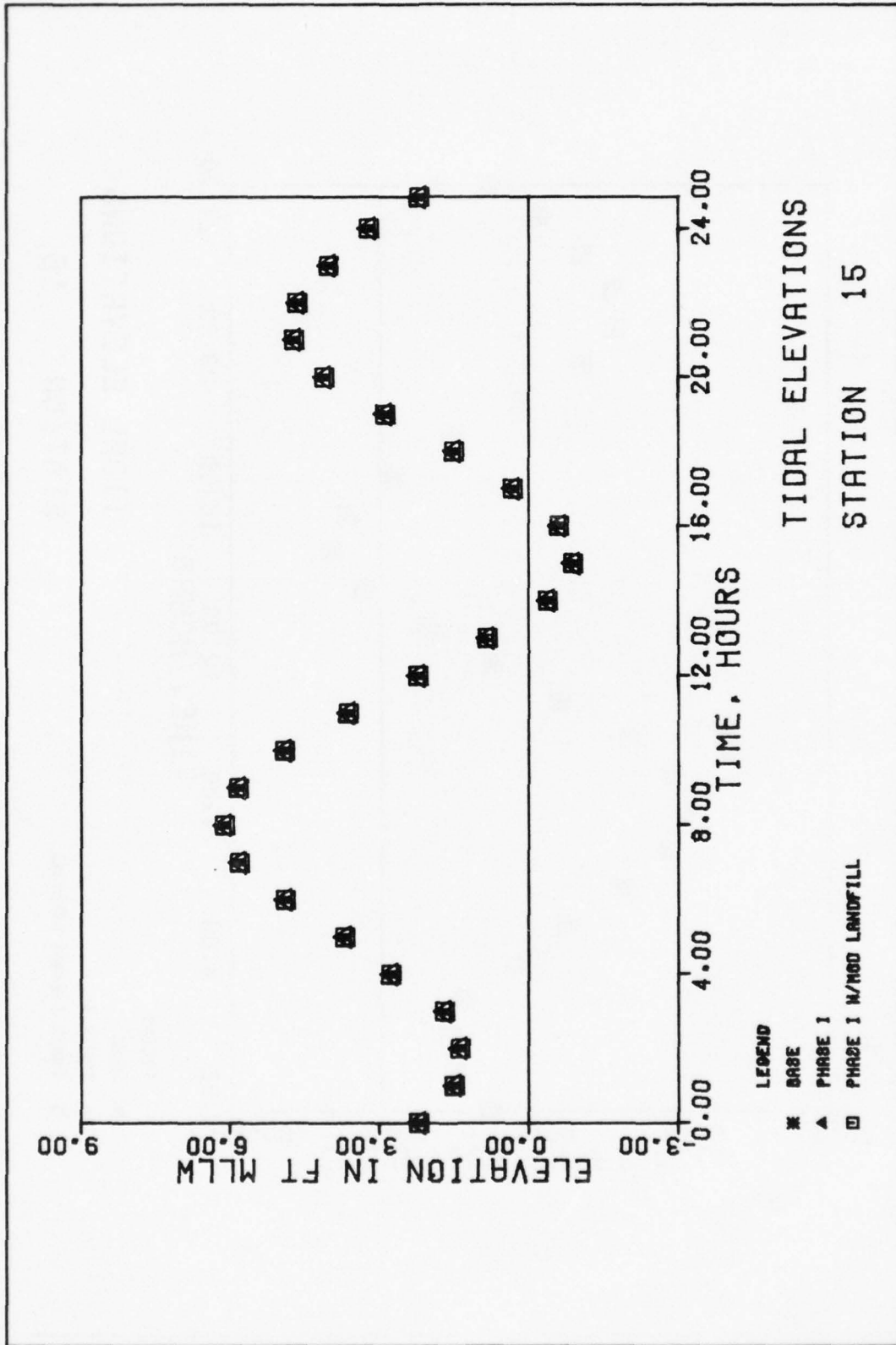


PLATE 13

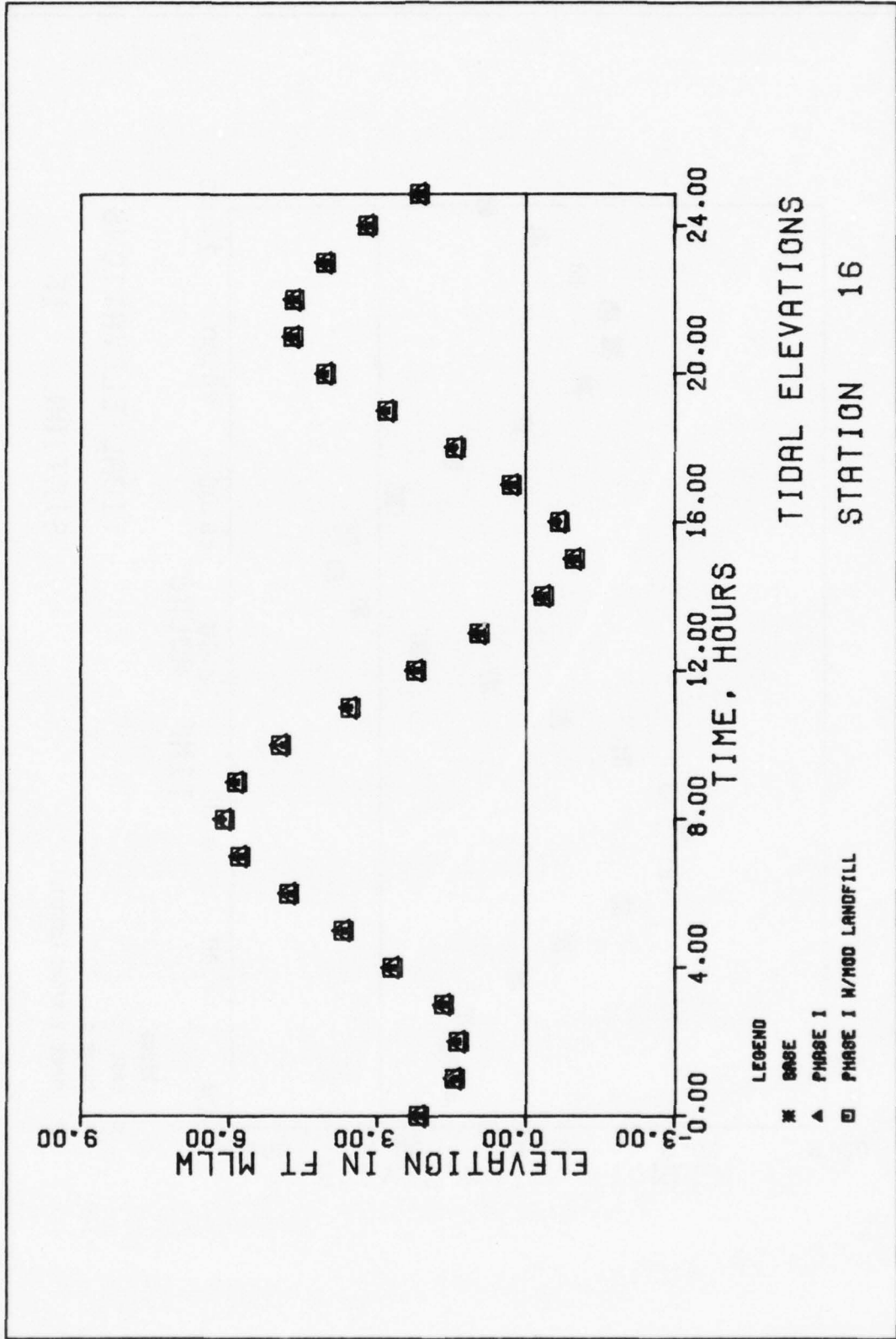


PLATE 14

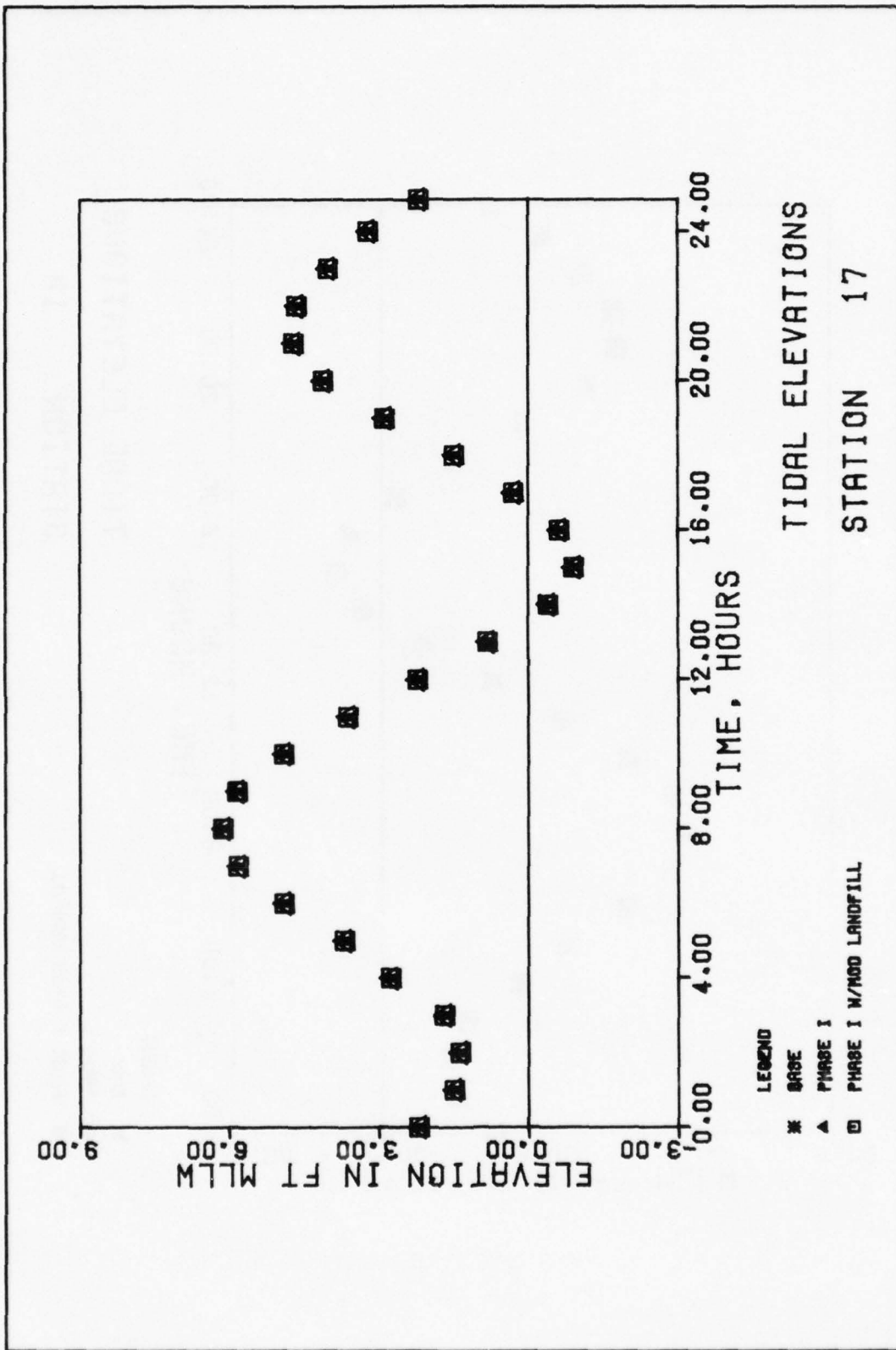


PLATE 15

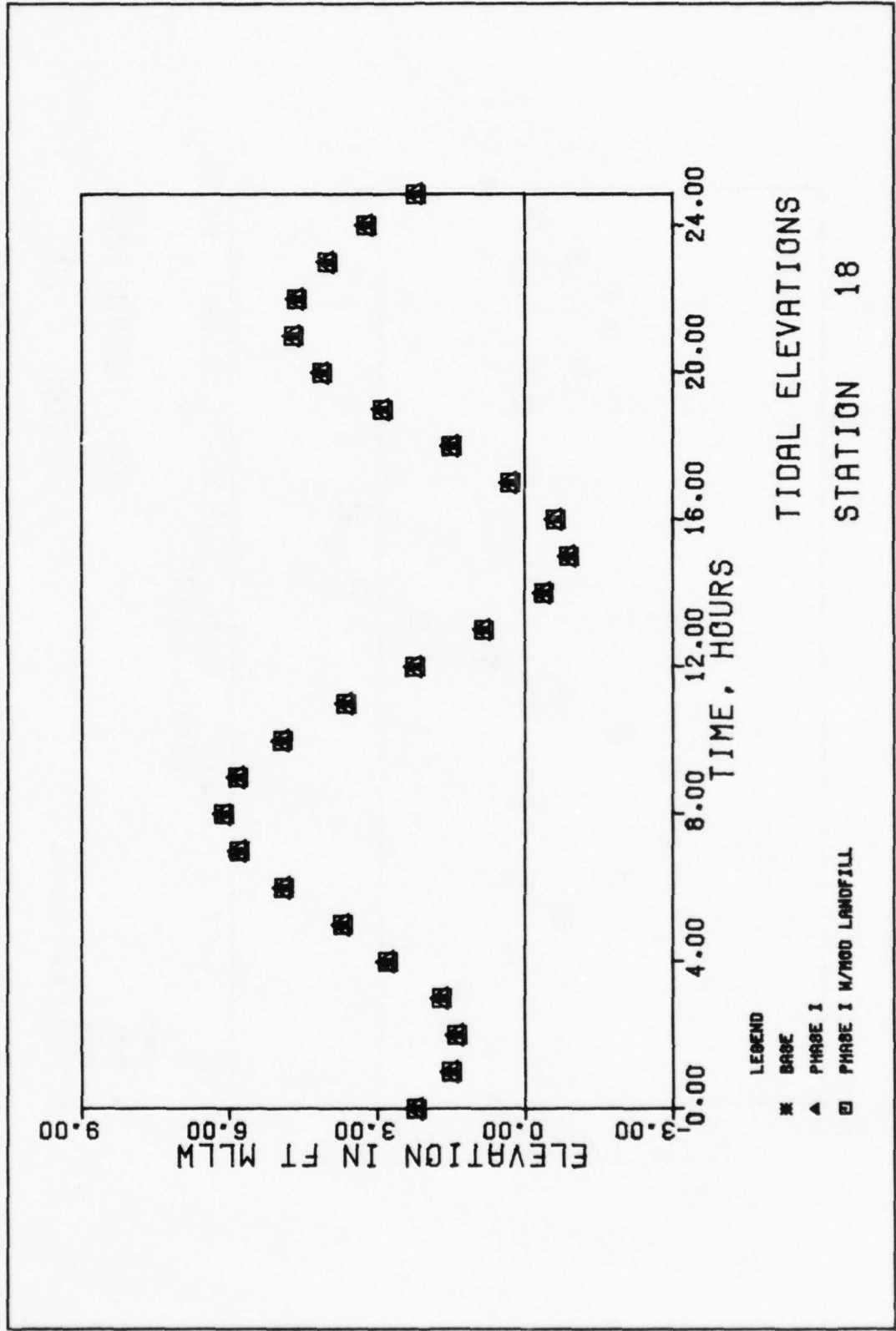


PLATE 16

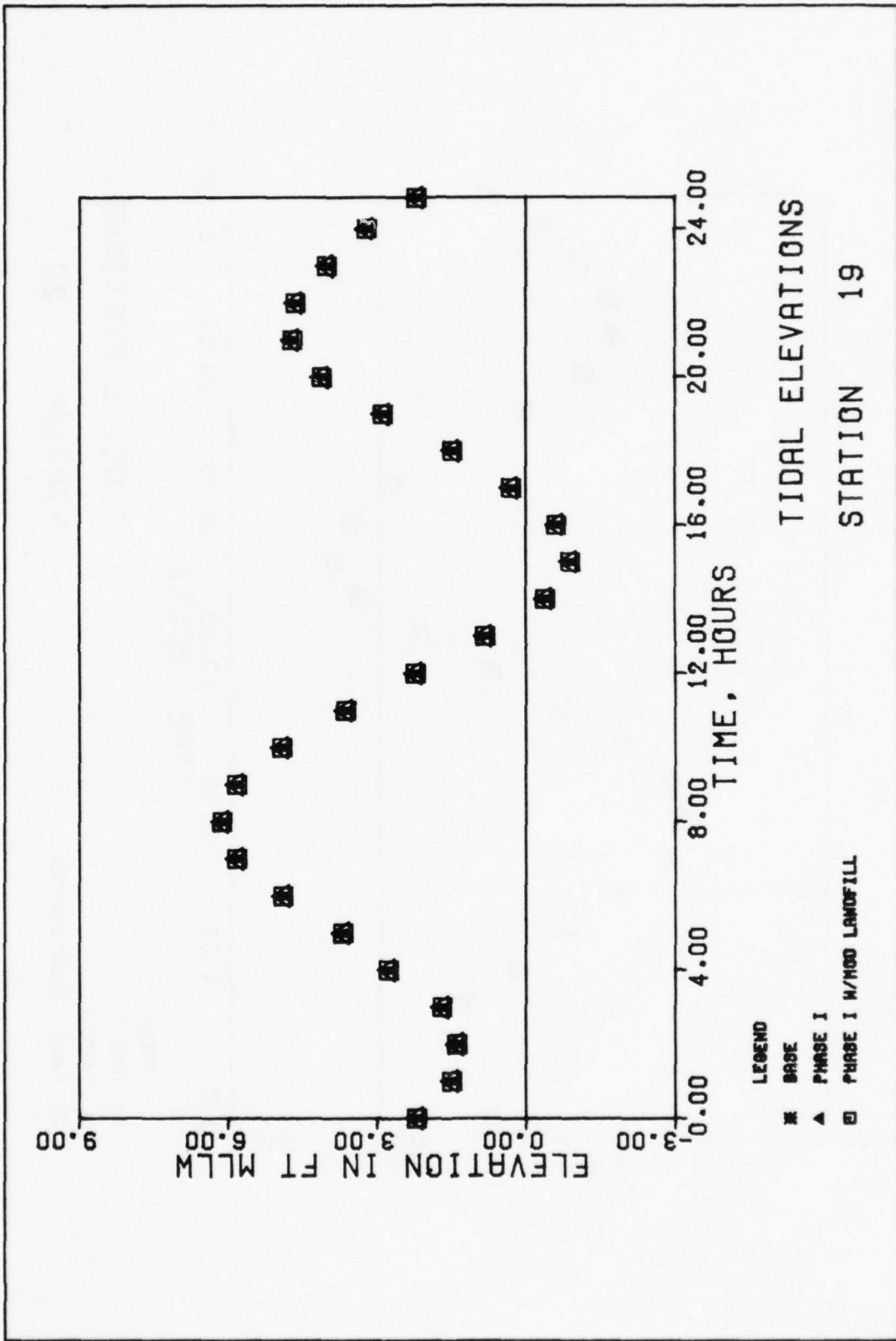


PLATE 17

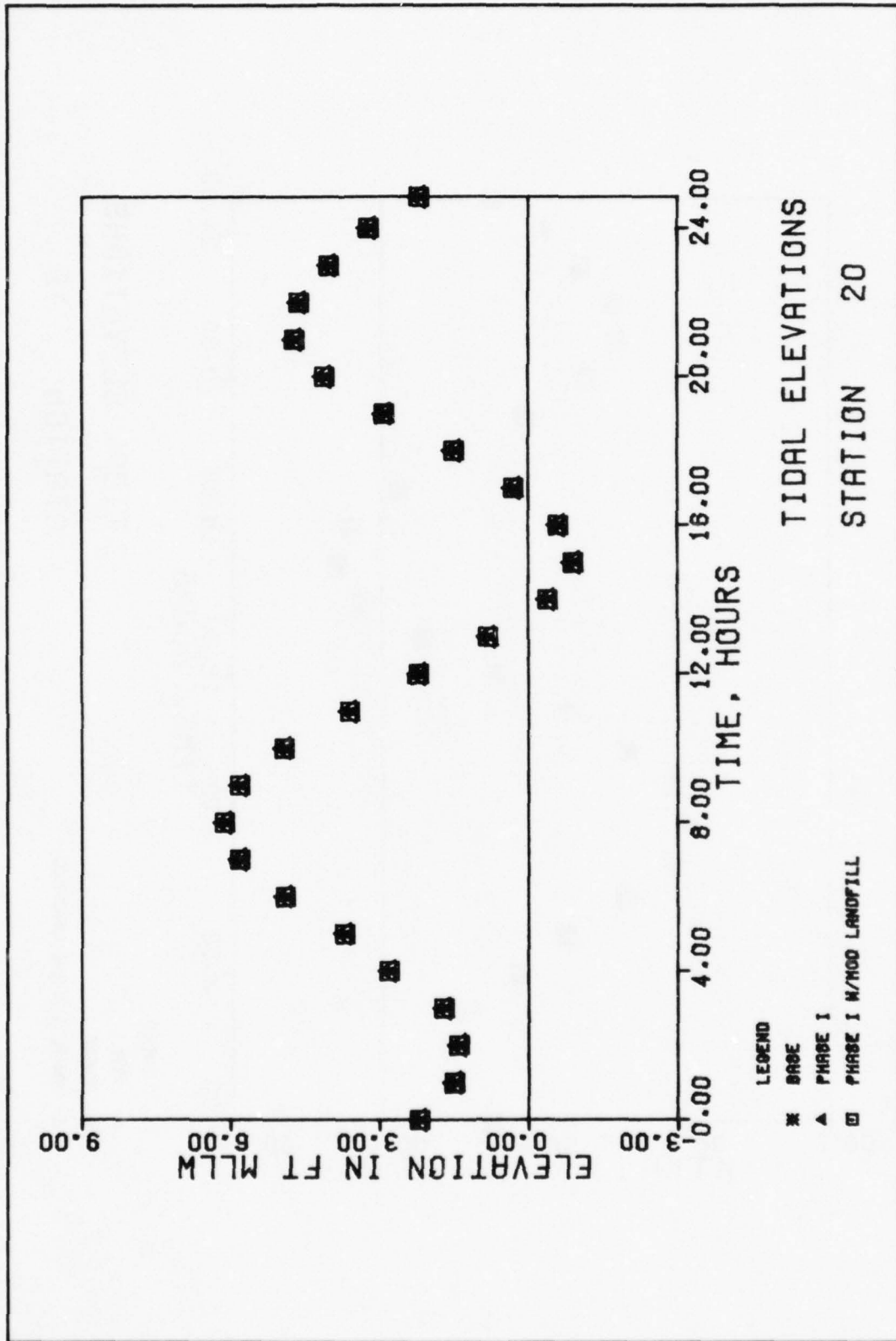
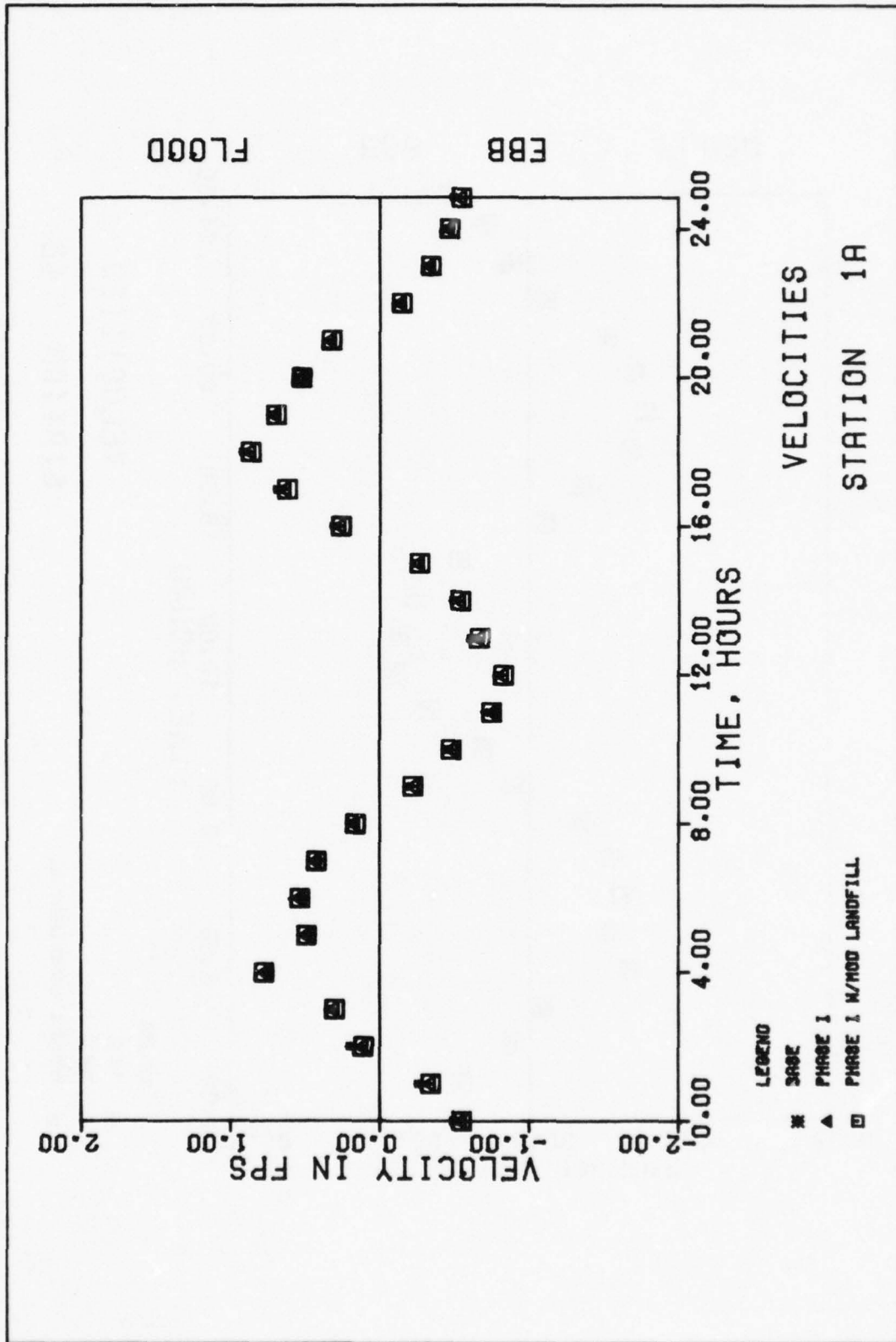


PLATE 18



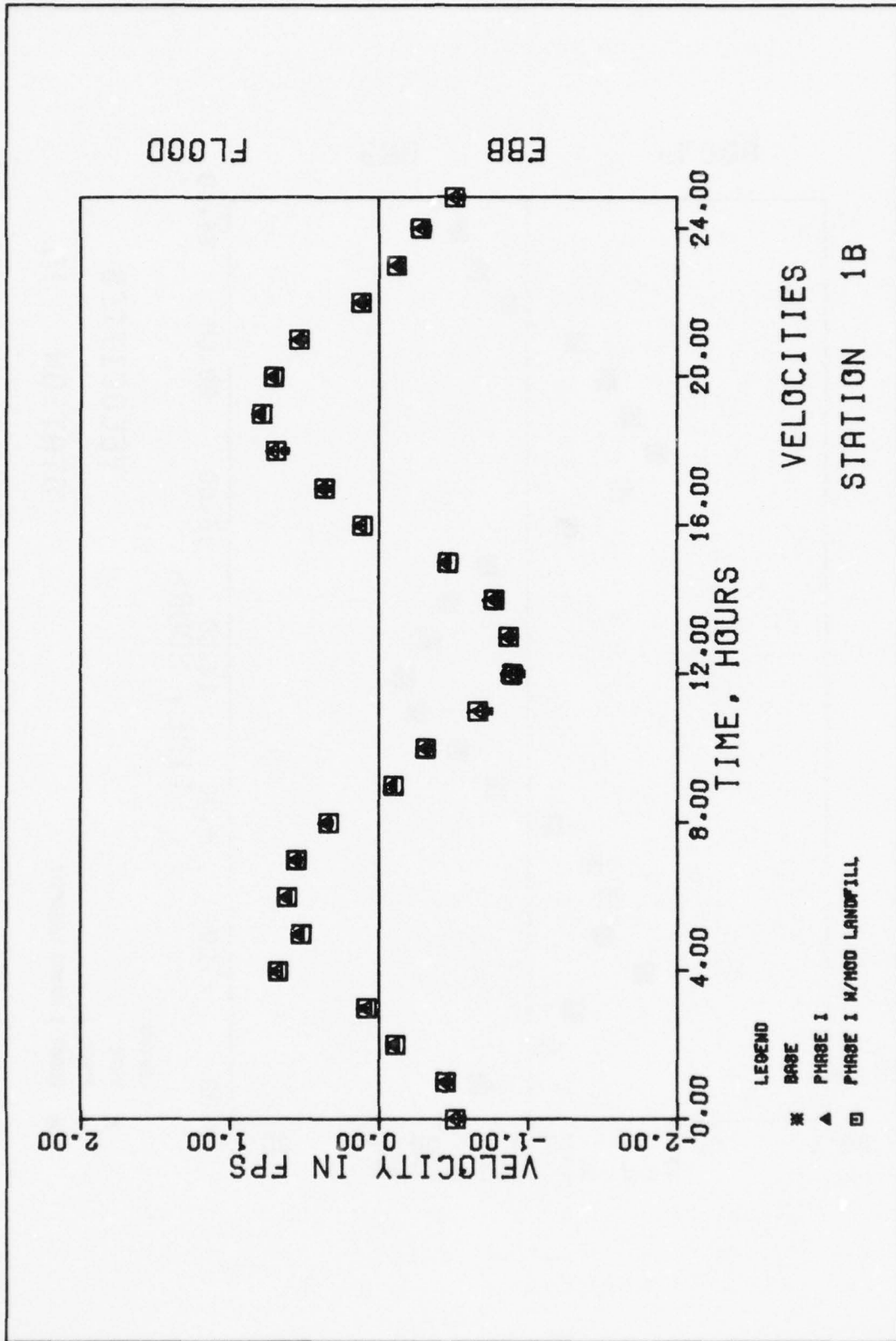


PLATE 20

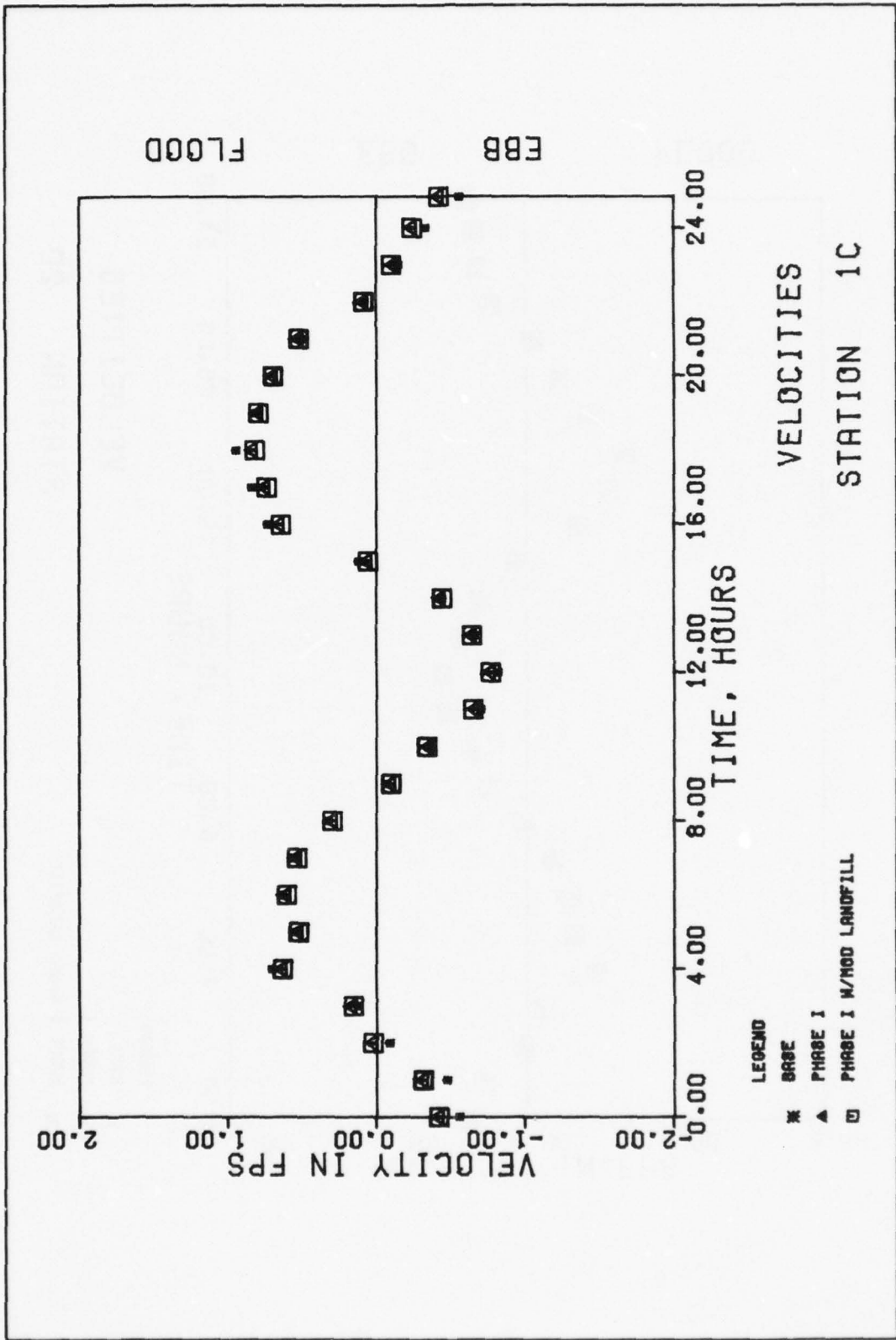


PLATE 21

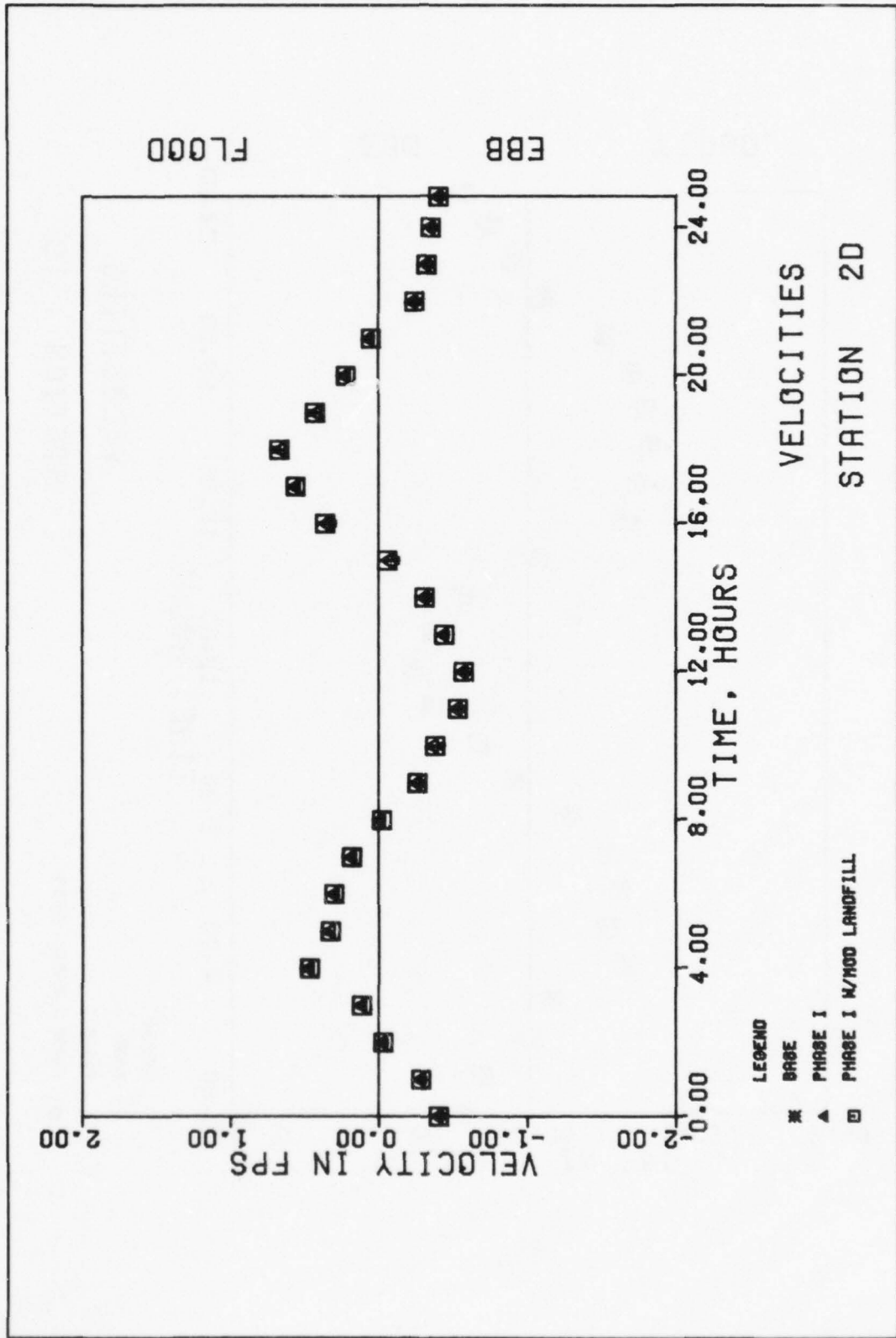
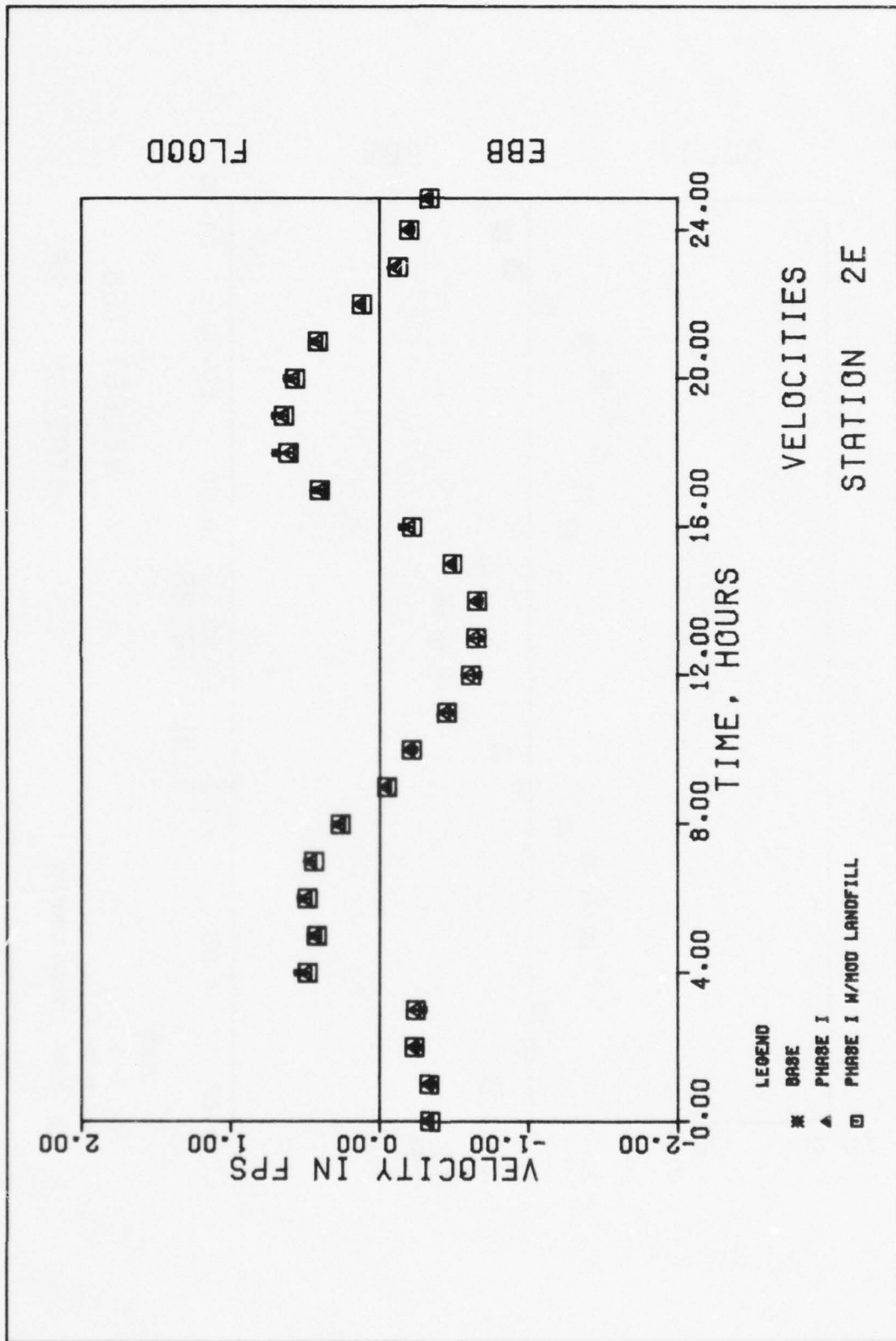


PLATE 22



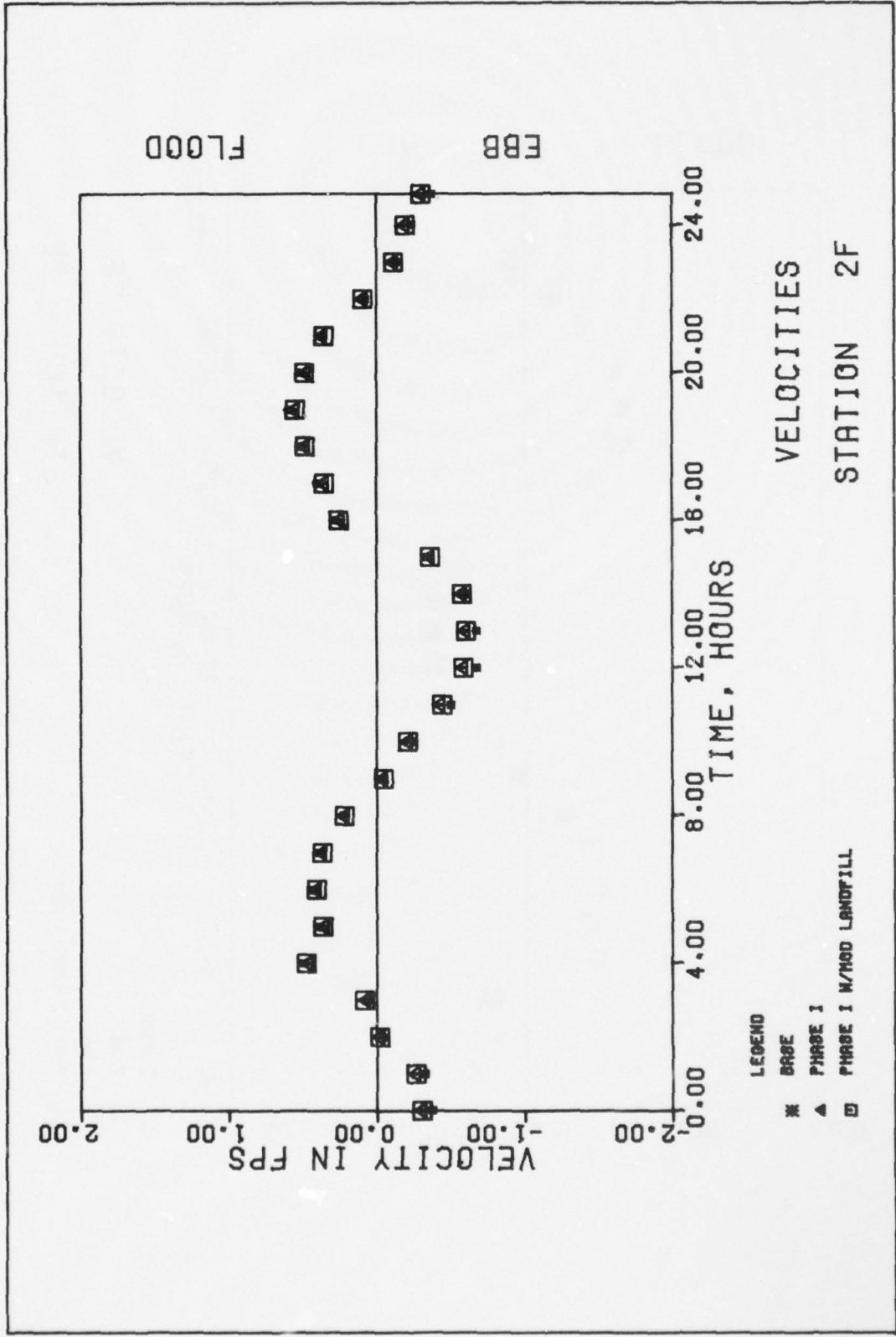


PLATE 24

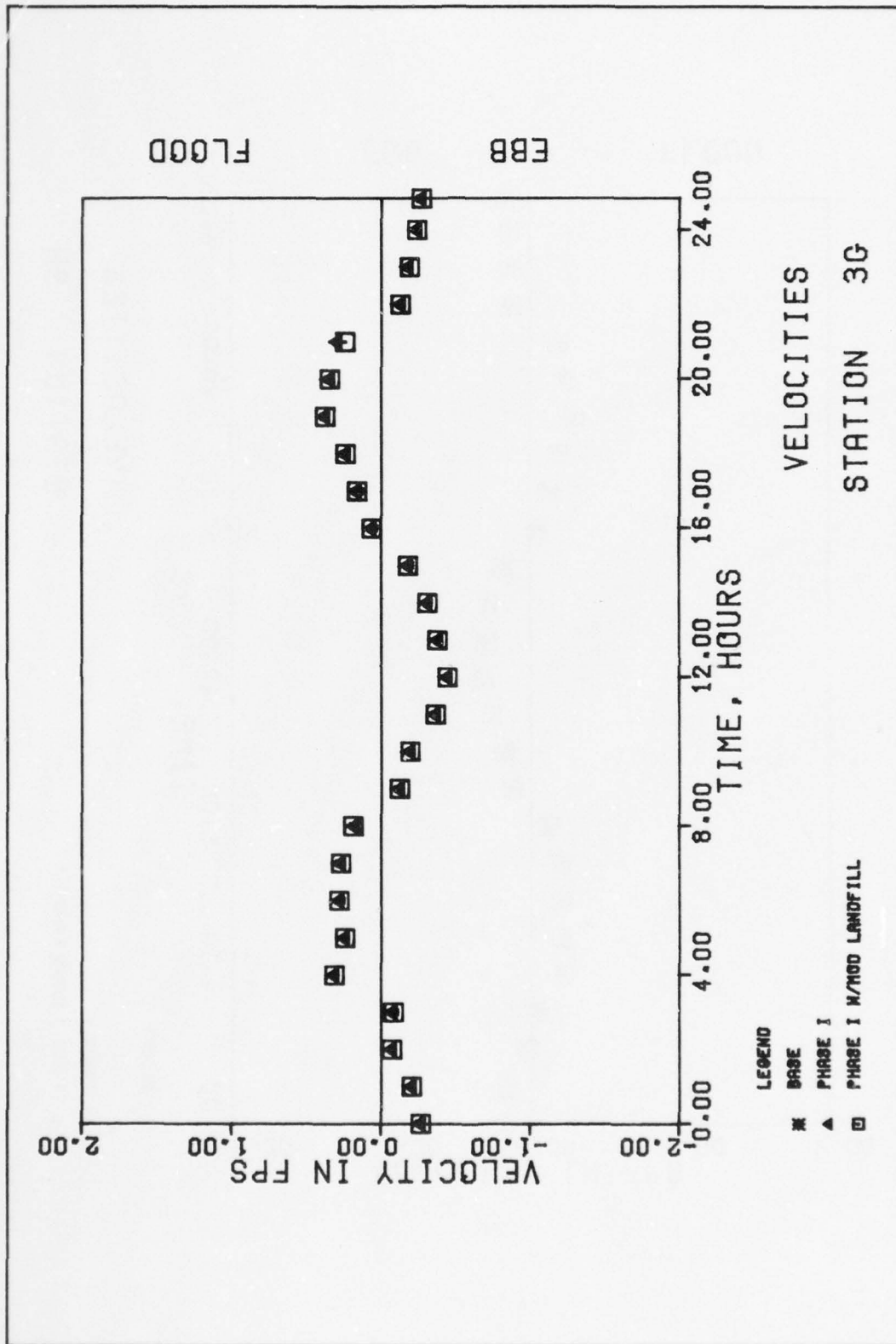


PLATE 25

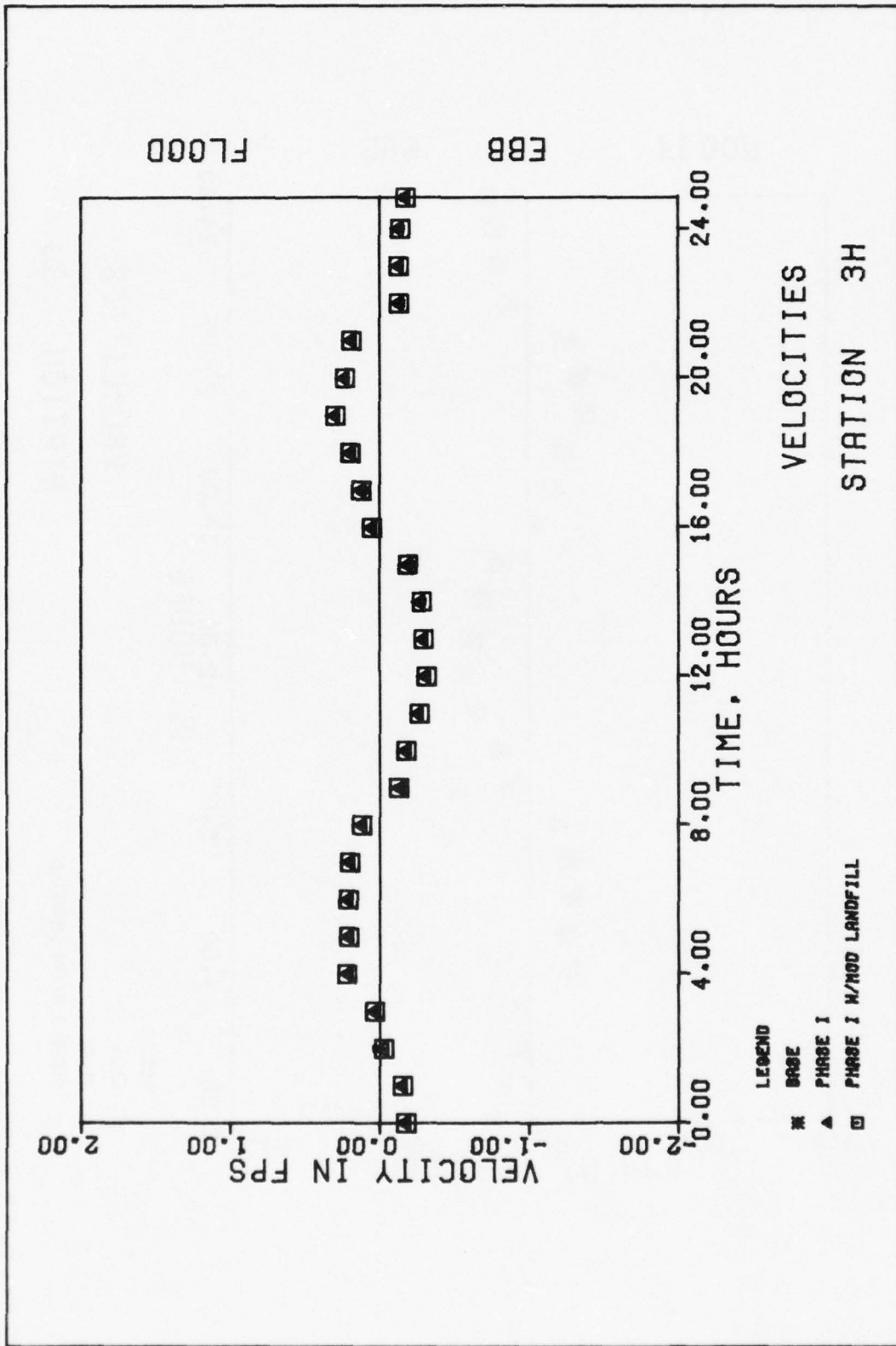
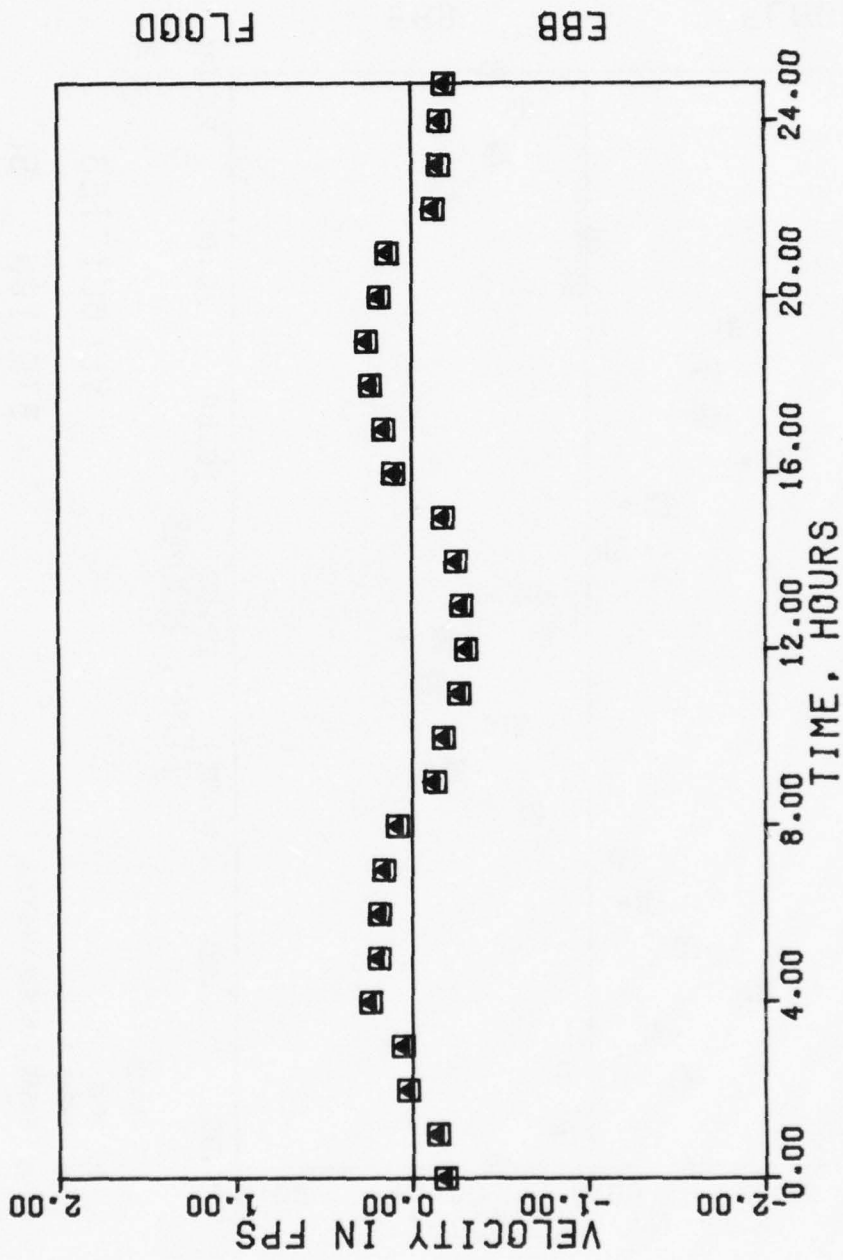


PLATE 26



VELOCITIES
STATION 31

LEGEND
* BASE
▲ PHASE I
▣ PHASE I W/MOD LANDFILL

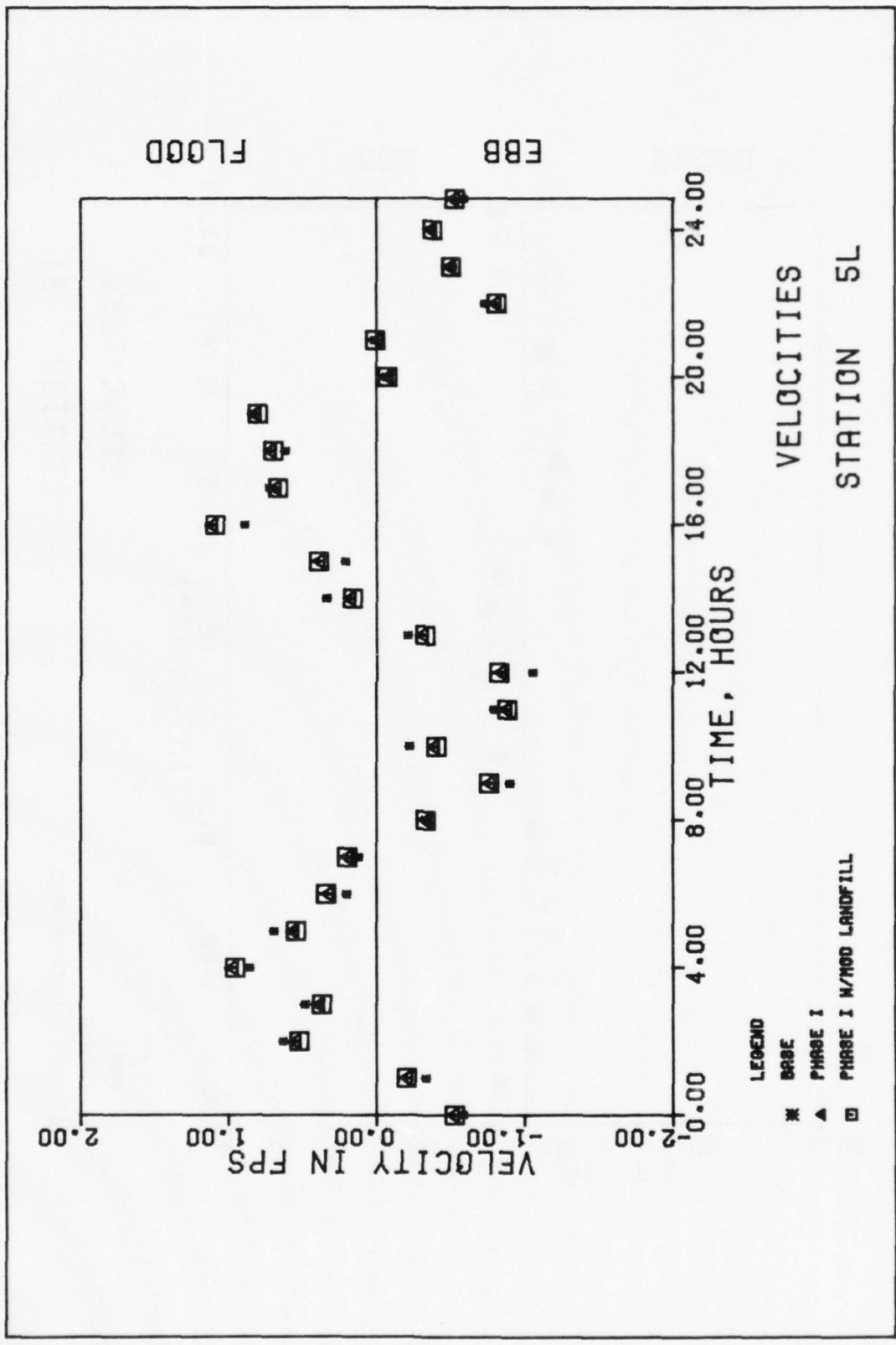
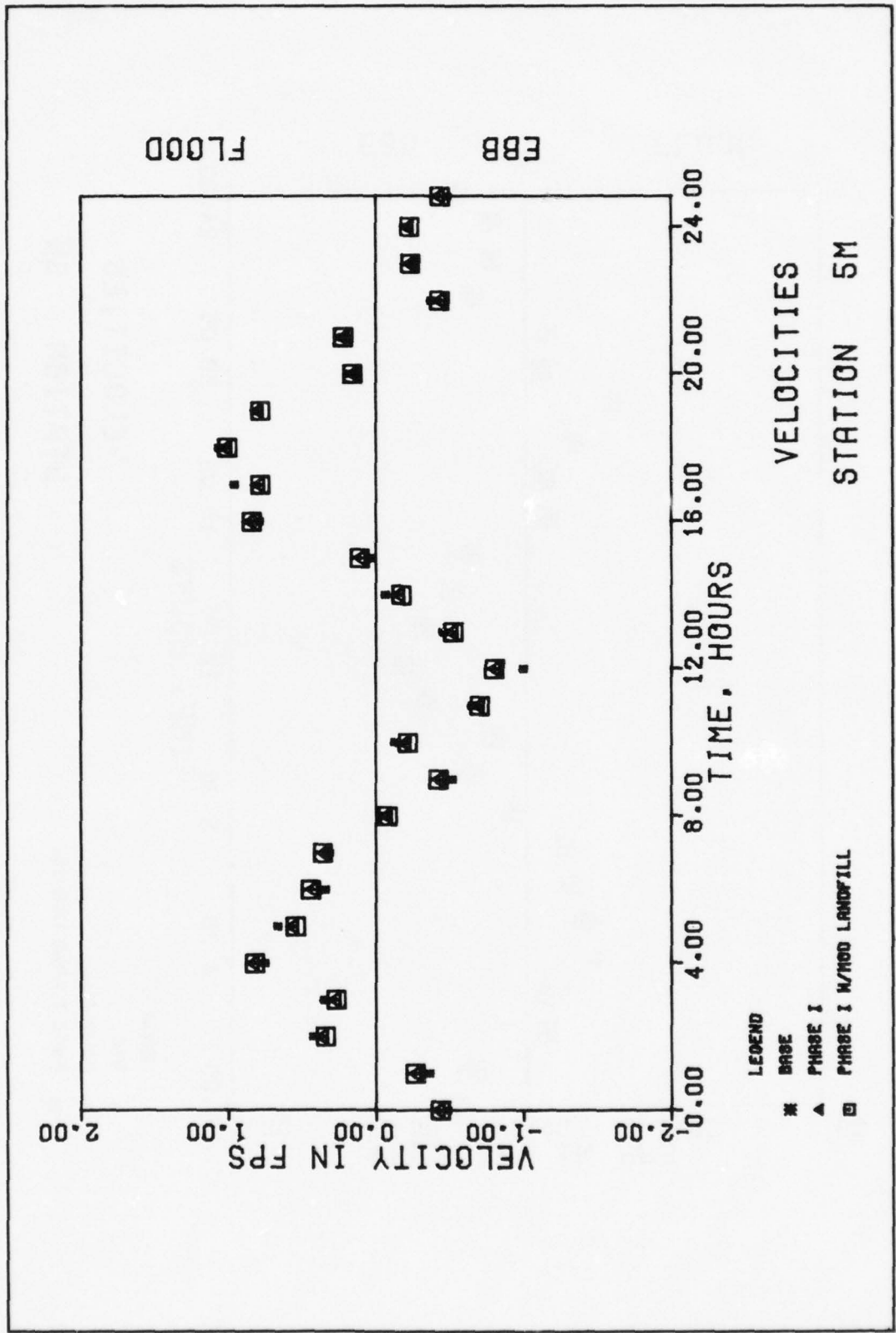


PLATE 28



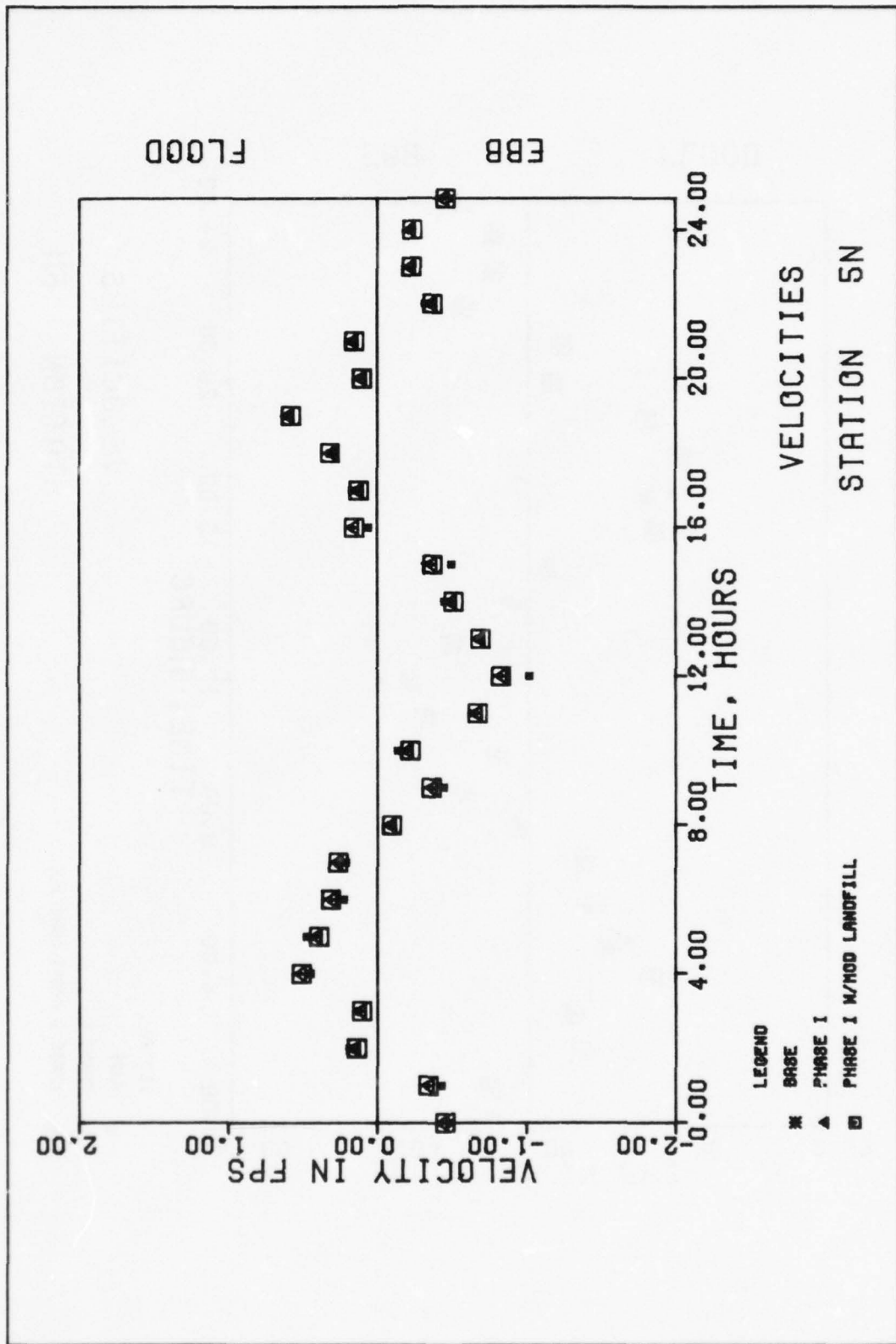
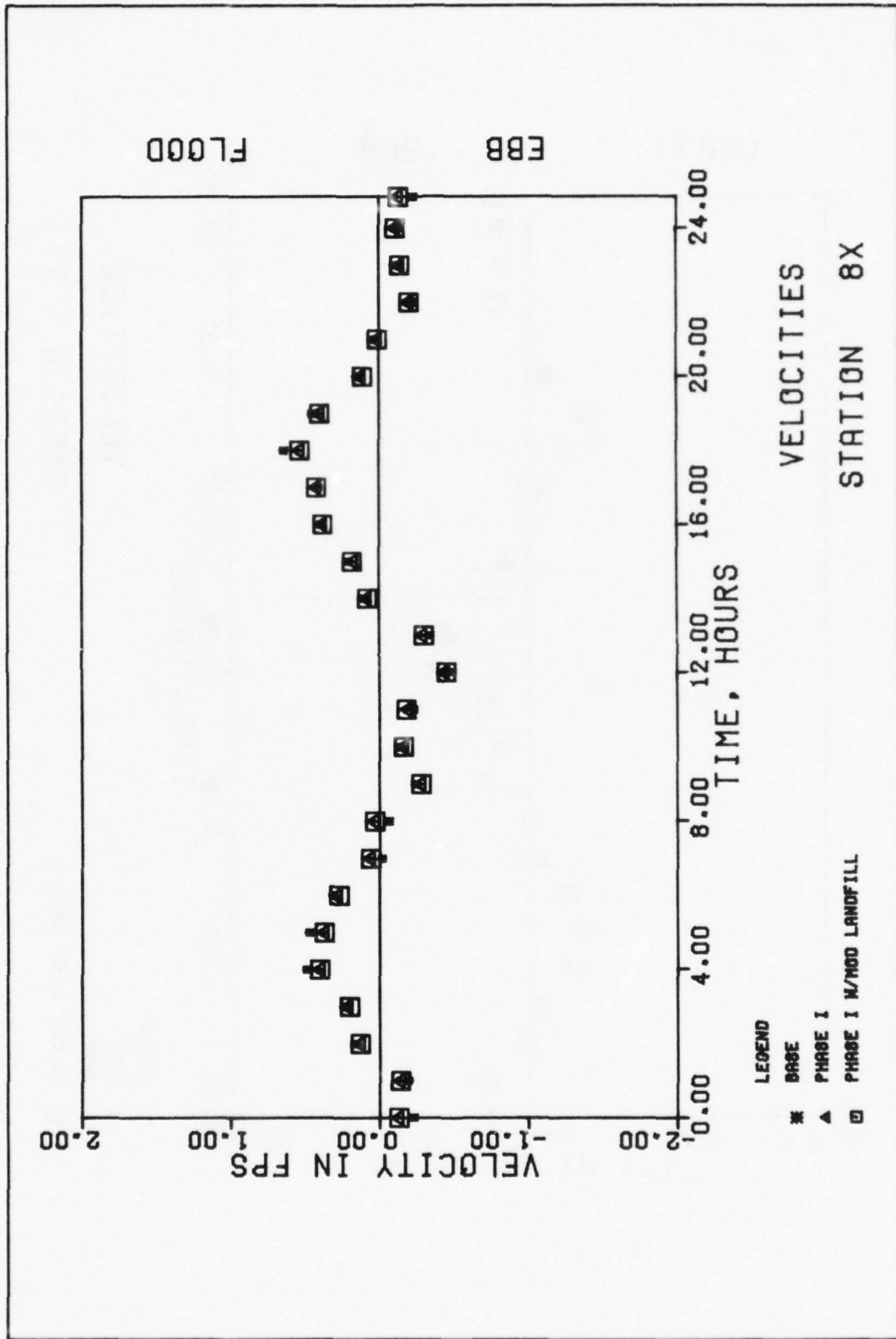


PLATE 30



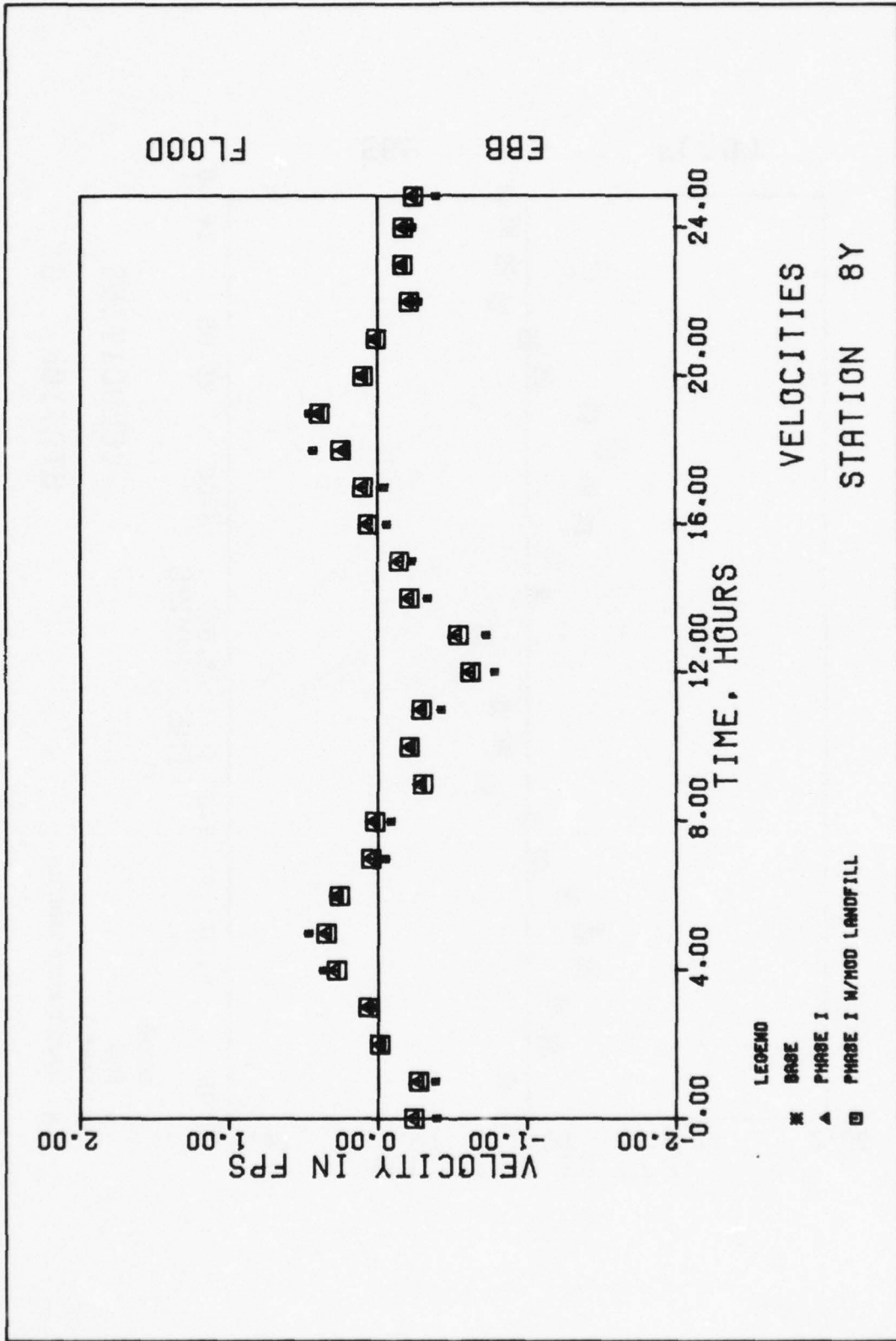
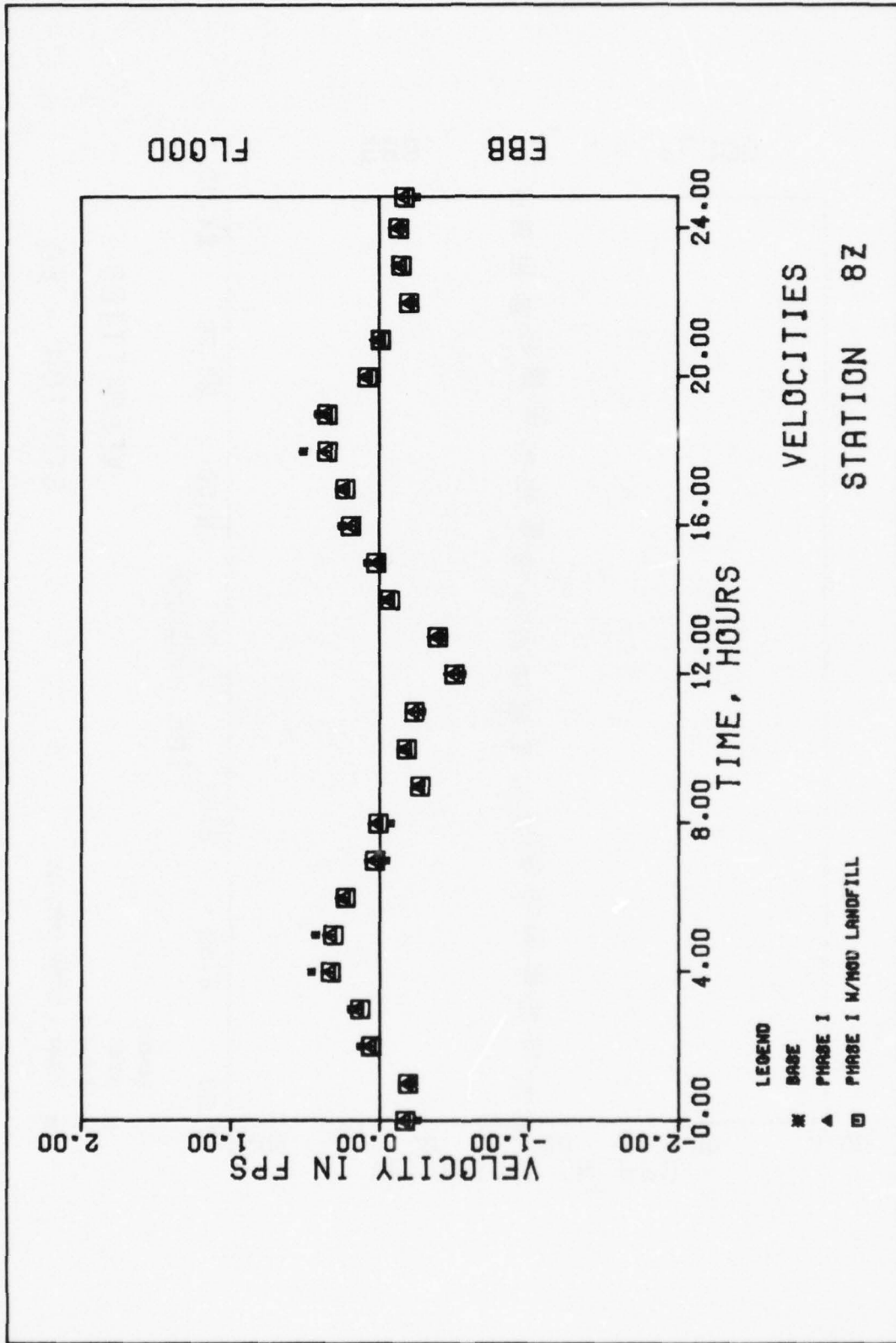


PLATE 32



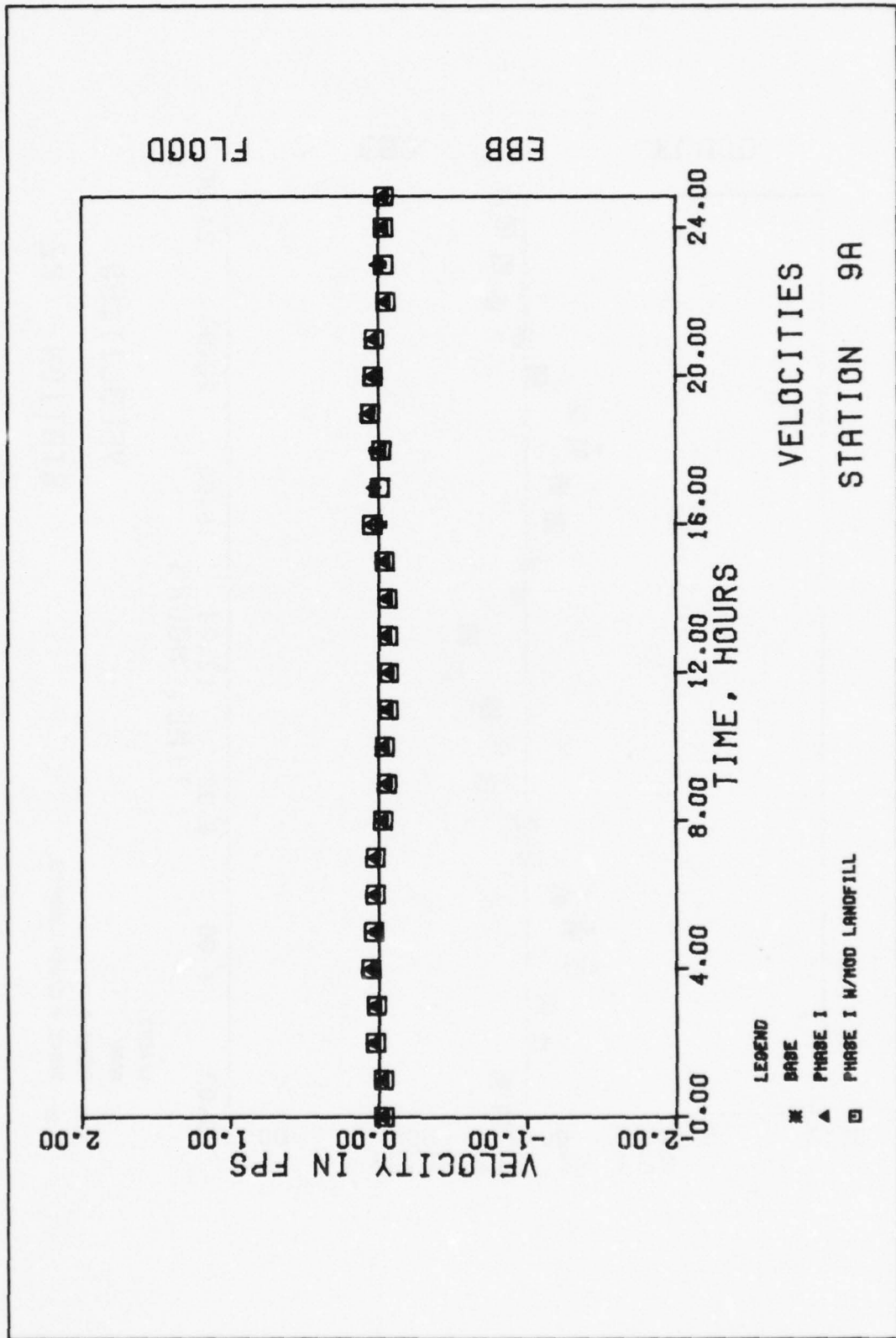
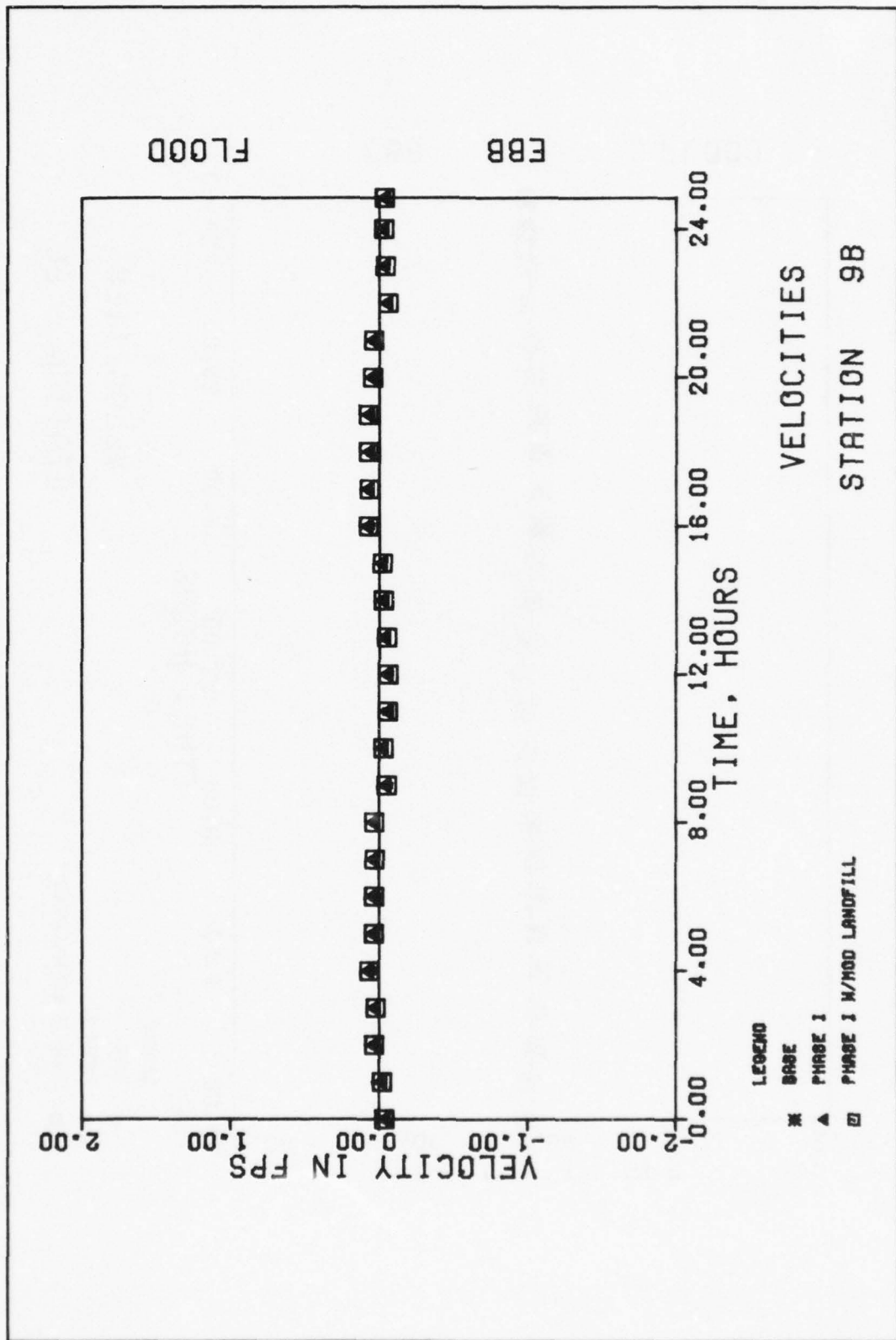


PLATE 34



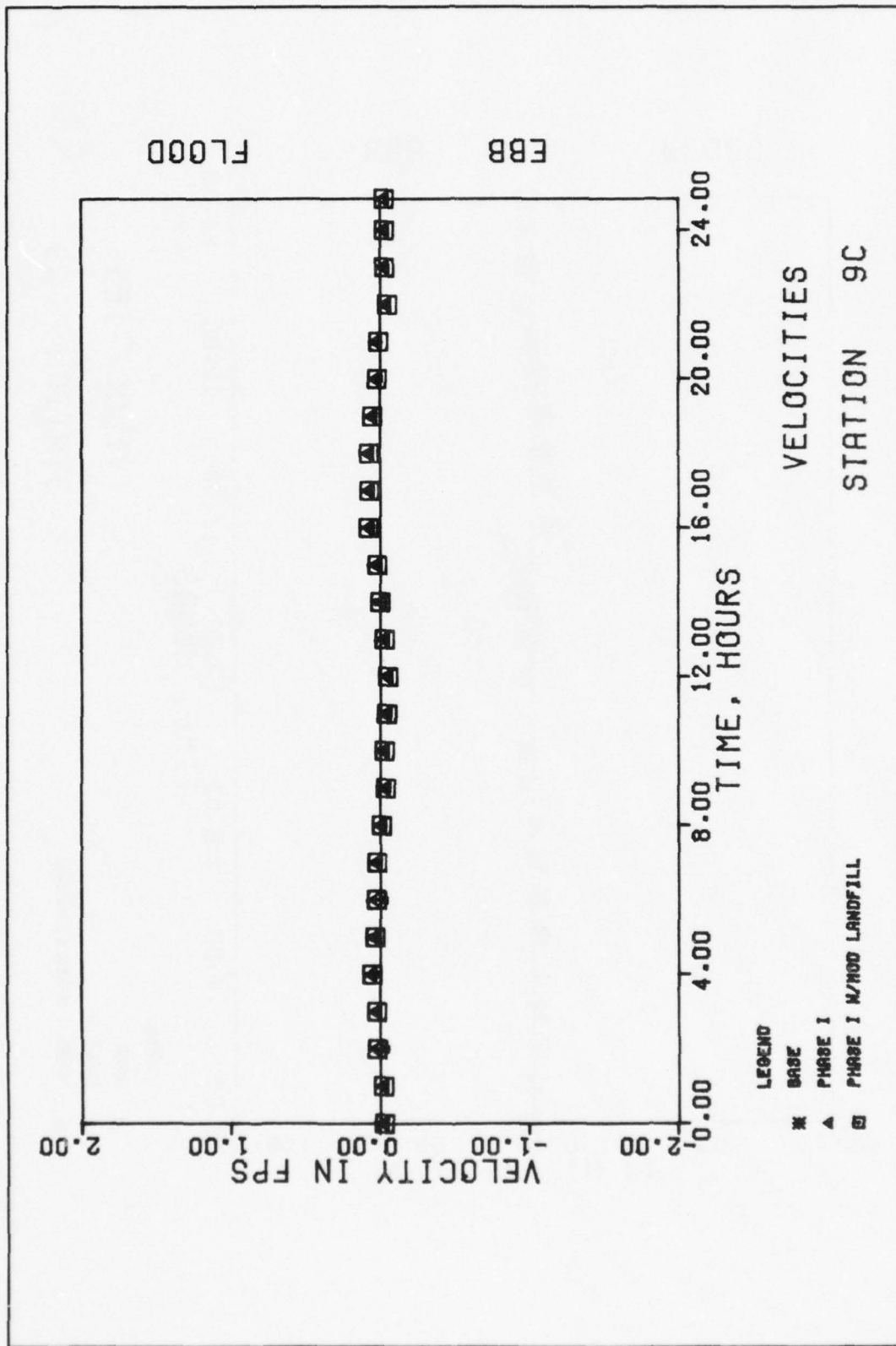


PLATE 36

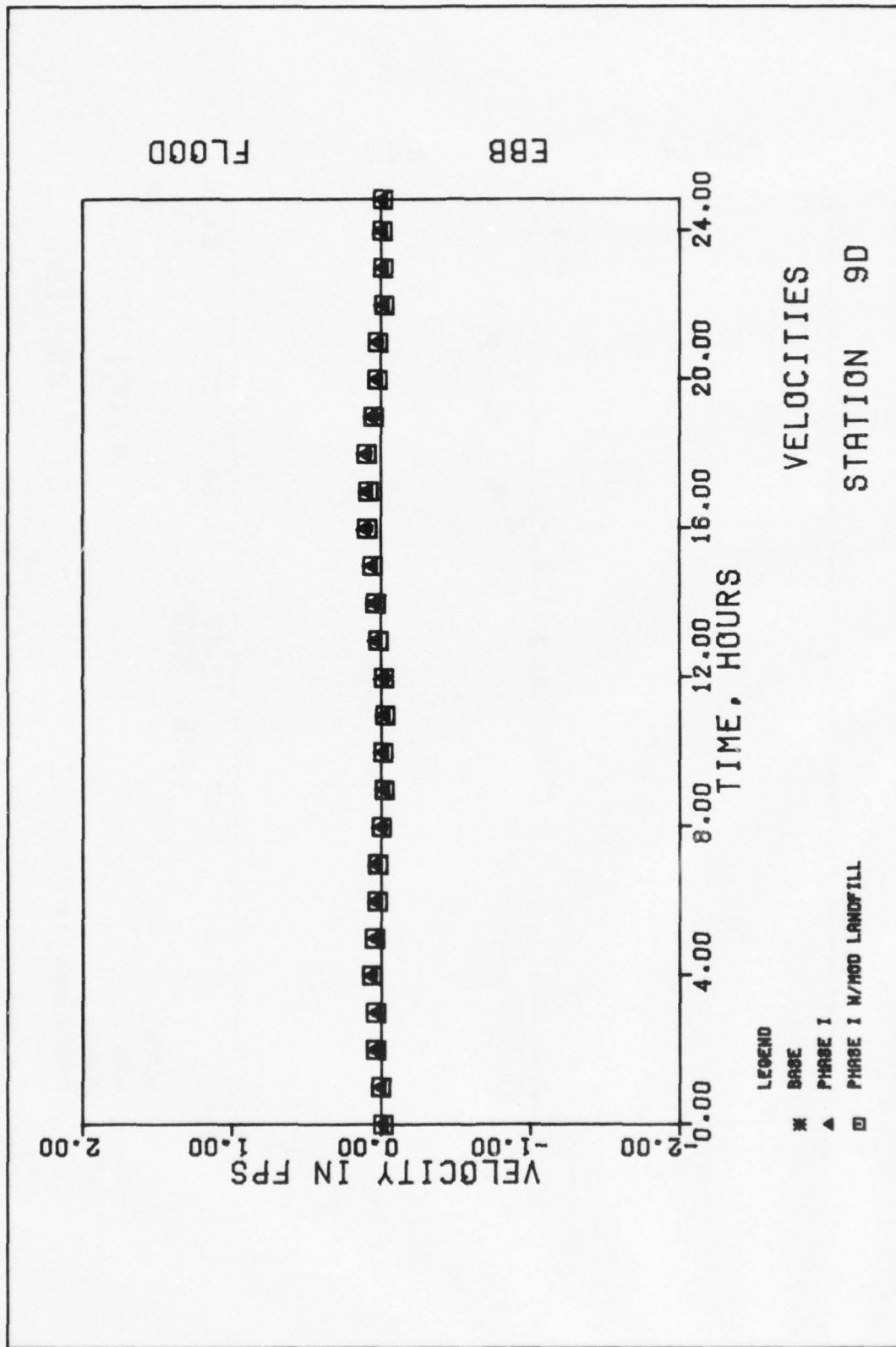


PLATE 37

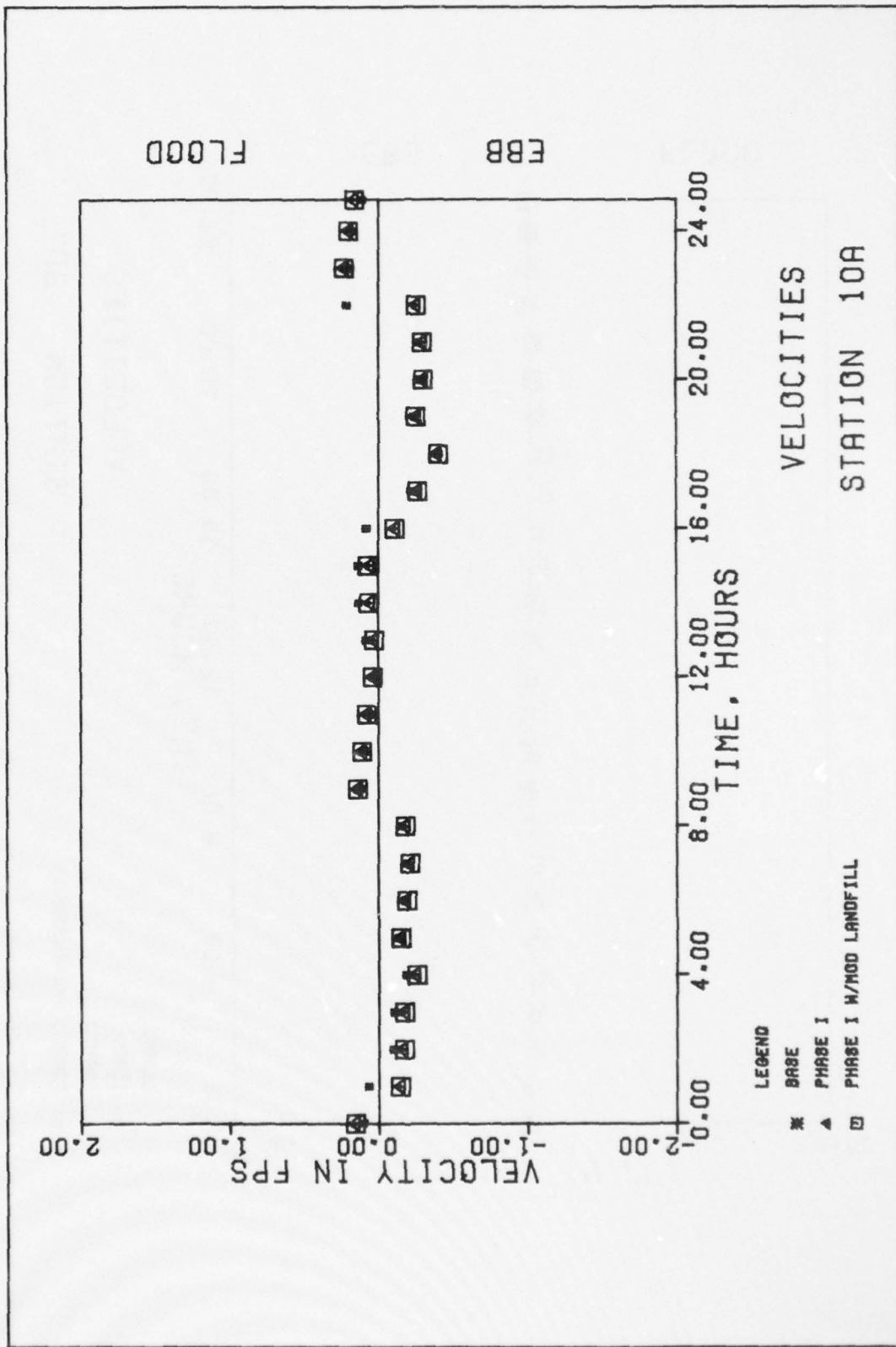
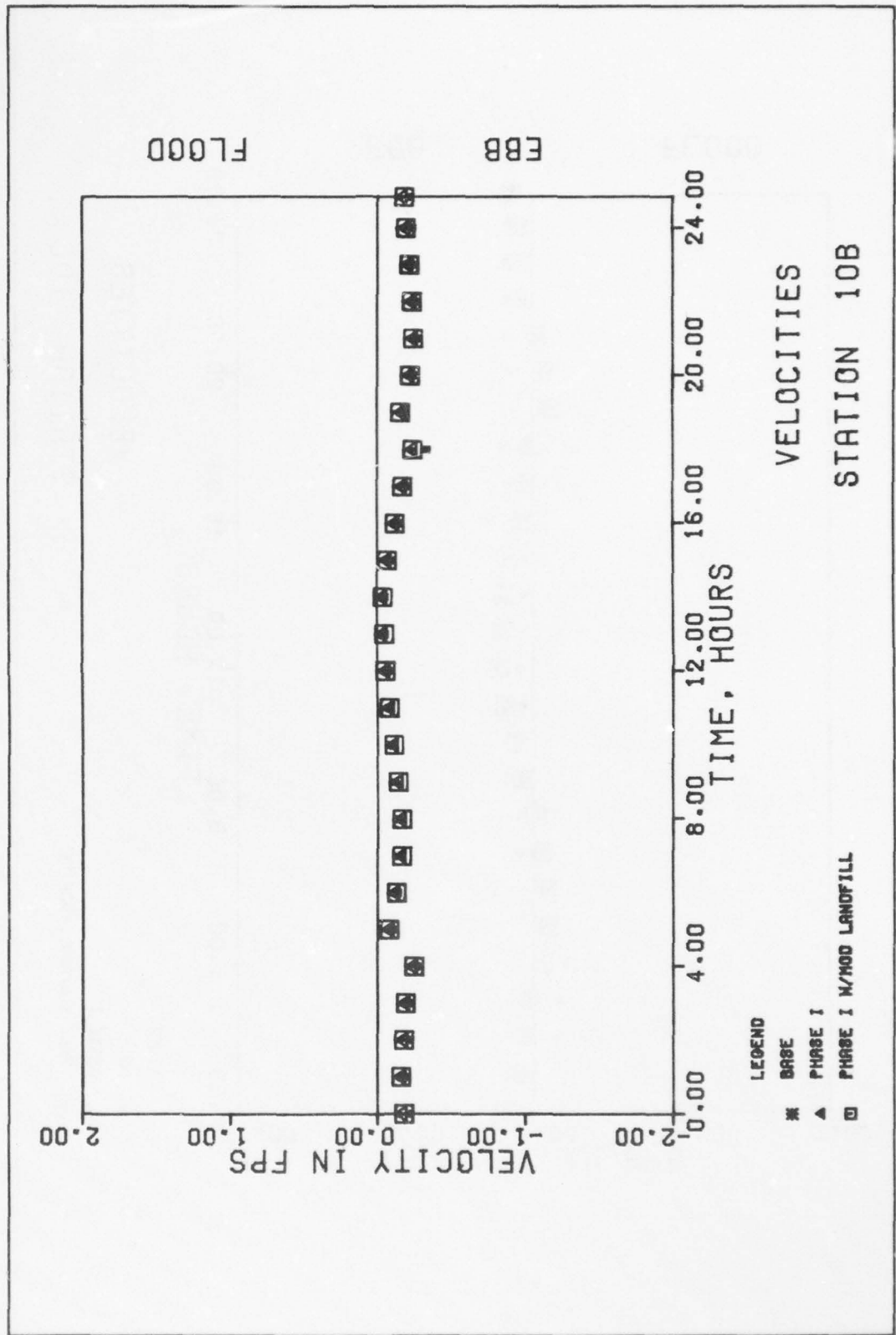


PLATE 38



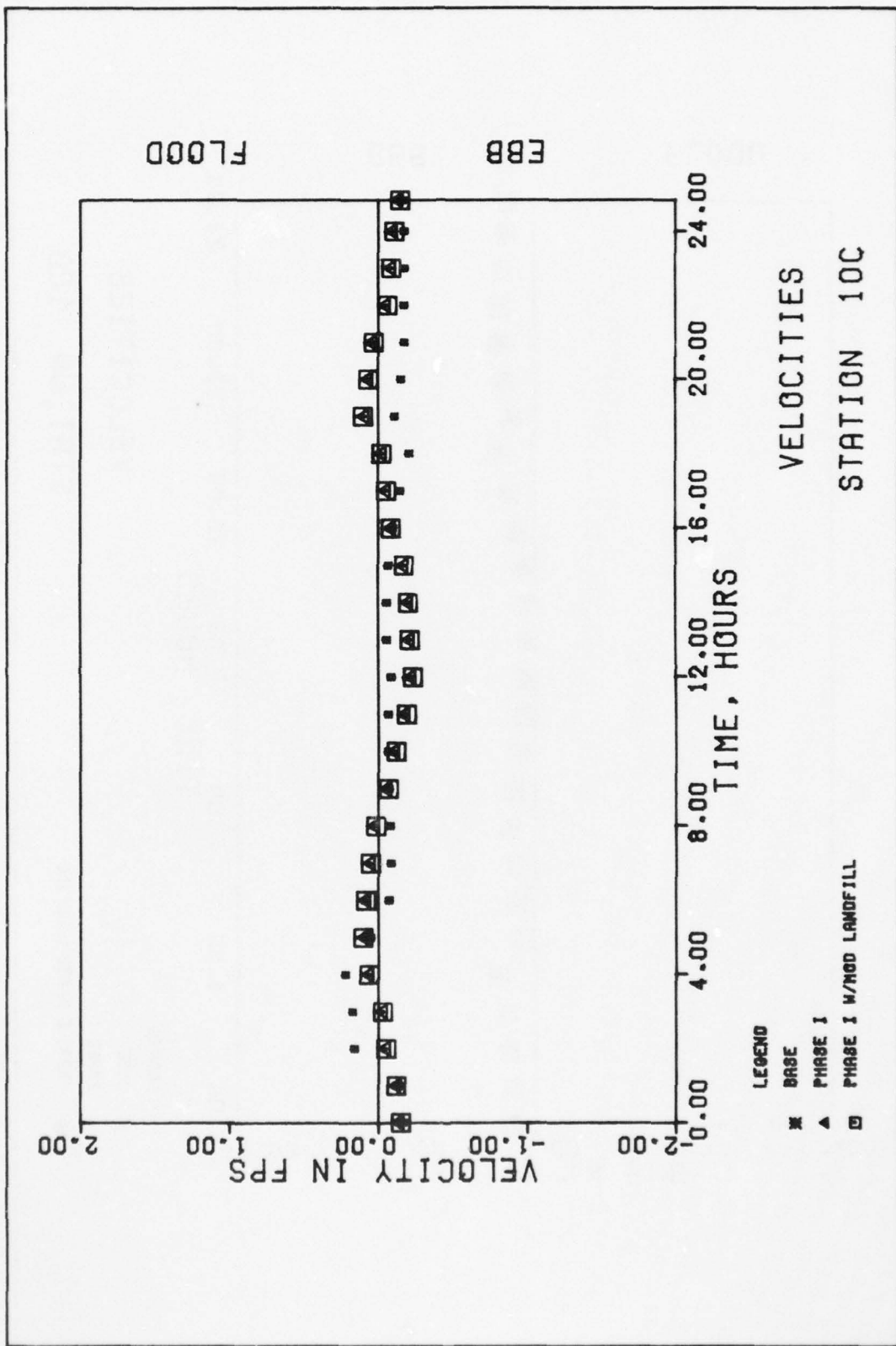
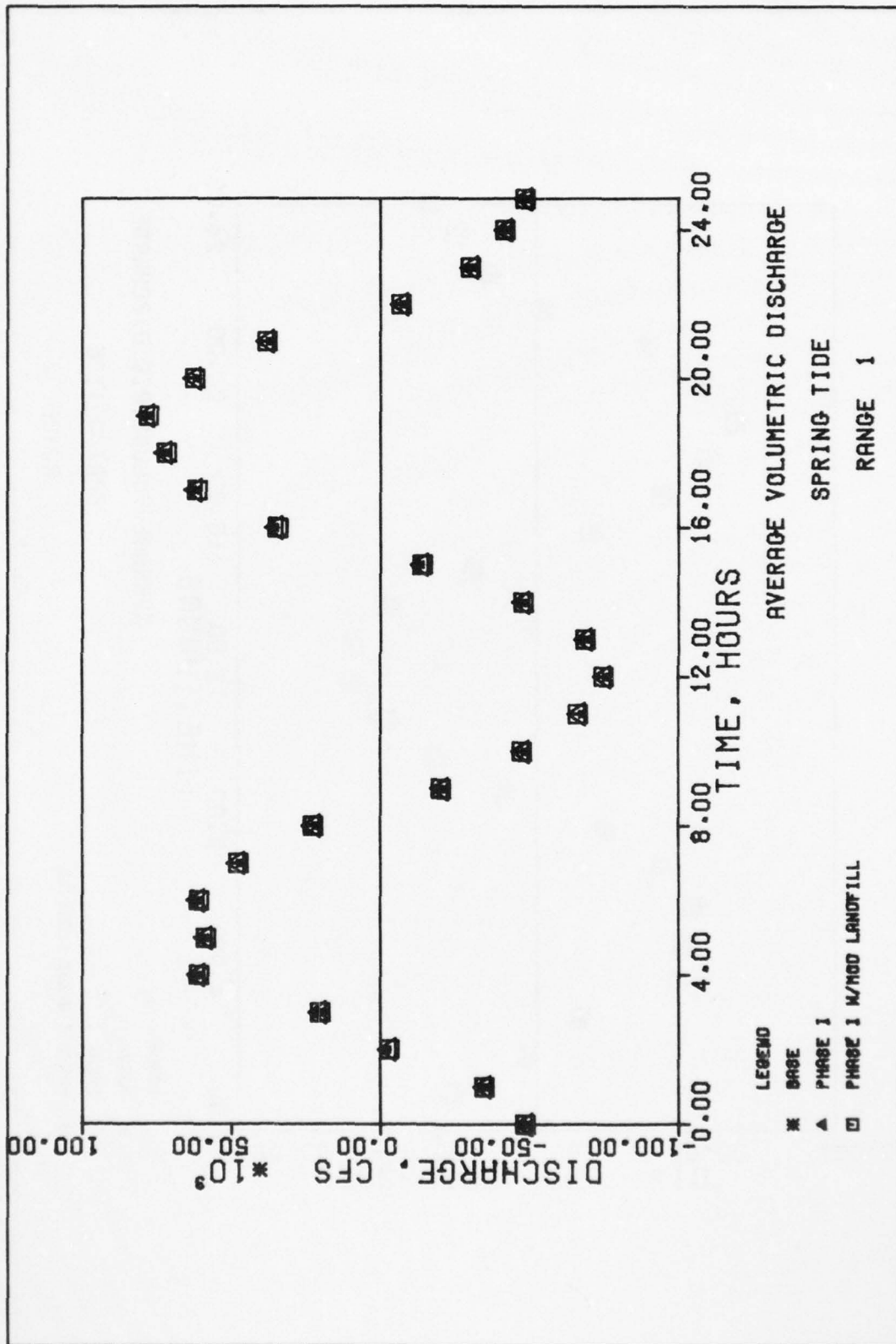


PLATE 40



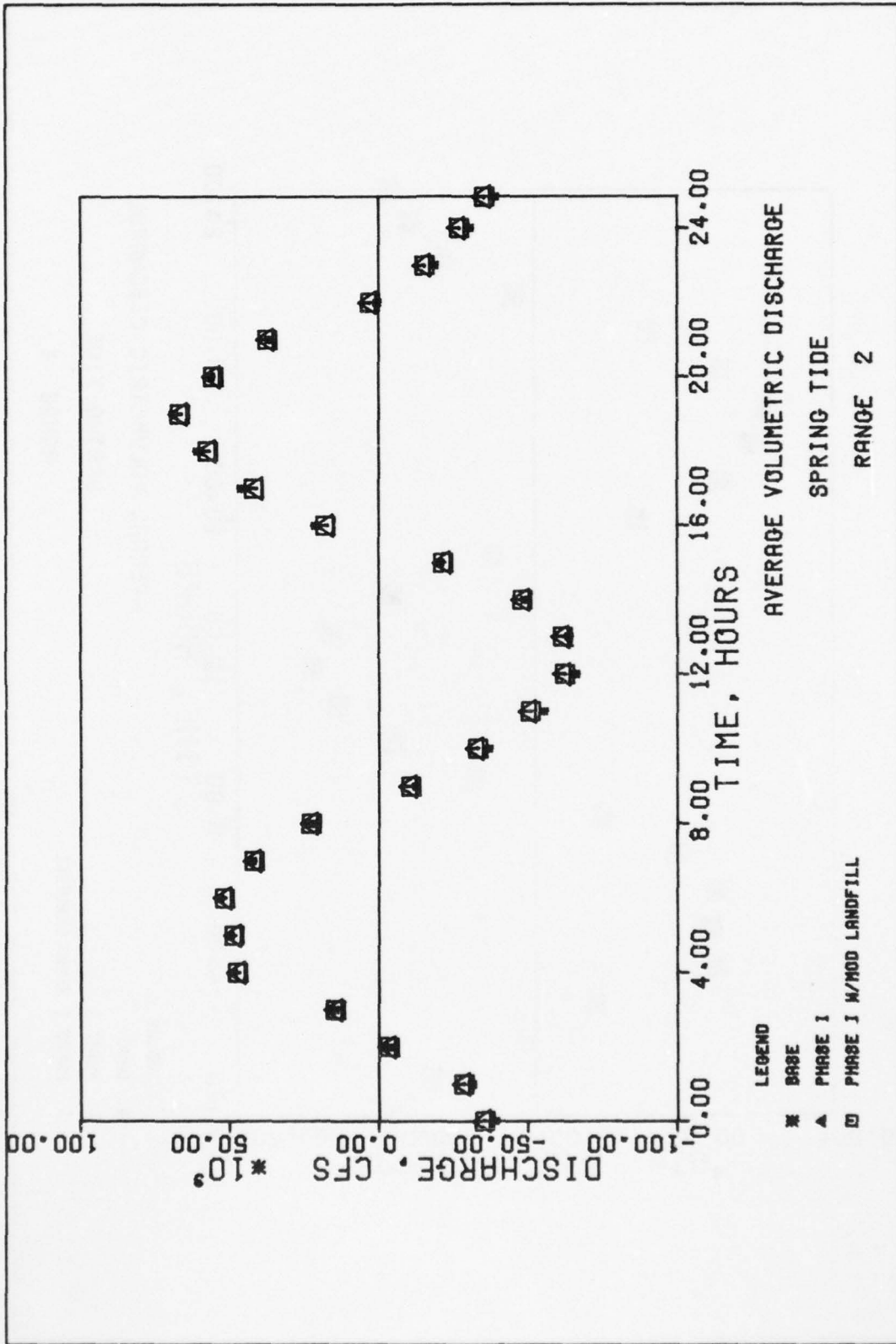
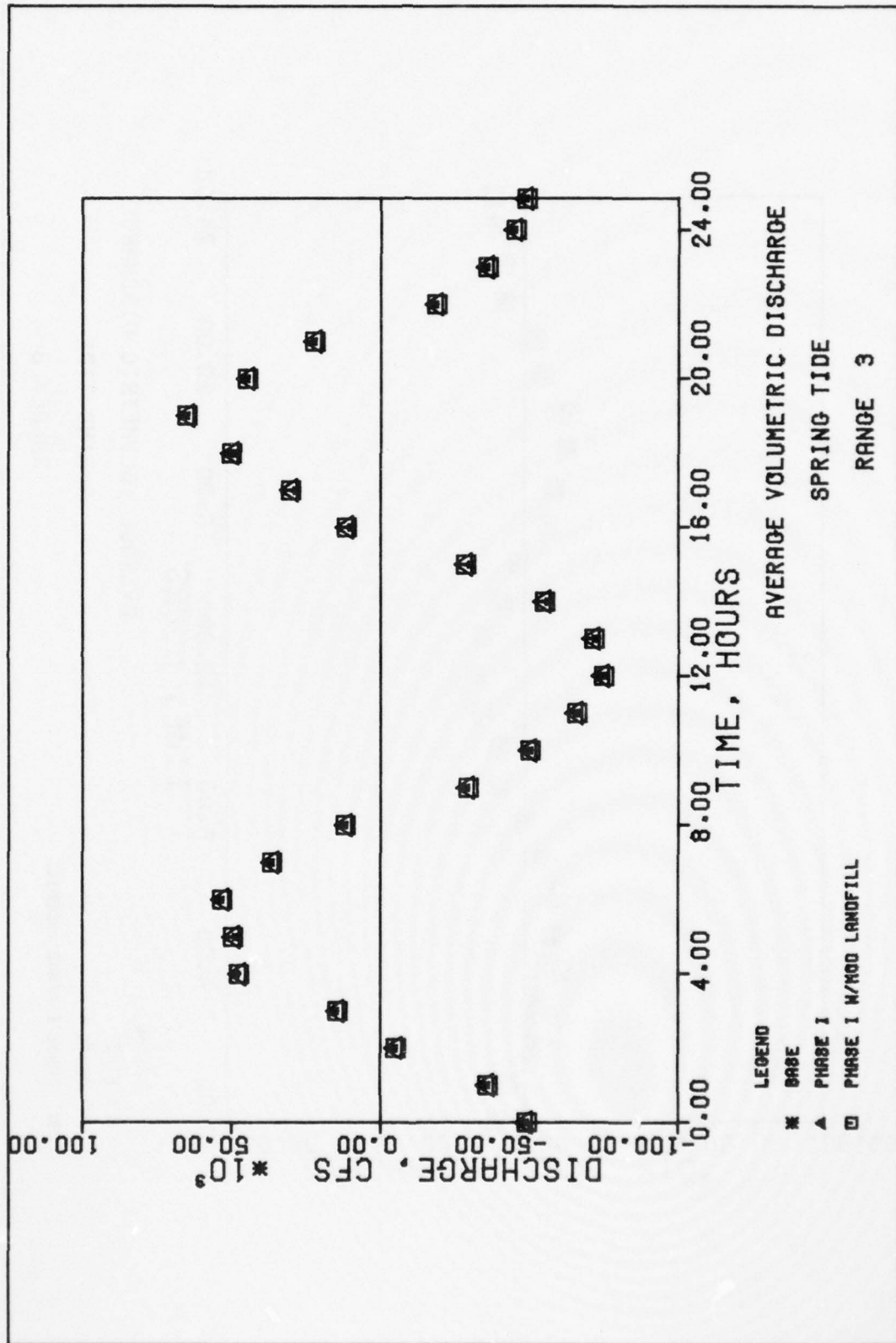


PLATE 42



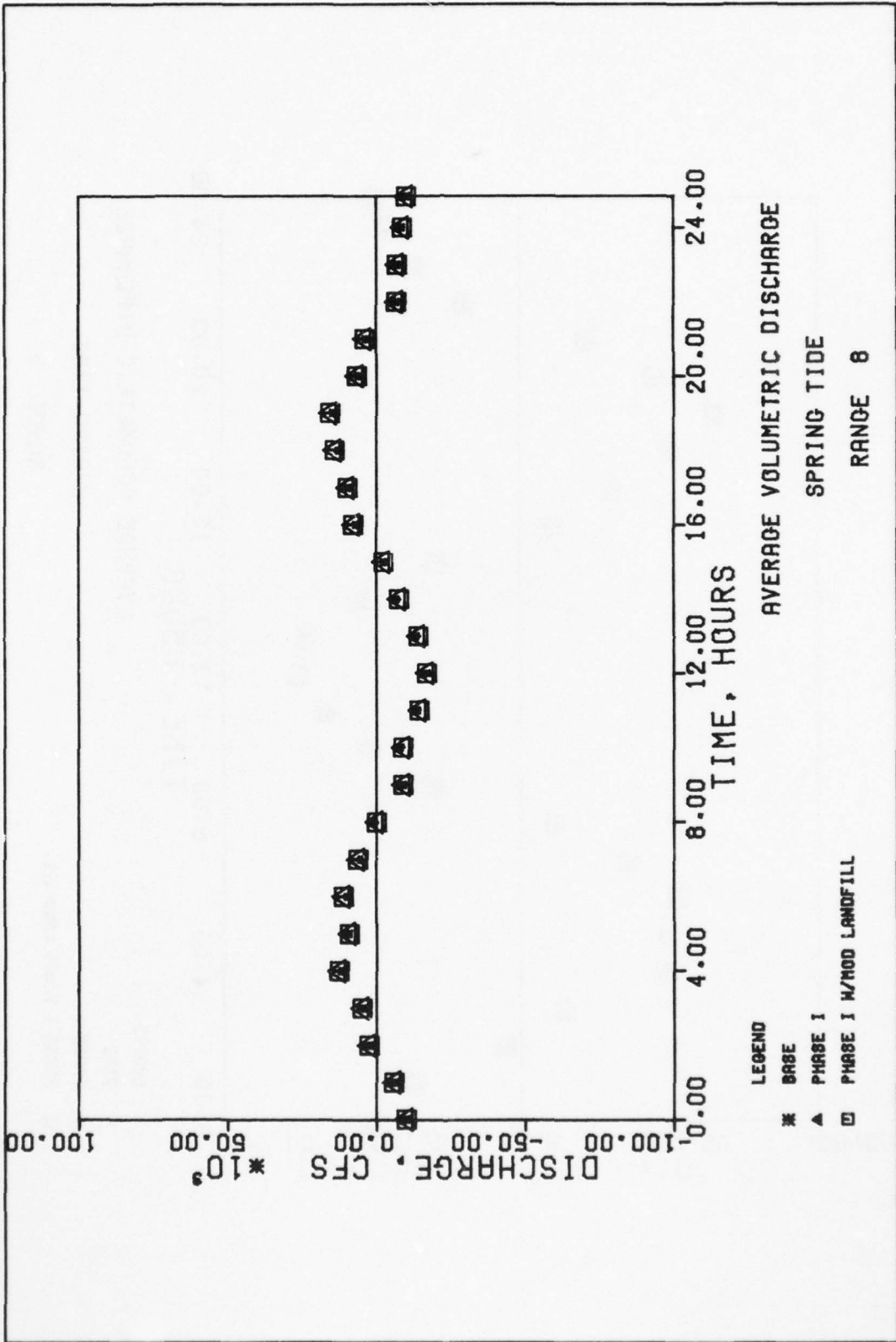
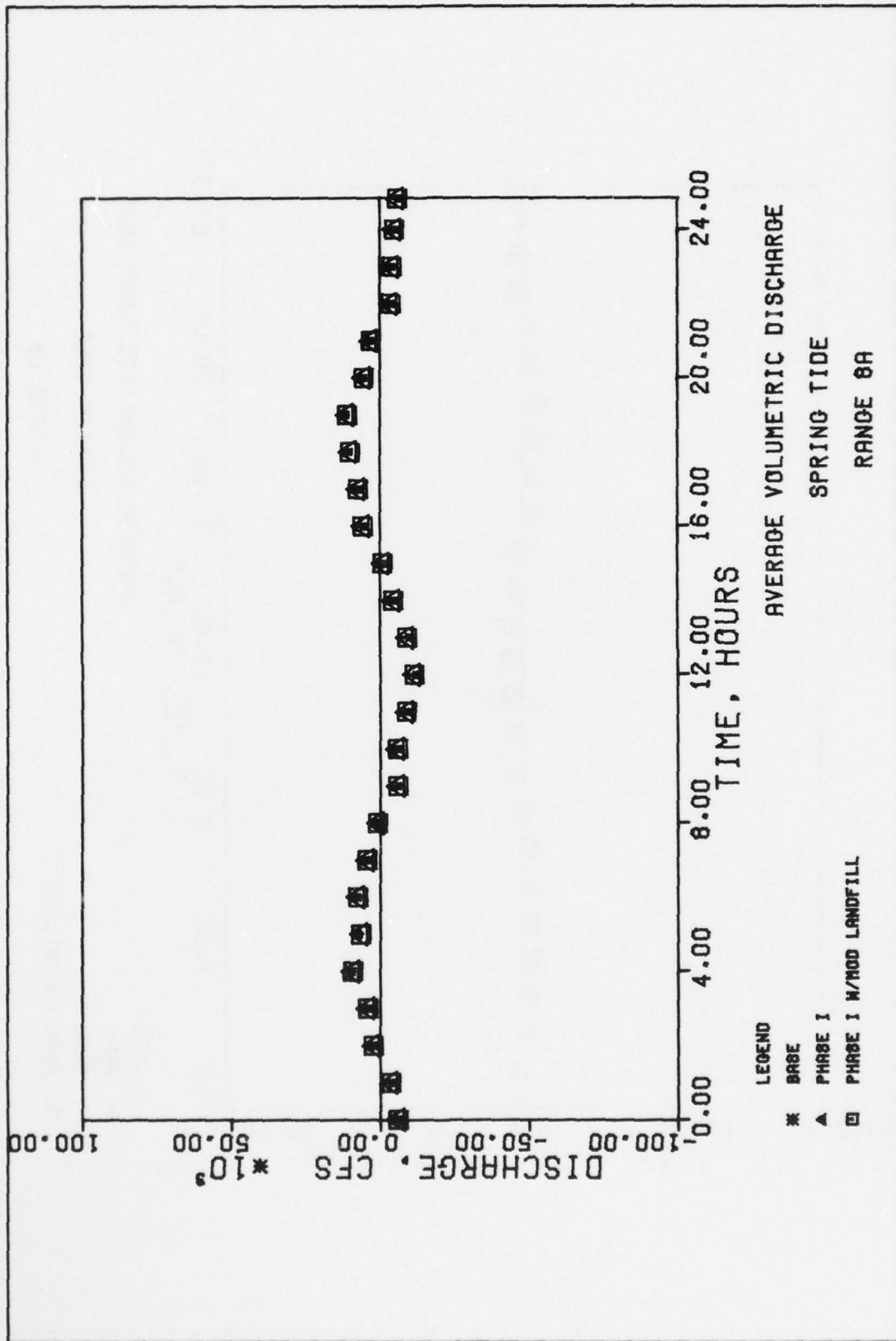
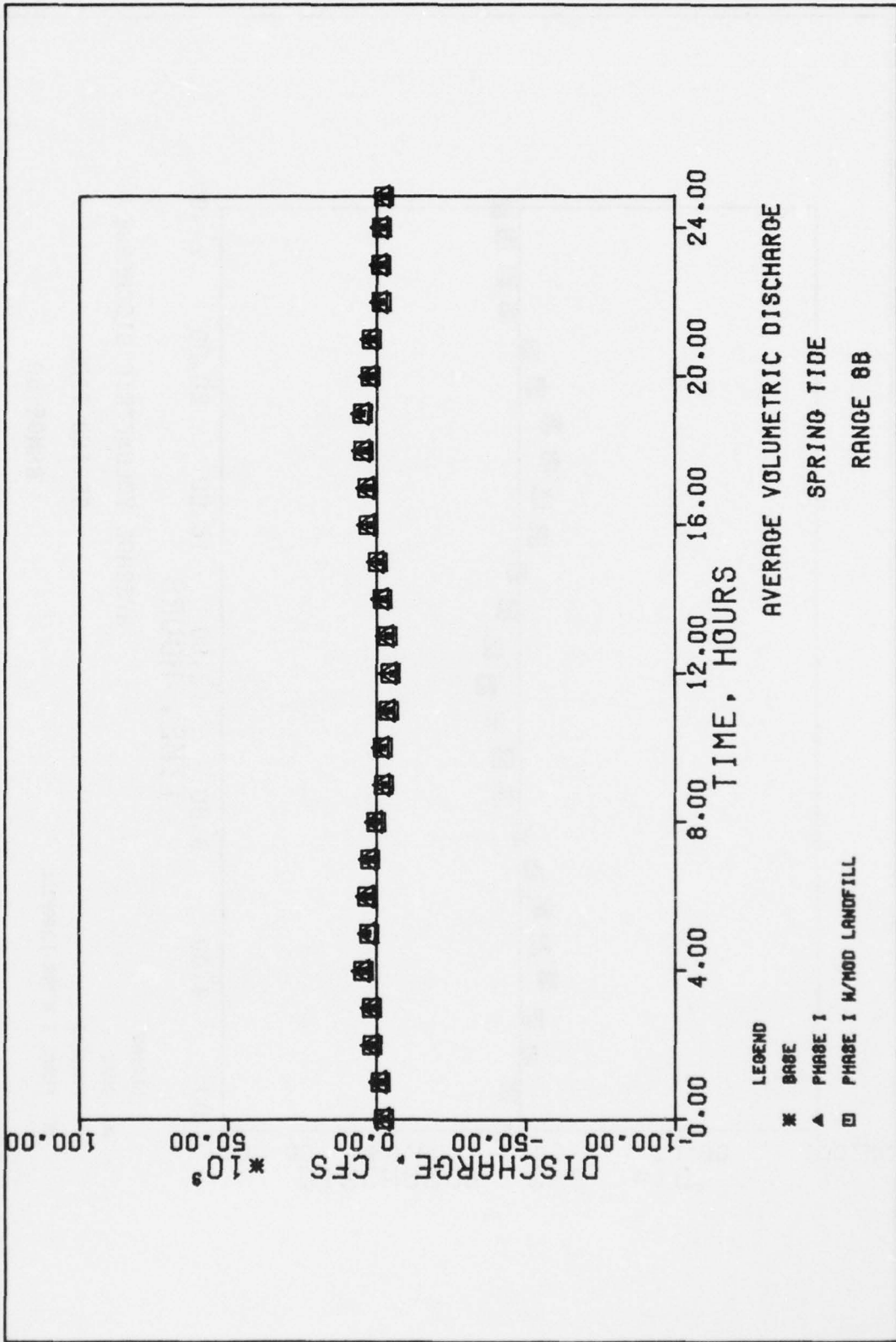


PLATE 44

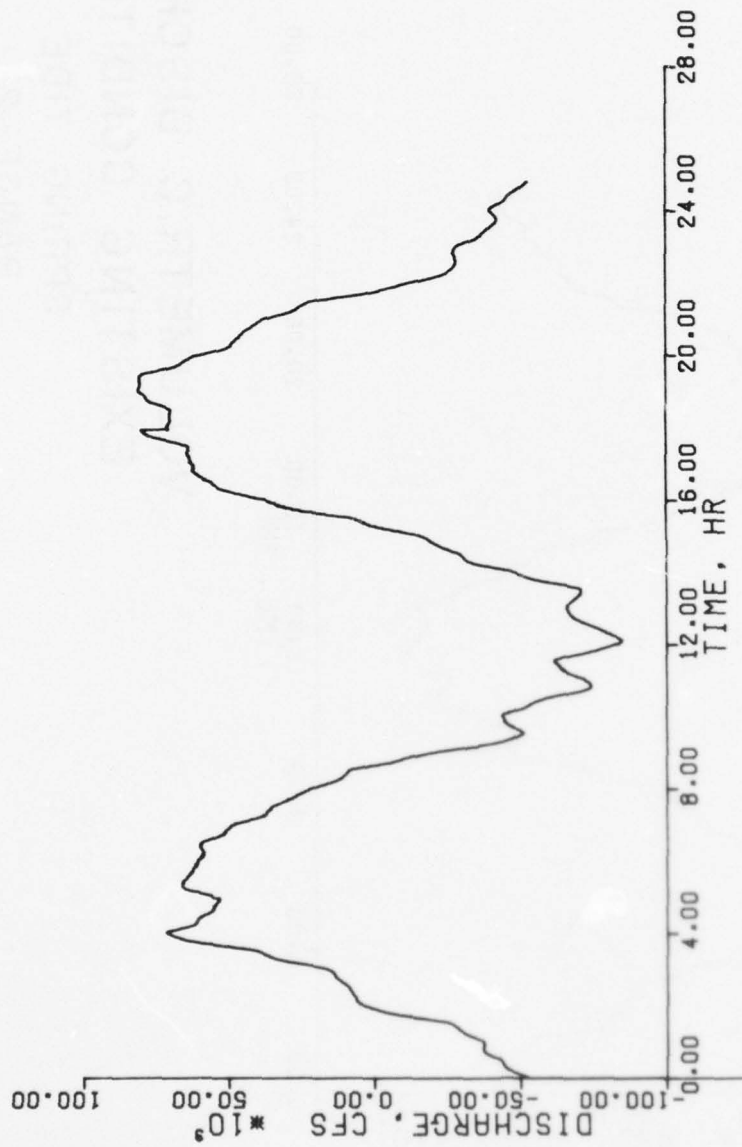




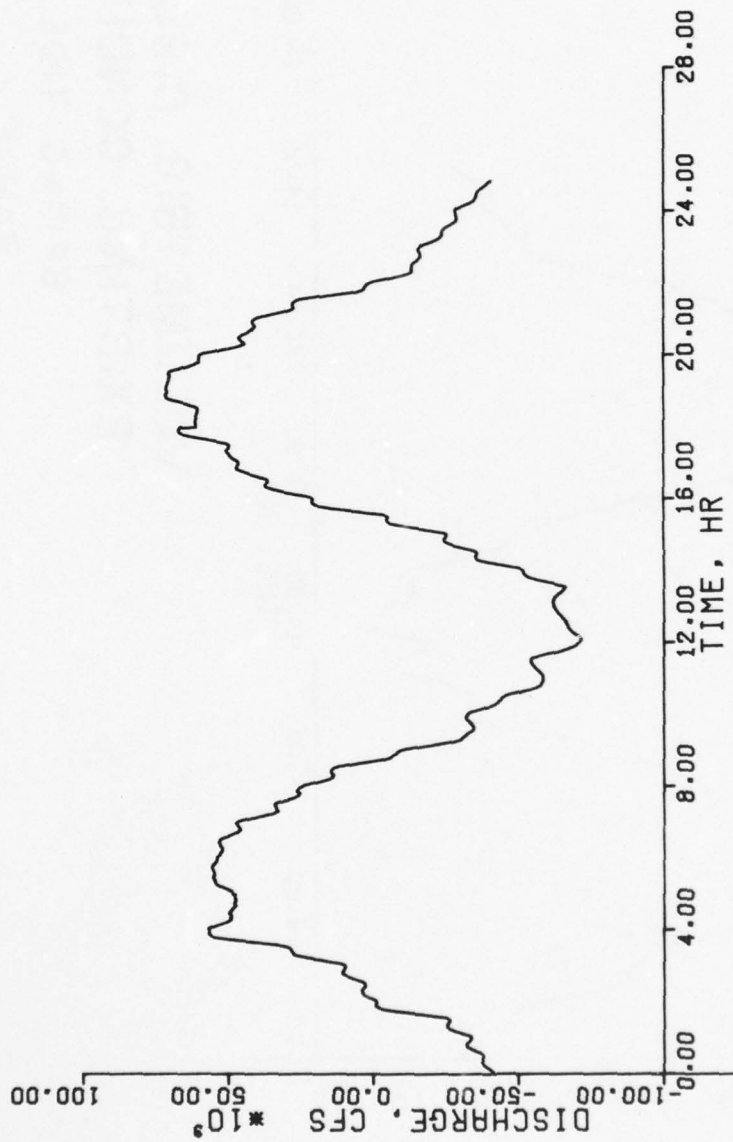
LEGEND
 * BASE
 ▲ PHASE I
 □ PHASE I W/MOD LANDFILL

AVERAGE VOLUMETRIC DISCHARGE
 SPRING TIDE
 RANGE 6B

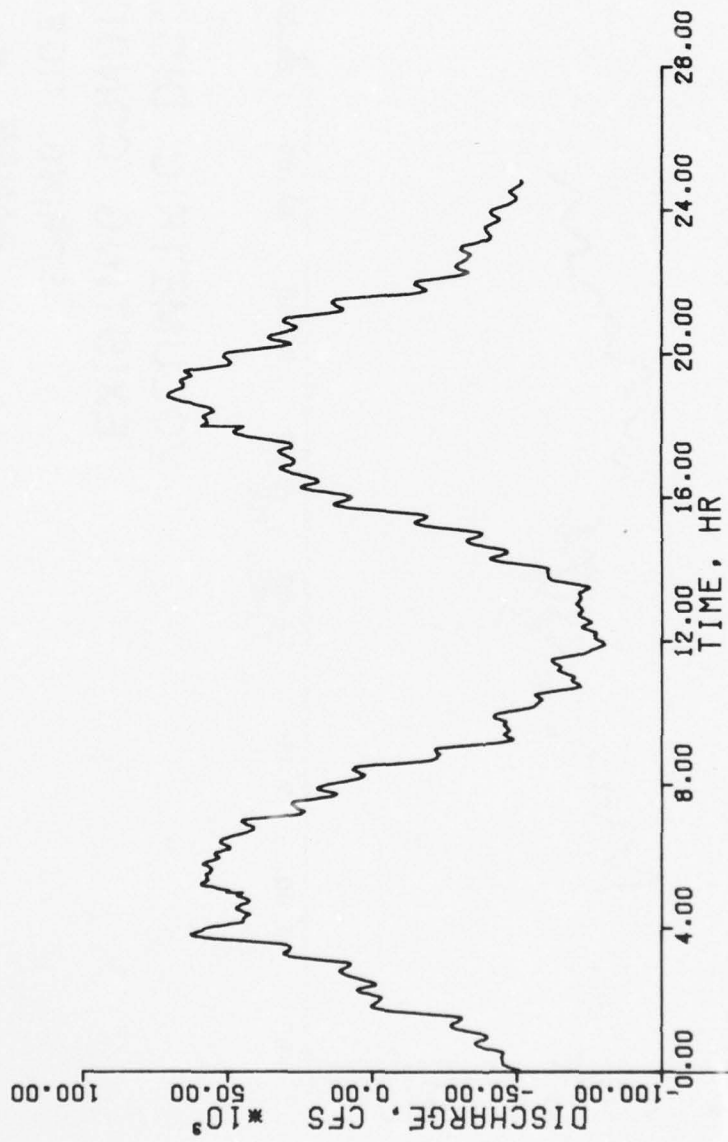
PLATE 46



VOLUMETRIC DISCHARGE
EXISTING CONDITIONS
SPRING TIDE
RANGE I



VOLUMETRIC DISCHARGE
 EXISTING CONDITIONS
 SPRING TIDE
 RANGE 2



VOLUMETRIC DISCHARGE
 EXISTING CONDITIONS
 SPRING TIDE
 RANGE 3

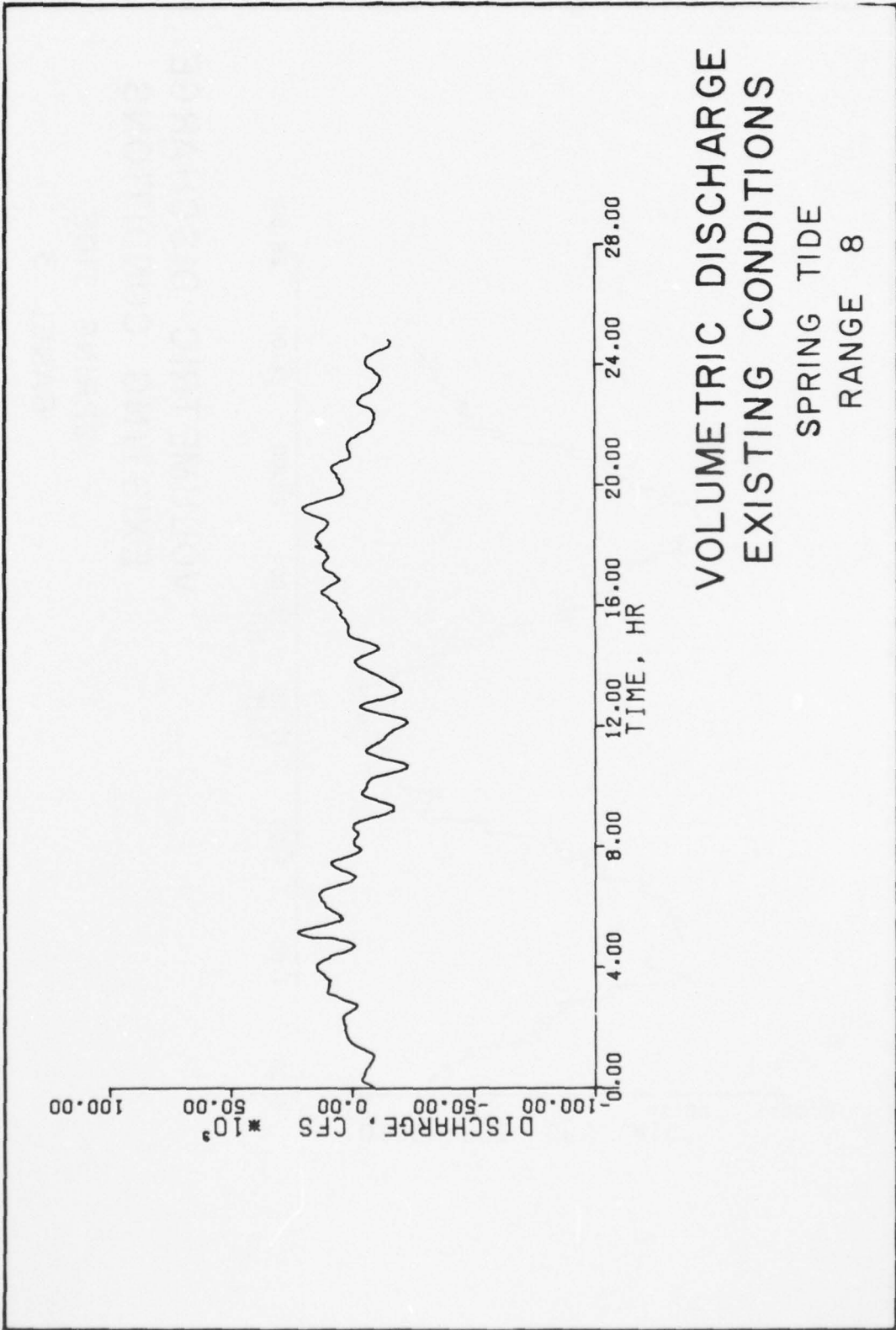
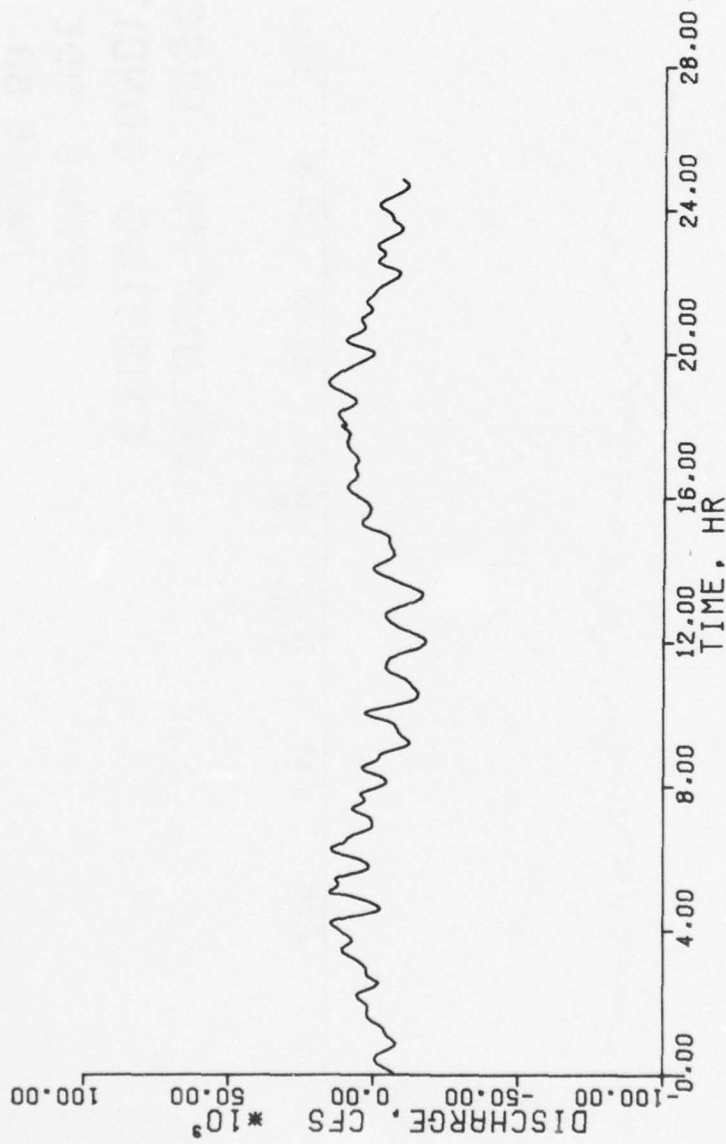
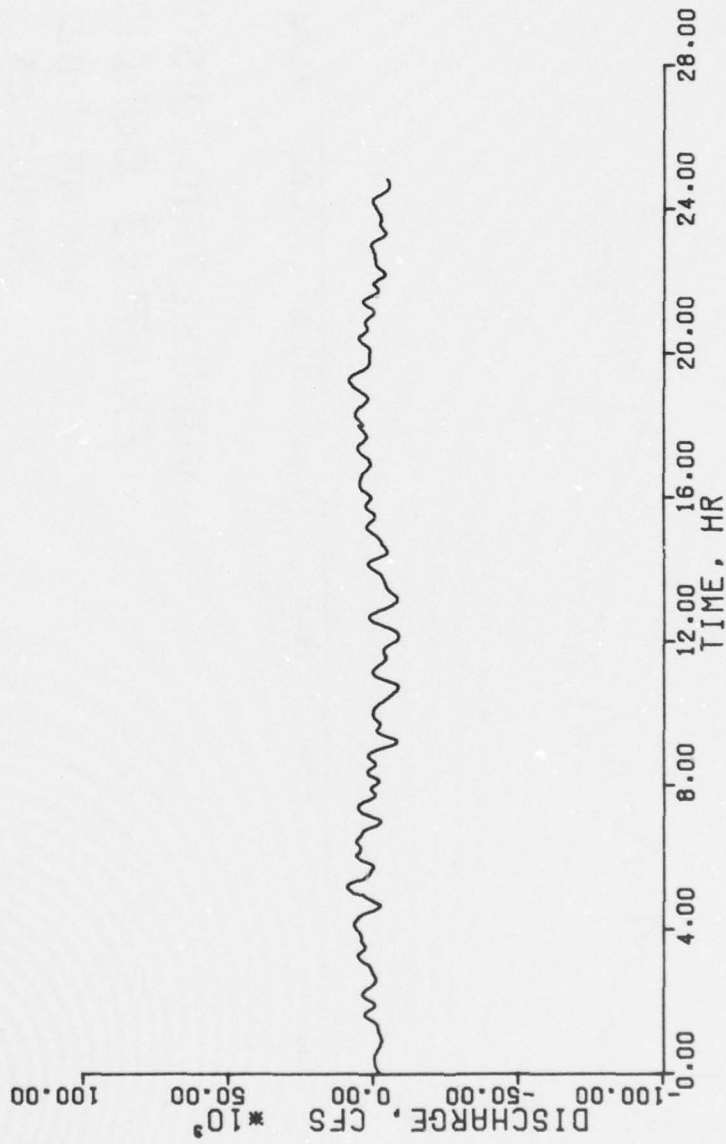


PLATE 50



VOLUMETRIC DISCHARGE
EXISTING CONDITIONS

SPRING TIDE
RANGE 8A



VOLUMETRIC DISCHARGE
EXISTING CONDITIONS
SPRING TIDE
RANGE 8B

AD-A069 796

ARMY ENGINEER WATERWAYS EXPERIMENT STATION VICKSBURG MISS F/G 13/13
NUMERICAL ANALYSIS OF TIDAL CIRCULATION FOR LONG BEACH OUTER HA--ETC(U)
MAY 79 D G OUTLAW, D C RANEY

UNCLASSIFIED

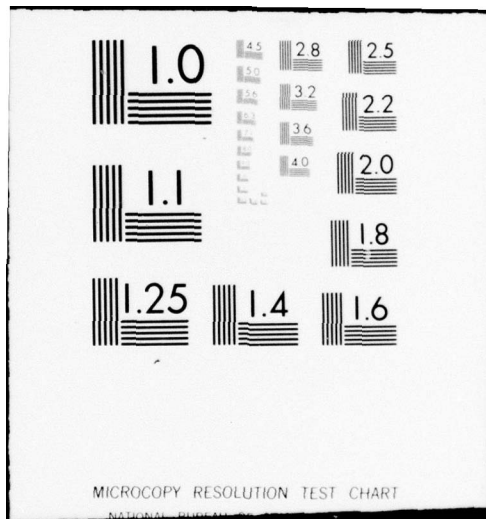
WES-MP-HL-79-5

NL

2 OF 2
AD
A069796



END
DATE
FILMED
7-79
DDC



MICROCOPY RESOLUTION TEST CHART

NATIONAL BUREAU OF STANDARDS-1963-A

APPENDIX A: NOTATION

C	Chezy coefficient
f	Coriolis parameter
g	Acceleration due to gravity
h	Water depth
j,k	Grid lines
L_x, L_y	Acceleration effect of the wind stress acting on the water surface in the x- and y-directions
n	Integer defining the calculation time-step
R_x, R_y	Effect of bottom roughness in x- and y-directions
t	Time
T_x, T_y	Wind stress components acting on the water surface
u	$u(x,y,z,t)$
v	Depth-averaged velocity component in the y-direction
\vec{V}_n	Normal component of velocity
w	Depth-averaged velocity component in the x-direction
x	Longitudinal coordinate measured along the estuary axis
x,y	Rectangular coordinate variables
y	Transverse coordinate
z	Vertical coordinate
η	Water-level displacement with respect to datum elevation
θ	Angle
ρ	$\rho(x,y,z,t)$

In accordance with letter from DAEN-RDC, DAEN-ASI dated 22 July 1977, Subject: Facsimile Catalog Cards for Laboratory Technical Publications, a facsimile catalog card in Library of Congress MARC format is reproduced below.

Outlaw, Douglas G

Numerical analysis of tidal circulation for Long Beach Outer Harbor proposed landfill / by Douglas G. Outlaw, Donald C. Raney. Vicksburg, Miss. : U. S. Waterways Experiment Station ; Springfield, Va. : available from National Technical Information Service, 1979.

39, [2] p., 52 leaves of plates ; ill. ; 27 cm. (Miscellaneous paper - U. S. Army Engineer Waterways Experiment Station ; HL-79-5)

Prepared for Port of Long Beach, Long Beach, California. Appendix B published in separate volume.

References: p. 39.

1. Earthfills. 2. Finite difference method. 3. Harbor oscillations. 4. Harbors. 5. Long Beach Harbor. 6. Mathematical models. 7. Numerical analysis. 8. Tanker terminals. 9. Tidal circulation. I. Raney, Donald C., joint author. II. Port of Long Beach. III. Series: United States. Waterways Experiment Station, Vicksburg, Miss. Miscellaneous paper ; HL-79-5.
TA7.W34m no.HL-79-5